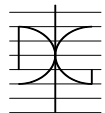


Trabajo de Investigación CST/MIH

Study of the Feasibility of Self-Healing Concrete with and without Crystalline Admixtures

Por:
Marta Roig Flores

March 2015

Autor / Author: Marta Roig Flores		Fecha / Date: 03/03/2015	
Título / Title Study of the Feasibility of Self-Healing Concrete with and without Crystalline Admixtures			
Directores del trabajo / Supervisores: Pedro Serna Ros		Código / Code: CST/MIH	Nº páginas / Pages: 115
Departamento / Departament: INGENIERÍA DE LA CONSTRUCCIÓN Y PROYECTOS DE INGENIERÍA CIVIL			
Universidad / University: UNIVERSITAT POLITÈCNICA DE VALÈNCIA			
Palabras clave / Keywords: Self-healing, concrete, crystalline admixtures, autogenous healing, autonomous healing, permeability, durability			
Código Unesco: 3305/05 Ciencias tecnológicas / Tecnología de la construcción / Tecnología del Hormigón			

Index

CHAPTER 1. INTRODUCTION	1
1.1 Research background.....	1
1.2 Objectives of this research.....	1
1.3 Outline of the document	2
CHAPTER 2. STATE OF THE ART	3
2.1 Introduction to self-healing.....	3
2.2 Mechanisms of self-healing in concrete.....	4
2.3 Autogenous healing	5
2.3.1 Principles of autogenous healing	5
2.3.2 About continuing hydration effect on autogenous healing	6
2.3.3 About carbonation effect on autogenous healing.....	9
2.3.3.1 Self-healing by carbonation in historical mortars	11
2.3.4 Limits of autogenous healing in traditional concrete.....	12
2.3.5 Strategies to enhance autogenous healing.....	16
2.3.5.1 Increasing cement content to high strength concrete.....	17
2.3.5.2 Adding pozzolanas	19
2.3.5.3 Restricting crack width	24
2.3.5.3.1 Fiber-Reinforced Concrete: SHCC+ECC.....	24
2.3.5.3.2 Application of compressive strength.....	30
2.3.6 Summary of autogenous healing.....	31
2.4 Autonomous healing.....	32
2.4.1 Types and classification.....	32
2.4.2 Cement as healing agent	33
2.4.2.1 Concepts.....	33
2.4.2.2 Without encapsulation (autogenous healing)	33
2.4.2.3 Encapsulation of the catalyst (water).....	33
2.4.2.3.1 Superabsorbent polymers	33
2.4.2.3.2 Natural fibers.....	35
2.4.2.3.3 Other methods for water encapsulation	36

2.4.3	Chemical powder or solution as healing agent.....	36
2.4.3.1	Concepts.....	36
2.4.3.2	Without encapsulation (self-healing admixtures)	36
2.4.3.2.1	Crystalline Admixtures.....	37
2.4.3.2.2	Expansive Admixtures	38
2.4.3.3	Located encapsulation	40
2.4.3.4	Dispersed encapsulation.....	42
2.4.3.4.1	Microcapsules	42
2.4.3.4.2	Porous aggregates.....	44
2.4.3.4.3	Natural fibers.....	45
2.4.4	Bacteria as healing agent	45
2.4.4.1	Concepts.....	45
2.4.4.1.1	Urea-based	45
2.4.4.1.2	Non-urea-based	46
2.4.4.2	Without encapsulation	46
2.4.4.3	Located encapsulation	47
2.4.4.4	Dispersed encapsulation.....	47
2.4.5	Summary of autonomous healing	49
2.5	Discussion.....	49
CHAPTER 3. EXPERIMENTAL PHASE.....		53
3.1	Specific objectives.....	53
3.2	Program of the campaign	54
3.3	Materials	56
3.3.1	Cement.....	56
3.3.2	Water.....	56
3.3.3	Aggregates and limestone powder	56
3.3.4	Superplastizer	57
3.3.5	Fibers.....	57
3.3.6	Crystalline admixtures.....	58
3.4	Methodology.....	59
3.4.1	Mix design.....	59
3.4.2	Control tests: slump and compressive strength	60
3.4.3	Self-healing methodology	61

3.4.3.1	Creation of a damage: pre-cracking process.....	63
3.4.3.2	Evaluation of properties: permeability test	64
3.4.3.3	Evaluation of properties: study of crack geometrical parameters.....	66
3.4.3.4	Exposure simulation	66
CHAPTER 4. RESULTS AND DISCUSSION.....		71
4.1	Introduction	71
4.2	Presentation of results	71
4.2.1	Structure of results and parameters.....	71
4.2.2	Relation between permeability and crack width measurements.....	73
4.2.3	Repeatability of results	77
4.3	Discussion.....	77
4.3.1	Qualitative evaluation of crack sealing	77
4.3.2	Effect of initial damage on self-healing.....	80
4.3.3	Effect of water/cement ratio and cement content	82
4.3.4	Effect of crystalline admixtures	84
4.3.5	Effect of healing exposure	86
4.3.6	Comparison between parameters	91
4.3.7	Comparison with other studies	93
CHAPTER 5. CONCLUSIONS AND FUTURE LINES.....		95
5.1	Conclusions	95
5.2	Future lines.....	96
REFERENCES.....		97
APPENDIX		107

Chapter 1. Introduction

This Master thesis describes a project performed from November 2013 until January 2015, at the Institute of Concrete Science and Technology (ICITECH) at the *Universitat Politècnica de València*, Spain.

1.1 Research background

The search for smart self-healing materials is justified by the increasing sustainability and security requirements of structures. The appearance of small cracks or defects in concrete is unavoidable due to its heterogeneous nature. Shrinkage, thermal effects or freeze/thaw cycles are examples of external actions that could originate small defects. These do not necessarily cause a risk of collapse for the structure, but do certainly accelerate its degradation process and diminish its service life. That degradation of the properties could force an increasing of the maintenance operations or the reparation/rehabilitation of the structure.

1.2 Objectives of this research

The three main aims of this research are to develop a state of the art on self-healing concrete, to set up a methodology in order to characterize the self-healing properties of a concrete with respect

to its permeability, and to evaluate the effects of crystalline admixtures as a healing agent on the properties of concrete under different conditions.

The goals of this research are:

- To prepare a state of the art on self-healing concrete
- To establish a methodology to evaluate self-healing based on permeability.
- To discern the effect of crystalline admixtures on the self-healing capability of concrete.
- To compare autogenous healing and self-healing by crystalline admixtures under different exposures.
- To detect and quantify any limits on effectiveness regarding the initial damage.

1.3 Outline of the document

This document is organized in five chapters:

- Chapter 1 is the current introductory chapter.
- Chapter 2 reports the state of the art on self-healing and includes a discussion on the different methodologies.
- Chapter 3 describes the experimental phase, which includes the specific objectives, experimental program and methodology used in this research in order to evaluate self-healing.
- Chapter 4 presents the outcome of the experimental phase and a discussion on the results.
- Chapter 5 summarizes the obtained results and provide ideas for further research.

Chapter 2. State of the Art

2.1 Introduction to self-healing

Self-healing is the process of recovery of lost or diminished properties after suffering some damage or degradation and with little to no external help. This process is well-known in bones and trees healing, which are able to repair damage and recover their strength. A self-healing material is that which presents self-healing capabilities.

Self-healing materials would extend the service life of structures built with them, lowering maintenance costs and avoiding complicated repairs, thus increasing the sustainability of the material itself. In the case of concrete, self-healing has been focused on the sealing of cracks and the associated recovery of properties.

The popularity of self-healing concrete has increased recently; it is a mechanism that has been known for years, however. Neville (1986) already talked about the autogenous healing of concrete, and Fernández Cánovas (1994) gave the phenomena the name of cicatrization. What is more, it has been registered that water reservoirs and historical lime and lime-pozzolana mortars have a self-healing capability due to their composition (ter Heide, 2005; Nijland, et al., 2007).

2.2 Mechanisms of self-healing in concrete

There are two main types of mechanisms of self-healing in concrete: autogenous healing and autonomous healing (van Tittelboom, et al., 2013).

Autogenous healing of small cracks in concrete is a natural process, intrinsic to the properties of the material itself. It is mainly caused by continuing hydration of cement and calcium carbonate precipitation, though other processes could also help it. This capability and the methods to increasing it will be explained in section 2.3.

Autonomous healing is an engineered healing process in order to improve the self-healing properties of a concrete element. There are different strategies of designing autonomous healing methods, which will be explained in section 2.4.

The available literature uses several nomenclatures regarding the self-healing phenomenon, such as *self-healing*, *self-sealing*, *self-repairing*, or *self-closing*, depending on the type of properties recovered or other factors, which are summarized in Table 2-1.

Reference	Criteria	Nomenclature
(Hearn, 1998)	Boundary conditions	<ul style="list-style-type: none"> ▪ Continuing hydration: will proceed as long as water is available. It does not depend on flow. ▪ Self-sealing: caused by the interaction between microstructure and the permeating fluid (swelling, chemical interaction, osmotic pressure, physical clogging...). It takes place in systems closed to CO₂. ▪ Autogenous healing: white crystals fill cracks from the reaction of calcium hydrogen carbonate from water and calcium hydroxide from concrete or the carbonation of calcium hydroxide. Does not take place in systems without CO₂.
(Schlangen, et al., 2006)	Type of mechanisms	<ul style="list-style-type: none"> ▪ Self-tightening: the crack is blocked with small particles from the crack faces or small parts present in fluids that flow through the crack. ▪ Self-healing: a chemical reaction takes place connecting the two crack surfaces.
(Igarashi, et al., 2009)	Type of process and design	<ul style="list-style-type: none"> ▪ Natural healing: cracks naturally clogged in humid environments. ▪ Autonomic healing: cracks clogged in concrete with special material design, such as using supplementary cementing materials. ▪ Activated repairing: cracks are clogged by devices embedded in concrete or the purpose of autonomically repairing cracks. ▪ Autogenous healing: autonomic healing + natural healing. ▪ Engineered healing/repairing: autonomic healing + activated repairing. ▪ Self-healing/repairing: the whole phenomenon of clogging cracks without human intervention.

Table 2-1 - Self-healing related phenomena.

Despite this wide range of nomenclature, there is a certain consensus on using the term autogenous healing for natural intrinsic healing (including continuing hydration and carbonation) and the term autonomous healing for specific tailored designs. Self-sealing would be the nomenclature for a superficial blocking by contaminants, however, because of the difficulty of distinguishing the healing effect in depth, most of the times it is not differentiated in the literature from pure self-healing. This nomenclature will be used hereinafter.

2.3 Autogenous healing

2.3.1 Principles of autogenous healing

Autogenous healing has been known for years, but there has been no clear consensus about its causes. An evidence of that is the lack of a clear differentiation of the chemical processes (which could be mostly caused from either continuing hydration or carbonation) in the literature and the predominance of carbonation models (Hearn, 1998).

Hearn and Morley (1997) summarized the different mechanisms that were thought caused self-healing in concrete in the literature:

1. Air in the matrix, due to:
 - a) Incomplete saturation of the test specimen.
 - b) Dissolution of air under pressure, into permeating water.
2. Swelling of the matrix.
3. Chemical interaction of water and the matrix:
 - a) Continued hydration of residual clinker.
 - b) Dissolution of soluble alkalis, such as Na^+ , K^+ and Ca^{2+} and crystallization along the flow path.
 - c) Carbonation of dissolved $\text{Ca}(\text{OH})_2$.
4. Osmotic pressure, due to ions concentration gradients.
5. Physical clogging caused by downstream movement of loose particles in the matrix.

Hearn and Morley experimented with concrete specimens in order to determine d'Arcy's coefficient by the flow of water through saturated concrete. They analyzed the cause of water flow reduction for 26-years old concrete specimens by measuring its permeability. Permeability remained almost constant for virgin specimens, while oven-dried and saturated specimens experienced a decrease of the water flow with the time, which was considered as an indicator of the autogenous healing behavior. In their testing setup the osmotic effect was negligible in comparison to the decrease of permeability. They affirmed that continued hydration of residual clinker was important for young and poorly cured specimens, while carbonation of dissolved $\text{Ca}(\text{OH})_2$ was more notable when high concentrations of CO_2 are available. They stated that even

when hydration is complete, the dissolution process could be the cause for the reduction of water flow. In their study they concluded that the dissolution and deposition of alkalis (Na^+ , K^+ , Mg^{+2} and Ca^{2+}) was the most important cause for self-healing by comparing the concentrations of the inflow and outflow water by means of atomic absorption (Hearn & Morley, 1997). The incomplete saturation and dissolution of air were concluded as no relevant for self-sealing.

Afterwards, the four main possible causes for autogenous healing were classified by ter Heide (2005). This is the most extended classification, and does not include osmotic pressure, deposition or crystallization (Fig. 2-1):

- Calcium carbonate formation:** calcium hydroxide (portlandite) in the concrete matrix can react with water, and if it contains carbon dioxide, calcium carbonate is formed as a precipitate filling the crack.
- Sedimentation of external particles:** particles of dust or concrete from the matrix itself could be transported by the flow and block the crack.
- Delayed hydration:** unhydrated cement particles in contact with water hydrate forming byproducts that would fill cracks.
- Matrix swelling:** increase of volume caused by the saturation of the matrix could close the crack.

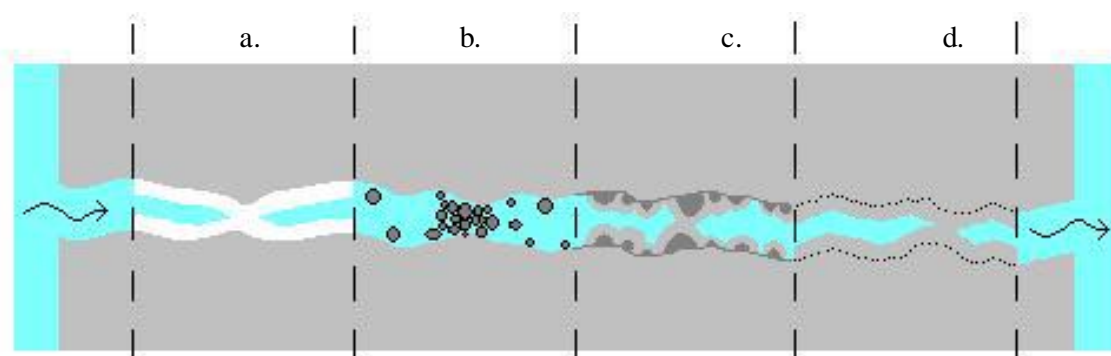


Fig. 2-1 - Possible causes for autogenous healing: (a) carbonation, (b) sedimentation of particles, (c) delayed hydration and (d) swelling of the matrix (ter Heide, 2005).

2.3.2 About continuing hydration effect on autogenous healing

Continuing hydration¹ effect on self-healing has not received as much attention as carbonation, but its contribution could be of considerable importance as the permeability of concrete decreases with the curing time. According to Hearn and Morley (1997) the permeability drop between the initial permeability of young paste and a well-hydrated system caused by hydration can be of four orders of magnitude. In old or saturated specimens, it is expected that almost complete hydration has occurred, so the autogenous healing caused by these mechanisms would be small.

¹ Also named, continued hydration, delayed hydration, further hydration or secondary hydration in the literature

In conventional concrete with water/cement ratio around 0.4, about 30% of cement particles remain unhydrated, even though, theoretically, that ratio is enough for complete hydration (van Breugel, 2007). That percentage is increased with coarser cements and higher amounts of cement. After cracking and being in contact with water (which could be from rain or exposure humidity) those particles hydrate forming byproducts that would fill cracks and pores, therefore, they could cause autogenous healing. This process will increase as the water/cement ratio is diminished, as there would remain a higher amount of unhydrated particles.

There are two main differences between the conditions for the chemical reactions in the hydration of cement bulk paste and in a hydration to fill a crack in a specimen, which could change the mineralogy of products (Huang, 2014). First, the water/binder ratio is much higher in cracks with access to external water than in the cement paste, thus there is more water available for the reaction. Second, the free space is much larger in cracked specimens than in the paste.

The healing capability of an Ordinary Portland Cement (OPC) concrete depending on its initial degree of hydration has been studied for early age cracks with initial openings of 20, 50, 100 and 150 μm by Schlangen, et al. (2006). This study was based on the recovery of mechanical properties by using three-points-bending tests on prismatic specimens, which were kept under water. They concluded that if the degree of hydration of the specimens is higher at the moment of cracking, *i.e.* if the specimen is older; the strength regain is less (see Fig. 2-2).

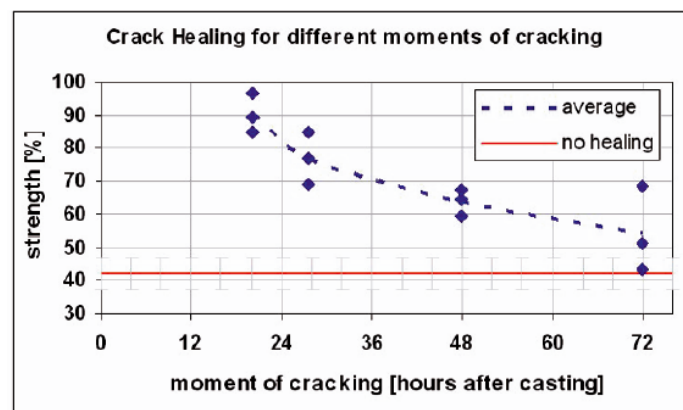


Fig. 2-2 – Influence of compressive strength and age of pre-cracking on healing (Schlangen, et al., 2006).

From that group of researchers, ter Heide (2005) did microscope observations of the products formed inside the crack, resulting in a needle-like network, which was probably ettringite. When re-loading the healed specimens, the cracks occurred mostly by the old-crack path, breaking the needle network (Fig. 2-3).

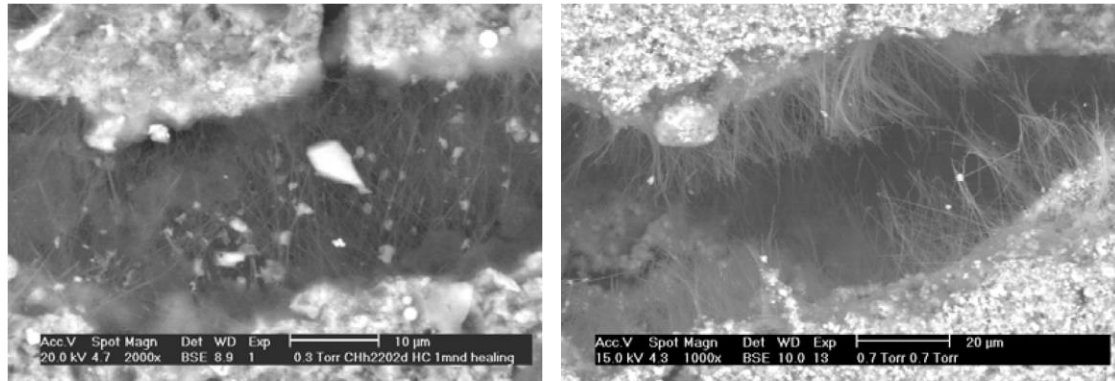


Fig. 2-3 – Needle-like network formed in a crack after healing (left) and broken after reloading (right). (ter Heide, 2005).

There are few studies about the self-healing produced by continuing hydration, as it is necessary to avoid the interaction with other processes, such as carbonation. In one of those studies the self-healing behavior of micro-cracks by continuing hydration in Portland cement pastes has been characterized (Huang, et al., 2013; Huang, 2014). In order to avoid the effect of the carbonation process the specimens were immersed in a sealed container, thus preventing the entrance of CO_2 in the water. The healing condition was the partial immersion of specimens; therefore the capillary action caused the absorption of water into cracks. In this study, artificial cracks (with a gap of 30 μm) were used for the characterization of the chemical precipitates while natural cracks (crack width around 10 μm) were employed for the quantification by back-scattered electron (BSE) image analysis. Fig. 2-4 shows the two series: series I for artificial cracks and series II for natural cracks.

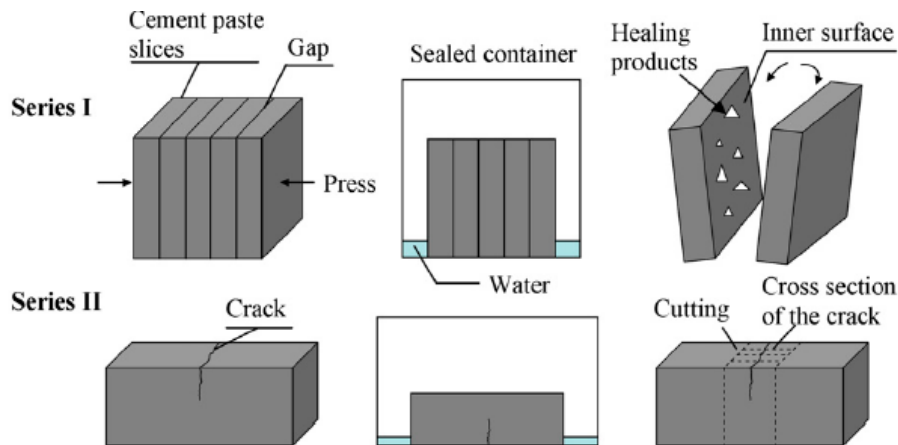


Fig. 2-4 – Artificial cracks for characterization (Series I) and natural cracks for image analysis (Series II) (Huang, et al., 2013).

In this process, two types of products were formed in the artificial cracks: gel-like and crystal-like products, the first formed mainly by hydrated calcium silicates (C-S-H) and the latter mostly formed by calcium hydroxide (CH). The main minerals of the reaction products in the artificial cracks (in the conditions of Fig. 2-4) were portlandite (78% of mass percentage for specimens under water and 80% under $\text{Ca}(\text{OH})_2$ solution) and C-S-H gels (15% of mass percentage for specimens under water and 17% under $\text{Ca}(\text{OH})_2$ solution). The rest of product was identified as

calcite. These compounds were produced when the cracked paste was cured in water and in $\text{Ca}(\text{OH})_2$ solution, meaning that the initial concentrations of Ca^{2+} and OH^- had not notable influence in the healing processes.

The quantification of healing by further hydration was performed by analyzing the BSE images and measuring the filling area of the natural cracks (Huang, 2014). Different values for the filling fraction of cracks were obtained for the pre-cracking ages and time of healing, with better results for younger cracks and higher healing time. The highest values of filling fraction (for 10 μm cracks) were around 50% after 200 hours of exposure to the conditions of partial immersion.

Despite of the influence of continuing hydration on self-healing, several authors agree to affirm that the effect of continuing hydration on autogenous healing is not as important as carbonation (Edvardsen, 1999; Joos, 2001).

2.3.3 About carbonation effect on autogenous healing

Carbonation is thought to be the most important process for autogenous healing, at least in older elements, in which cement particles are almost completely hydrated. It has been noticed for years in structures in water contact, such as water tanks. Carbonation is produced in concrete when water dissolves and transports the soluble compounds out of the concrete matrix. In concrete, the compound of higher solubility is portlandite, $\text{Ca}(\text{OH})_2$, which dissolves in water. When calcium ions contact with carbon dioxide contained in water, they would form calcium carbonate. Fig. 2-5 shows a summary of the compounds in a water tank with a crack in a wall and the carbonation process (Edvardsen, 1996).

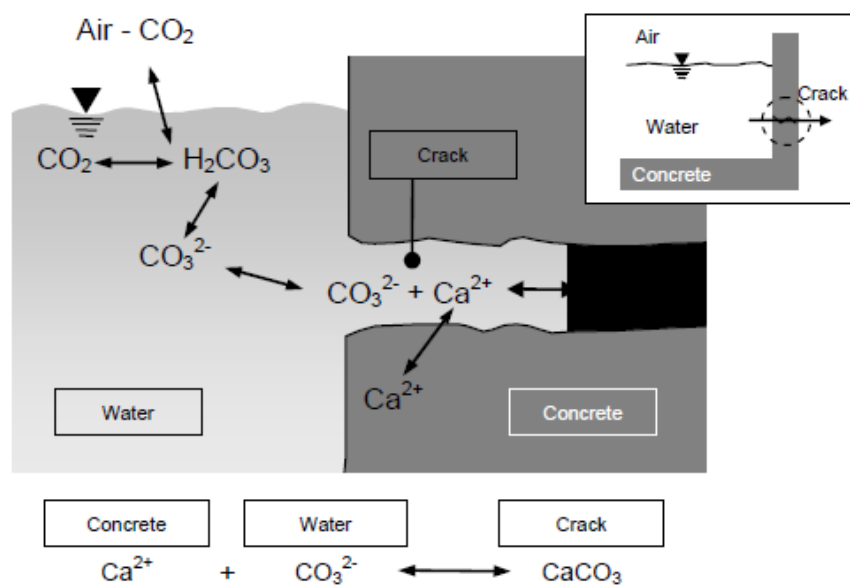
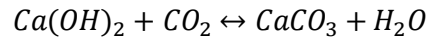


Fig. 2-5 – Carbonation process in a crack produced in a water tank (Edvardsen, 1999).

Carbonation process affects all the compounds in the hydrated cement matrix: the calcium hydroxide, and when that element becomes depleted, the carbonation of hydrated calcium silicates

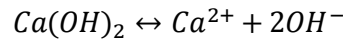
(C-S-H gels) starts, forming silica gel, which is a high porosity material and promote even further carbonation (Neville, 2011). The reaction of carbonation of C-S-H gels, has been taken from Morandau, et al. (2014). These authors affirm that the exact stoichiometric coefficients of this reaction are not clearly defined. For instance, the amount of water inside the silica gel SH_t is unknown, as well as the exact kind of calcium carbonate which it forms (calcite, vaterite or aragonite).



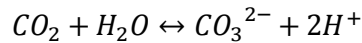
In most studies the carbonation process is mostly referred to the calcium hydroxide carbonation and it will be the referred reaction in this work. The process can be divided in two phases:

1) Dissolution of ions:

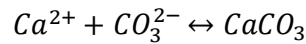
- a. Dissolution of calcium hydroxide in the water.



- b. Dissolution of carbon dioxide from the environment in the water at high pH.



2) Reaction of calcium and carbon ions at high pH (Joos, 2001):



Edvardsen (1999) studied profoundly the autogenous healing by analyzing the water permeability of cracked concrete specimens for different static crack widths and water pressure. She obtained higher initial flows for larger cracks and higher pressure, as it was expectable, but the test presented a high dispersion due to the nature of the test setup.

She obtained two behaviors, the surface-controlled phase and the diffusion-controlled phase, as shown in Fig. 2-6. The first phase would be controlled by the presence of ions in the surface of the crack, while the second would start as calcium carbonate layer does not allow direct contact of calcium ions with water, so the process depends on the diffusion of ions from the concrete to the crack. Autogenous healing mostly took place in the first 5-7 days of water immersion (phase 1 in Fig. 2-6). The study also concluded that precipitation of calcium carbonate was the main cause for autogenous healing by using X-ray diffraction of the healing products, as the main product detected as healing filling fraction was calcite (see Fig. 2-7).

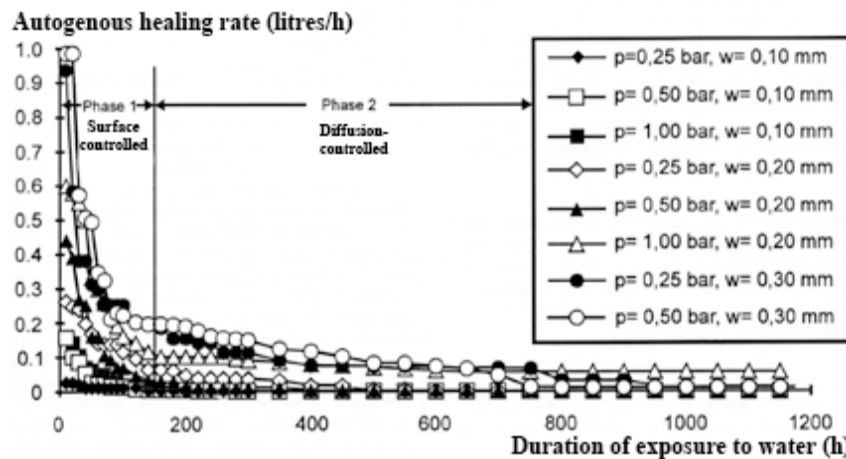


Fig. 2-6 – Healing rate for different crack widths and water pressures (Edvardsen, 1999).

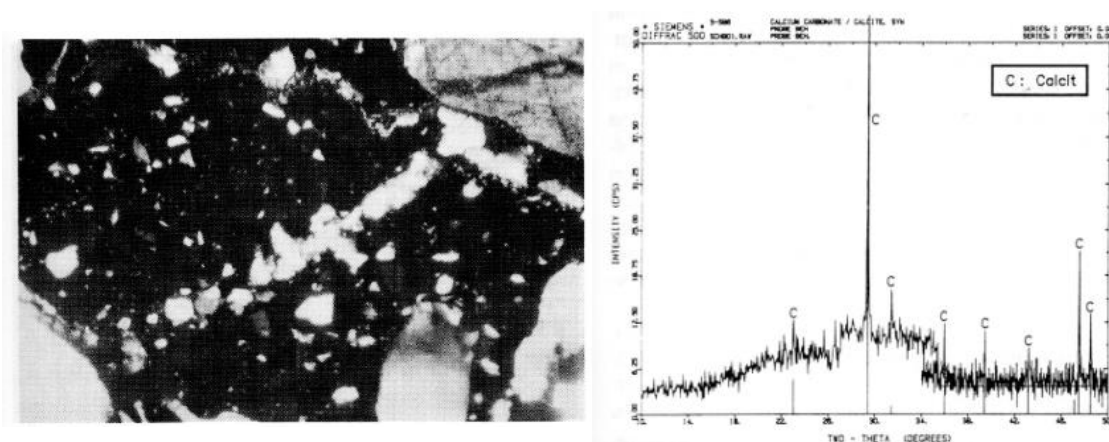


Fig. 2-7 – Crack of 0.2 mm filled by calcite (left) and X-ray diffraction of healing products showing the predominance of calcite (right) (Edvardsen, 1996).

2.3.3.1 Self-healing by carbonation in historical mortars

Though Portland cement was introduced in late 18th century constructions, lime and lime-pozzolana mortars have been used for years as binder. Their composition is based in calcium oxide and calcium carbonates; therefore, they could give a hint about the self-healing reactions based on carbonation.

In fact, the self-healing process in historical lime and lime-pozzolana mortars from the 18th, 19th and 20th centuries, demonstrates the importance of the carbonation process in autogenous healing. In contrast to Ordinary Portland Cement, those lime mortars showed the filling of small microcracks (< 70 μm). The more important chemical reactions in this case were thought to be the alkali-aggregate reactions and the crystallization of water-soluble salts (Nijland, et al., 2007).

Fig. 2-8 (left) shows a lime-fired clay pozzolana mortar from 1814, with a composition similar to medieval mortars. This mortar presented large portlandite crystals formed inside a void, which were formed in wet conditions that prevented carbonation, and it is thought to be an arrested self-healing process. Fig. 2-8 (right) shows a 19th century masonry mortar from a quay wall, which had cracks due to frost action. Its cracks were filled by calcium carbonate, which was thought to

be in calcite form. Even for not completely immersed masonry structures, healing by leaching of calcite has been registered, such as in an old bridge from 1728 at Amsterdam (Nijland, et al., 2007; Lubelli, et al., 2011).



Fig. 2-8 - Microphotograph showing large portlandite crystals in air void in early 19th century lime (left) and a crack filled completely by calcite (right) (Nijland, et al., 2007).

2.3.4 Limits of autogenous healing in traditional concrete

The main causes proposed in the literature for autogenous healing in concrete have been explained in the sections above. The causes are not completely clear and there are still grounds for research. Autogenous healing in traditional concrete has limits of effectiveness: it is not a reliable phenomenon in which an engineer could trust when projecting a concrete structure.

In the research by Edvardsen (1996; 1999) several factors were analyzed and the related findings are summarized in Table 2-2. Self-healing was analyzed by measuring water permeability of cracked concrete specimens before and after water immersion. The main water flow reduction was produced in the first 200 hours (approx. 8 days).

Factor	Studied Ranges	Self-healing Conclusions
Crack width	0.10, 0.20 and 0.30 mm	The most important parameter: smaller cracks heal better, but 0.3 mm cracks can heal by carbonation.
Water pressure head at testing	Variable between 2.5-20 m of water	Great influence: lower pressures, better healing rates.
Hardness of water	Soft water (70 mg CaCO ₃ /l), Hard water (480 mg CaCO ₃ /l) and distilled water	Lesser influence.
Type of cement	OPC, slag and SR cement	
Type of aggregate	Granite, limestone and basalt	
Type of filler	Limestone dust and fly ash	
Crack motion	Dormant crack / Active crack	Both are able to heal, but active cracks take longer time.
Substances in water	Microcement, silica fume and bentonite	Only general conclusions: bentonite seems to be problematic. The particles block the cracks.
Crack branching	Different skin reinforcement	Produces a reduction of crack width, thus of water flow.

Table 2-2 - Summary of the findings by Edvardsen (1996; 1999).

With a similar idea, Aldea, et al. (2000) studied the self-healing effect of a normal strength concrete, water/cement ratio of 0.45 by means of permeability of cracked specimens. In their research, the average induced crack widths range from 14 to 350 μm . The permeability setup was fixed and the healing exposure was water soaking. Fig. 2-9 shows the reduction of the permeability coefficient of a specimen at different times, with complete healing around 15 days after the first test. They also studied autogenous healing by means of signal transmission, which showed an improvement after 100 days of water flow; however the results were not as clear as by permeability.

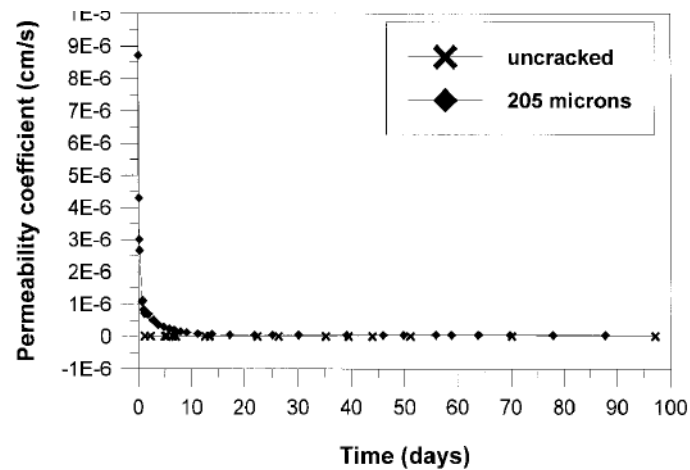


Fig. 2-9 – Permeability coefficient as function of time, initial crack width 205 microns (Aldea, et al., 2000).

Later on, ter Heide (2005) studied early age cracks and some of the conditions to achieve self-healing. She analyzed autogenous healing for cracks generated at 20, 24, 48 and 72 hours and compared the effect of healing time (from 2 to 12 weeks), crack widths (20, 50, 100 and 150 μm), relative humidity (60%, 95% and 100% or water immersion). This research used prismatic mortar specimens, pre-cracked by means of three-points bending test, and measured the strength recovery after healing. Fig. 2-10 shows an example of the obtained curves in this research, showing an increase of the strength after healing during 2 weeks, specially on stiffness terms. With this criteria, a crack healing of 100% means that the healed strength equals the strength of uncracked specimens.

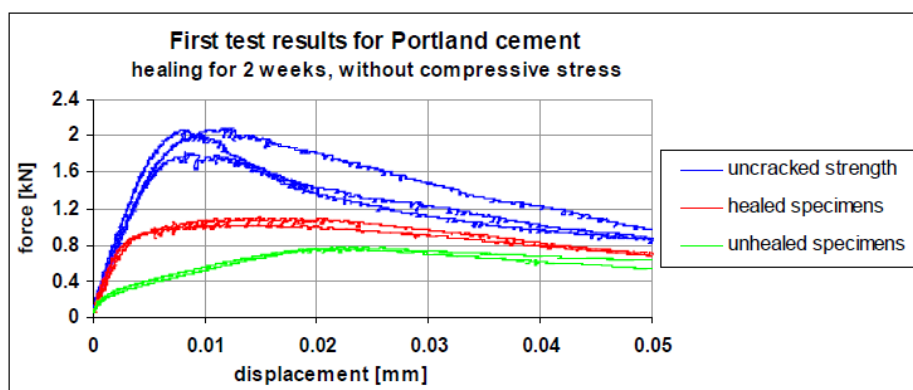


Fig. 2-10 – Strength recovery of healed, unhealed and uncracked specimens (ter Heide, 2005).

In the results of ter Heide (2005), it is concluded that larger initial crack widths reach lower strength recoveries. She did few tests for analyzing the effect of quantity of water, and thought affirms more studies are needed, it was registered a better response for specimens stored under water immersion in comparison to those in humidity chambers at 95% or 60% of relative humidity. In regards to the healing time, between one and two months of water immersion the strength recovery is stabilized, but the behaviour needed further investigation.

A few years later, Zhong & Yao (2008) analyzed the effect of damage degree on autogenous healing in normal strength concrete by means of ultrasonic pulse measurements and mechanical properties. Their research show that there is a damage threshold for high strength concrete and normal strength concrete. If the damage is lower than the threshold, the self-healing ratio is increased for higher damage degree; on the contrary the self-healing ratio is decreased with the increase in damage degree. They also concluded that the damage threshold for normal strength concrete is higher than that for high strength concrete. That threshold was obtained when comparing the strength recovery measured by the mechanical compressive strength before and after the healing with the degree of damage, whose results are represented in Fig. 2-11 for normal concrete. This study led to the idea that very small cracks could be more difficult to heal than moderately large cracks.

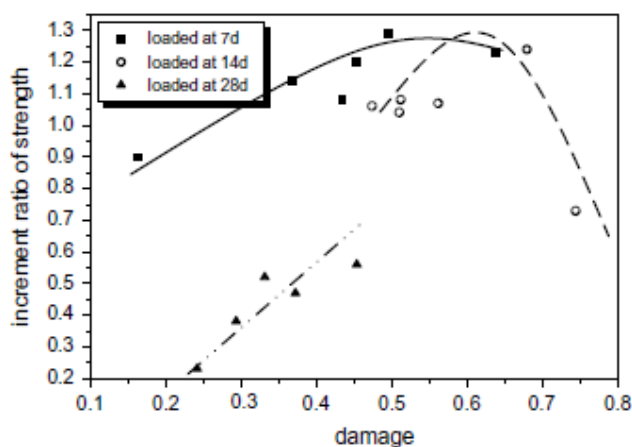


Fig. 2-11 – Relation between Damage and increment ratio of strength, for normal strength concrete (Zhong & Yao, 2008).

Fagerlund & Hassanzadeh (2010) investigated the amount and type of precipitations in the crack after long-term exposure in three types of water, three types of exposure and also the effect of crack-healing on the ingress of chloride ions in cracks of different width. Only one type of concrete was analyzed, which had a water/cement ratio of 0.40 and 440 kg/m³ of cement. Specimens were pre-cracked at 14 days and placed in different baths for 375-385 days. Two levels of crack width were studied, 0.2 and 0.4 mm and their results showed that cracks of 0.2 mm can heal but an opening of 0.4 mm was too large for complete healing. They analyzed three types of water exposure: permanent and complete immersion, cyclic (1 week immersed in water / 1 week in lab air) and one-sided capillary suction (immersed few millimeters in water) in three types of

water (sea from the west-coast of Sweden, brackish from south Baltic Sea, or tap water). Their results by means of visual observation of cracks show that permanent immersion in sea water presents better results, and the sealing of the mouth of the crack avoids the internal healing of crack.

Li, et al. (2011) studied the influences of particle size and mixing content of coarse cement, analyzing self-healing by non-destructive testing by comparing ultrasonic head wave amplitude before and after healing. After healing during 42 days in a standard moist chamber, they tested the specimens to compressive strength and ultrasonic tests. They registered a recovery of strength up to 16% and even higher recoveries for the non-destructive testing. They noticed a damage threshold, similar to that from Zhong & Yao (2008), which is shown in Fig. 2-12. Their results show that for equal mixing content of coarse cement, self-healing ratio increases with the diameter of cement.

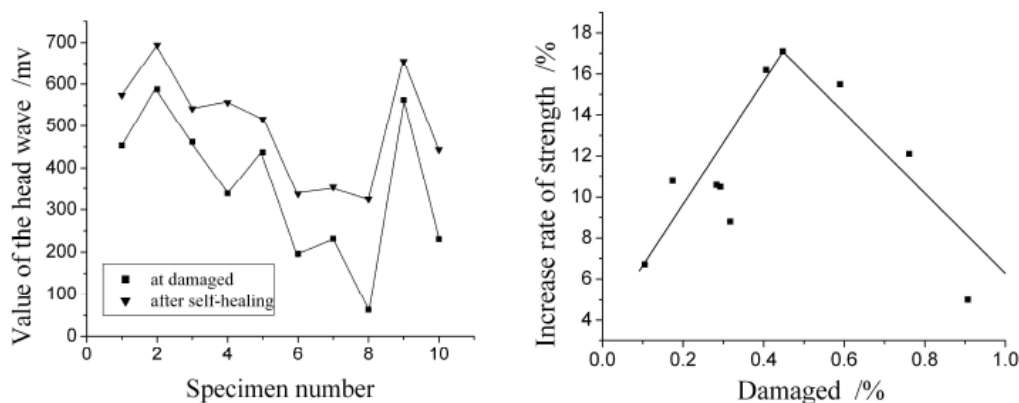


Fig. 2-12 – Relationship of the head wave amplitude for damaged and healed specimens (left) and relationship between damaged degree and increase rate of strength (right) (Li, et al., 2011).

Zhou, et al. (2011) studied the effect of sand ratio (sand/aggregates), as it affects the size particles distribution and the density of concrete. For low values of sand ratio, concrete would have got more gravel content, but for higher ratios concrete strength would be smaller. In this research, the optimal sand ratio was obtained in which the self-healing ability of concrete was the highest (33% of recovery).

Van Tittelboom, et al. (2012) analyzed the composition of concrete mix in the autogenous healing by continuing hydration or carbonation. They analyzed the effect on permeability of cracked specimens due to an increasing of the water/binder ratio from 0.4 to 0.5. They pre-cracked the specimens by means of splitting test to levels between 50 and 250 μm . The age of pre-cracking was fixed at 55 days and the healing exposure was 71 days of wet/dry cycles for the microscopic and strength tests in order to activate the carbonation process; while for the calorimetric and water permeability tests, the specimens were exposed 71 days to water immersion, in which the only expected mechanism was continuing hydration. Their microscopic measurements showed that calcite was the main precipitate in cracks. Their results did not showed any difference between

the two ratios on autogenous healing. They compared the global healing capability depending on the closing rate of the crack width observed visually. In their research, 0.15-0.2 mm cracks achieved more healing rates than 0.1-0.15 cracks. They concluded that cracks larger than 0.2 mm were unlikely to achieve complete closing of the crack, while cracks under 0.1 mm seal completely by 75% of the time by autogenous healing under the designed conditions.

Gagné & Argouges (2012) investigated the autogenous healing of mortars by means of air-flow permeability through pre-cracked specimens. They analyzed three mix designs, with water/binder ratios of 0.35, 0.45 and 0.60 and three crack categories 50 ± 15 , 105 ± 15 and 220 ± 35 μm . Cracks were generated at the age of 28 days and 6 months and after the damage, were stored for healing at 23°C and 100% of relative humidity for 5 months.

Their results show that effective crack opening decreases for all cases and the velocity of healing is higher in the first month, while at 3/5 months healing is still active but at notably lower rates. Autogenous healing was registered more effective for smaller cracks. Moreover, early age cracks (1 month) healed only slightly better than those pre-cracked at older ages (6 months). That could be caused by an almost complete hydration of specimens pre-cracked at 1 month. It was expected that early age cracks had higher amount of anhydrous cement for continuing hydration, but lower amount of calcium hydroxide available for carbonation for early ages; while old age cracks, would show the opposite behavior. The same research did not discerned clear effect of water/cement ratio on self-healing. The reaction products were composed mostly of calcium carbonate, which blocked the crack. That obstruction of the crack slowed the reaction, as the diffusion of CO_2 became more difficult.

2.3.5 Strategies to enhance autogenous healing

It is clear that autogenous healing in traditional concrete has got a limited effect. That is the reason why there are different strategies in order to enhance it by changing its composition:

- a. Increasing cement content or reducing water/cement ratio, in order to have more anhydrous cement in the matrix.
- b. Introducing pozzolanas (such as blast furnace slag or fly ash) that react with calcium hydroxide and have a delayed reaction, thus being more probable that it remains a reaction capability when a crack appears.
- c. Restricting crack width, which can be done in two different ways:
 - i. Introducing fiber reinforcement that restricts crack width, or the use of Strain-Hardening Cementitious Composites or Engineered Cementitious Composites, which have got smaller crack widths.

- ii. Introducing compressive strength, which ties both sides of the crack, using specific devices for generating the strength or using memory shape materials, which have an effect similar to prestressed concrete.

The following sections analyze the studies made for enhancing autogenous healing by using these types of strategies.

2.3.5.1 Increasing cement content to high strength concrete

Increasing cement content is a potential method to improve autogenous healing as the amount of unhydrated particles is increased. Nevertheless, as mentioned above, van Tittelboom et al. (2012) analyzed the effect of increasing the water/binder ratio from 0.4 to 0.5, and their results did not show any difference between the two ratios on autogenous healing. In the same direction, the results by Gagné and Argouges (2012) show that there is not a clear effect of water/cement ratio on self-healing in humid environment comparing ratios of 0.35, 0.45 and 0.60. On the contrary, Qian, et al. (2009) reported better healing behavior for concrete with much higher contents of cement when comparing water/binder ratios of 0.30 to 0.60, with different addition contents.

High performance concrete could have different behavior regarding to self-healing, mostly due to the much higher amount of unhydrated particles. There are several authors that analyze the autogenous healing in those types of mixtures.

Already in the mid-90s, Jacobsen et al. investigated the autogenous healing behavior of high performance concrete after being damaged by freeze/thaw cycles. They used with water/binder ratio of 0.4 with silica fume contents between 0 and 5% by the weight of cement. After the pre-cracking process, concrete beams were exposed 2-3 months under water immersion, and afterwards they were measured by regained resonance frequency. Resonance frequency values after deterioration were around 47-87% of initial frequency and after self-healing 85-99% of initial frequency. However, healing only implied a minor recovery of lost compressive strength on frost deterioration, since from the 22-29% of strength loss, only 4-5% was recovered, while the dynamic modulus was almost the initial (Jacobsen, et al., 1995; Jacobsen & Sellevold, 1996).

In their study, they obtained that main healing products were identified as C-S-H, which were observed bridging cracks after self-healing but not after damaging (Jacobsen, et al., 1995). Portlandite and ettringite were observed locally, as well. They measured crack size which was between 1-10 μm after damaging and presenting a partial closure after self-healing for cracks smaller than 5 μm while larger cracks (10 μm), hardly presented any healing. This poor filling of cracks was thought to be the reason for the low recovery on compressive strength. They also noticed that concrete with silica fume had smaller healing results (which could be done by the consumption of portlandite), but their results were not conclusive because of the different damage rates of each specimen and the presence of portlandite in the healing products.

Later on, Reinhardt and Jooss (2003) studied for high strength concrete (w/c ratio of 0.37, cement 360 kg/m³, microsilica 40 kg/m³) for different crack widths and temperatures of water at the healing exposure. They compared the reduction of water flow through concrete cracked specimens for crack widths of categories of 0.05, 0.10 and 0.20 mm and studied water temperatures of 20, 50 and 80°C. Their results show a better response for smaller cracks and higher temperature of water, with the main decrease of permeability around the first 100 hours in the smaller cracks for the higher temperature, that is approximately 4 days (see Fig. 2-13).

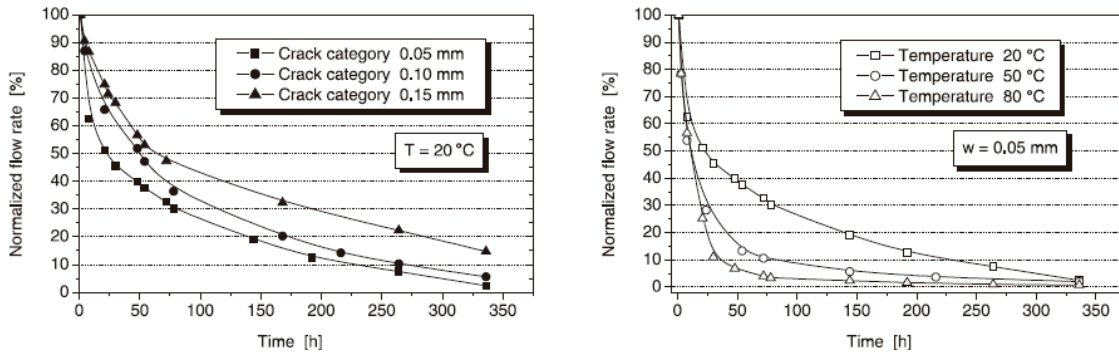


Fig. 2-13 – Decrease of normalized flow rate for different crack widths and water temperature at healing (Reinhardt & Jooss, 2003).

Granger et al. (2005) analyzed the healing properties of ultra-high performance concrete (W/C ratio close to 0.2 and with Silica Fume) using three-points bending tests and non-destructive testing (acoustic emissions and resonance frequency). They pre-cracked the prismatic specimens to crack openings of approximately 30 μm with residual cracks between 5 μm and 15 μm and they were stored to heal. They noticed a regain of stiffness at the reloading stage compared with the pre-cracking curve, which depended on the time of healing (1, 3 or 6 weeks) and the exposure (air or water immersion). This results show no regain of stiffness when specimens were stored in air, while those stored in water for more than 3 weeks showed self-healing behavior, with stiffness tending towards initial stiffness, almost being equal to that of the non-cracked concrete. In fact, their results show the average regain of stiffness when specimens were healed immersed in water, as the healing time was increased (Fig. 2-14). However, their results show that there is no recovery of the peak load under reloading after self-healing.

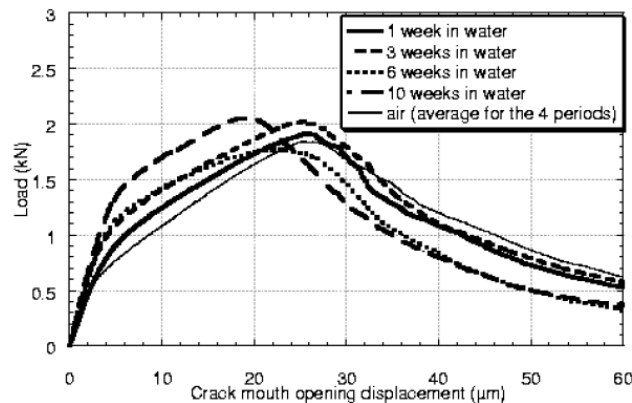


Fig. 2-14 – Reloading curves for different times cured in water and in air. (Granger, et al., 2005).

More recently, Fukuda, et al. (2013) have analyzed the self-healing behavior of 2-years old high performance concrete under marine environments by means of X-ray computed tomography. They showed the healing in depth of the concrete specimens, but only up to a certain depth. They took images each 24 μm from the surface (END-1 or END-2) to the interior of the specimen, achieving data for almost 3 mm depth. Their results show that for crack widths of 0.10 mm (END-1) there is a significant sealing (around 85% of sealing of the crack) while 0.25 mm cracks (END-2) barely heal during the 49 days of exposure (23%). This confirms the dependence on the initial crack width for the self-healing mechanisms and this effect was registered in a volume near the surface of the specimen (see Fig. 2-15).

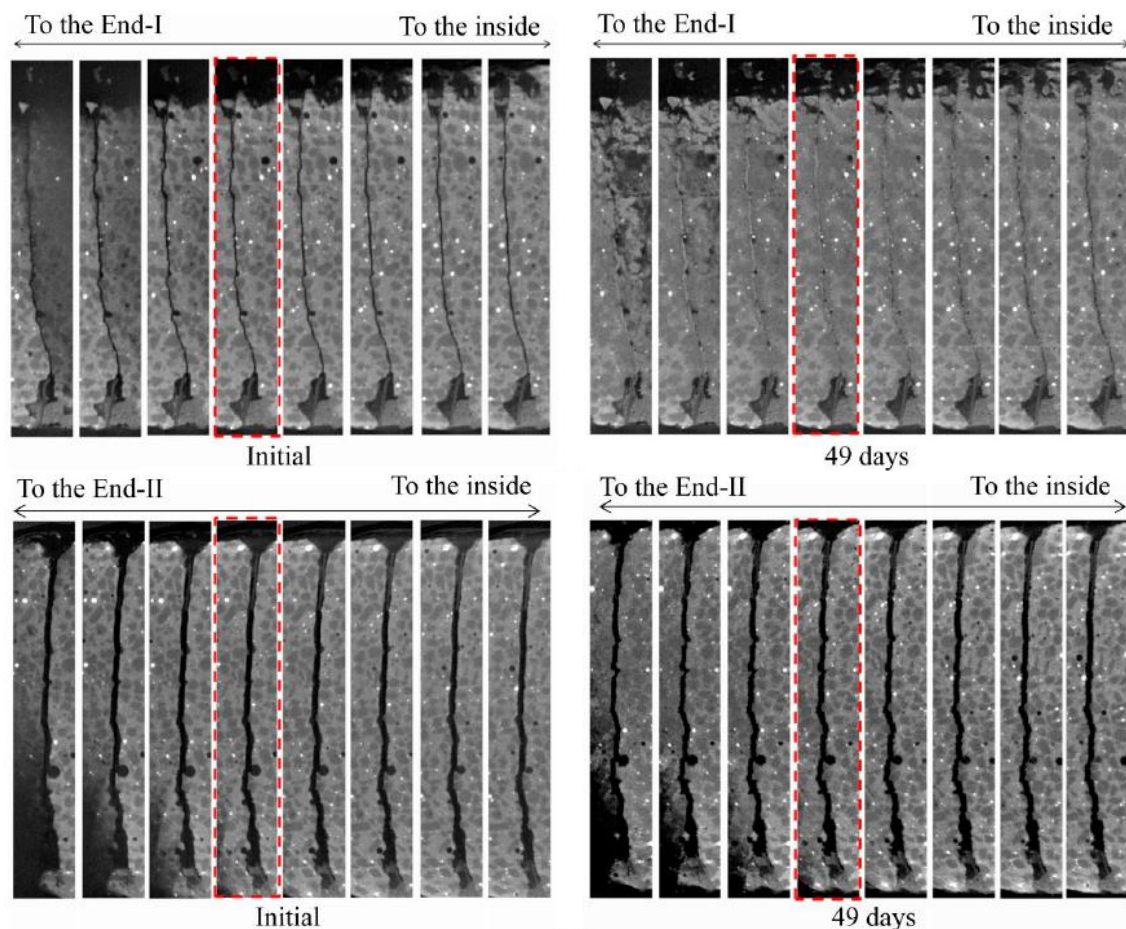


Fig. 2-15 – Comparison between the self-healing effect on 0.1 mm (top) and 0.25 mm (bottom) cracks before and after exposure to seawater (left and right, respectively). (Fukuda, et al., 2013).

2.3.5.2 Adding pozzolanas

Pozzolanas are mineral products that react with portlandite (calcium hydroxide) and in general have a delayed reaction, thus being more probable that it remains a reaction capability when a crack appears in concrete. These minerals react slower compared to cement, thus more unreacted material was available in the pre-cracking and healing moments. Nevertheless, pozzolanas consume portlandite, which could decrease the capability of carbonation for the matrix. Some of the pozzolanas used in concrete are silica fume, fly ash and blast furnace slag.

In this section, the studies have been gathered depending on the type of property they have focused on: mechanical properties, durability properties or crack closure.

a) Mechanical properties

According to Schlangen, et al. (2006), the differences of healing process for mechanical properties by using a Blast Furnace Slag Cement (BFSC) and an Ordinary Portland Cement (OPC) are not notable, and in any case, with slightly better results for OPC. In this study, the concrete mix is changed from CEM III (BFSC) to the same amount of CEM I 52.5 R (OPC). Three-point bending test was used for pre-cracking the specimens to crack widths of 50 μm (before unloading), and also to analyze the strength regain after healing. The results for the age of pre-cracking of 1 day are shown in Fig. 2-16, where it can be seen that BFSC has got significantly lower strength when pre-cracking, in comparison to OPC specimens. When reloading these specimens, they recover their whole initial strength, with better results when using OPC. When pre-cracking at the age of 15 days (Fig. 2-17) the strength recoveries are significantly lower than when pre-cracking at 1 day, thus remarking the significance of the hydration degree in autogenous healing. At 15 days, there are hardly any differences between BFSC and OPC in pre-cracking or in reloading.

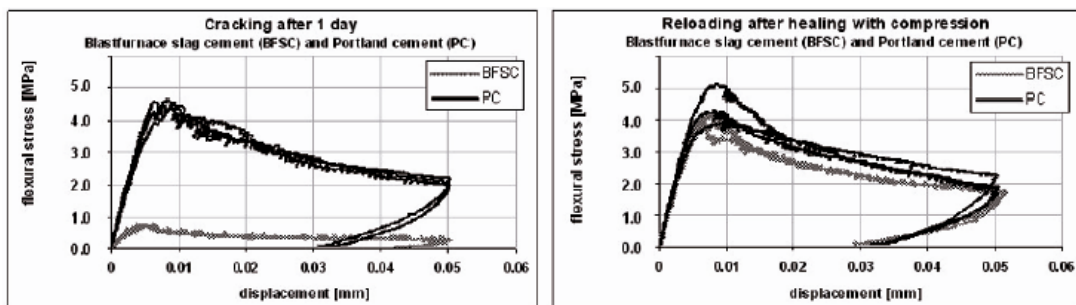


Fig. 2-16 – Flexural stress versus crack opening for pre-cracking age of 1 day and reloading after self-healing, for BFSC and PC concrete (Schlangen, et al., 2006).

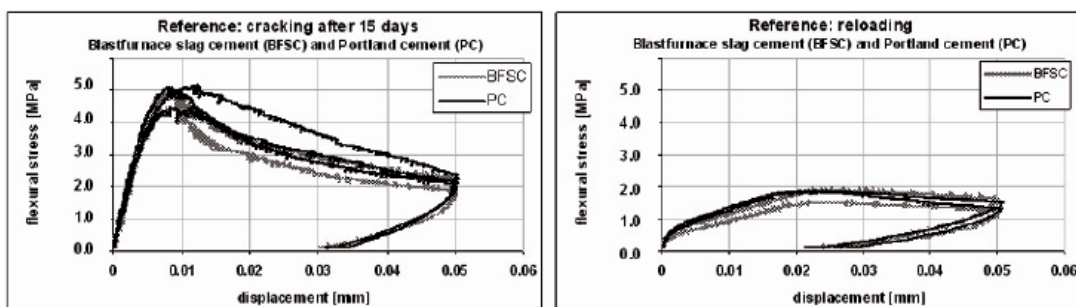


Fig. 2-17 - Flexural stress versus crack opening for pre-cracking age of 15 days and reloading after self-healing, for BFSC and PC concrete (Schlangen, et al., 2006).

In a similar direction, van Tittelboom, et al. (2012) reported that based on the recovery of mechanical properties, mixes with OPC, BFS or FA showed poor healing capabilities. Other authors have noticed a more positive effect from using pozzolana as autogenous healing enhancers, such as Termkhajornkit, et al. (2009), who registered a recovery of compressive

strength when using a 25% of Fly Ash, and also an improvement for durability properties, after letting the fly ash react up to the age of 91 days.

Zhou, et al. (2011) analyzed the influence of slag and fly ash content on self-healing by means of compressive strength recovery and SEM observations, both before and after self-healing. They compared for the contents of slag and fly ash of 20%, 30%, 40%. Their results show that the self-healing ability of concrete was maximized when the mixing content of slag and fly ash were 30% and 40% respectively, but only with percentages of recovery of compressive strength around 5-6% of the initial strength.

In the same direction, Na (2013) analyzed the effect of fly ash blended cement with different cement replacement ratios (10%, 20%, and 30% by volume) and three types of cement, comparing with OPC samples (named N sample). They used high early strength and low heat Portland cement. Specimens were exposed during 13 weeks to CO₂, in order to provoke the damage. They analyzed the properties of compressive strength, bending strength and dynamic modulus of elasticity for virgin specimens (no cracking), just after deterioration (relative damage of 60%), healing in water immersion at 20°C for 1 week and healing in water immersion at 40°C for 4 weeks. The results show a notable recovery of all the properties after deterioration for most cases, with higher degree of healing in mortar samples with fly ash (20 and 30% of replacement). Curing 1 week at 20°C was not enough for any significant recovery of most properties, while specimens under water immersion at 40°C for 4 weeks achieved the highest healing degrees.

b) Durability properties

Van Tittelboom, et al. (2012), analyzed the effect on self healing produced by Blast Furnace Slag and Fly Ash. Cracks up to 200 µm could close completely due to CaCO₃ precipitation with higher efficiency for CEM I mixes, but for larger cracks there were not significant differences. That was thought to be caused by the higher amount of portlandite, since as more Ca(OH)₂ is available, more Ca(OH)₂ can react with CO₂ from the air to precipitate as CaCO₃ crystals. From both the water permeability test and the calorimetric measurements, a decrease in the W/B ratio of the CEM I mixes from 0.5 to 0.4 and the presence of BFS and FA improved the autogenous crack healing efficiency due to further hydration.

Termkhajornkit, et al. (2009) studied the self-healing capability of fly ash systems to recover properties on cement paste, which was damaged by shrinkage. Most of shrinkage cracks occur before 28 days, and fly ash hydrates mostly after that time, thus it was expected to show a healing capability because of its reaction as pozzolana. When using a 25% of Fly Ash, they registered a recovery of compressive strength, but also a reduction of porosity and chloride diffusion coefficient (which was not significant at 28 days but was notable after 91 days) after letting the fly ash react up to the age of 91 days. They also compared the effect of on the carbonation

coefficient in the FA mortar samples FAX, FA20 and FAY and the carbonation depth in mortar with 30% of FA with two curing conditions. Results show that the carbonation depth after curing in water 20°C for 1 week was almost the same than for after deterioration, while specimens cured in water at 40°C for 4 weeks had carbonation depth lower than 1 mm, being even lower than for the case of virgin specimens. Their results (Fig. 2-18) show that FA specimens with lower w/c had lower carbonation coefficient and better self-healing performance when healing under water immersion for 4 weeks at 40°C.

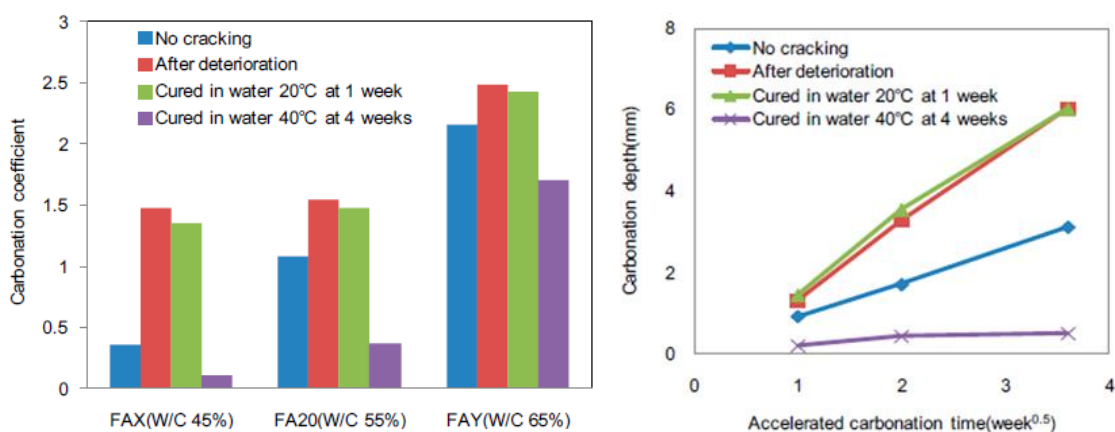


Fig. 2-18 - Change of carbonation coefficient for fly ash mortar samples with different water to cement ratio, exposed to CO₂ for 13 weeks (left) and change of carbonation depth for specimens with 30% of fly ash after different curing cases (right) (Na, 2013).

Yildirim, et al. (2014) studied the influence of hydrated lime on self-healing of engineered cementitious composites with high content of fly ash. Three different mixtures were analyzed with hydrated lime contents of 0%, 2.5%, and 5.0%. Resonant frequency and rapid chloride permeability tests were used to measure the deterioration. Their results show that the addition of hydrated lime enhanced the healing effect. Also the XRD patterns of self-healing products in the different mixtures show that for specimens without additional lime the most of the precipitates are SiO₂ while for specimens with 5% of additional lime the precipitates had significantly higher amount of calcite (CaCO₃), but also presenting silica.

Zhang, et al. (2014) compared the three ECC mix proportions with different volume of fly ash after healing 30 days under water immersion. Healing behavior was investigated by sorptivity and rapid chloride penetration tests. Sorptivity test results indicates that specimens with the highest investigated fly ash/cement ratio (4.0 by weight) may have the highest self-healing behavior, however this is not evident for the intermediate contents comparing with reference mix. Nevertheless, virgin specimens exposed to the same healing conditions, also experienced a high decrease of the charge passed in the chloride penetration tests, thus influencing the measure of self-healing, as most of the recovery produced also was produced in the un-cracked specimens exposed to the test. The observed self-healing products were mostly calcium carbonate, with few silica content.

c) Crack closing

Jaroenratanapirom and Sahamitmongkol (2011) compared the visual closure behavior of several mineral additions: silica fume (SF), fly ash (FA), limestone powder (LP) and reference OPC in the same study, hence it can give a hint about their effectiveness. They also compared these additions with expansive agents and crystalline admixtures, but this will be further explained in section 2.4.3.2 as they are considered a type of autonomous healing. These authors analyzed the effect of pre-cracking age (3 and 28 days) and the effect of the crack opening (< 0.05 mm, 0.1-0.2 mm and 0.2-0.3 mm). Their results show that most types of mortars showed healing processes with different optimal conditions of pre-cracking age and crack width, even for OPC. Silica Fume had the best behaviors for older pre-cracks, and notably good for early cracks of 0.1-0.2 mm. Limestone powder had good results only for early and larger cracks. Nevertheless, Fly Ash was found to be ineffective to improve self-healing for most cases.

Olivier, et al. (2013) studied the self-healing effect in mortar with blast furnace slag cement with a 50% of replacement compared with Portland cement (CEMI 52.5N), when exposed 28 days and 42 days to underwater conditions. They compared optical 2D and 3D measures with tomography in order to evaluate the phenomenon, showing that OPC heals better for less than 25 days, but for longer healing times, BFS behaves better, mostly because of its delayed reaction. After 1 week of water exposure, more than 20% of the crack was sealed, and after 2 weeks, crack was not visible.

In fact, Sahmaran, et al. (2013) compared the self-healing enhancement by using type F and C Fly ashes² and Slag, in reference to the behavior of OPC. The fiber-reinforced concrete specimens were pre-cracked and exposed to three healing conditions: continuous wet, continuous air, and freeze–thaw cycle, for 2 months. Their results show that, although samples with fly ash had more unhydrated cementitious materials (so an expected higher capacity for self-healing), more self-healing precipitates were observed from the mixture incorporating slag, composed by calcite and C-S-H gels, in general, but for slag specimens, only calcite.

Huang, et al. (2014) investigated the enhancement on autogenous healing by replacing 66% of cement by blast furnace slag in pastes and activating it with a saturated calcium hydroxide solution has been investigated. In this case, the products were C-S-H gels (which represented the higher fraction), ettringite (whose presence was also important), hydrogarnet and OH-hydratalcite. The amounts of ettringite showed the leaching and recrystallization of SO_4^{2-} ions. The results suggested that unreacted blast furnace slag in the matrix contributes to self-healing of microcracks when activated by $\text{Ca}(\text{OH})_2$ solution. Fig. 2-19 shows the filling products inside cracks in comparison with the original limits of the crack.

² Class F Fly Ash contains less than 20% lime (CaO) while Class C Fly Ash generally contains more than 20% lime.

Huang, et al. (2014) used two main methods to compare the behavior, the filling fraction of microcracks (with openings up to 30 μm) or the air permeability. Both tests show a better behavior for slag cement paste when cured in $\text{Ca}(\text{OH})_2$, but it is noted more significantly according to the filling fraction (Fig. 2-20) than by air permeability, which could be caused by the permeability coefficient of the filling material.

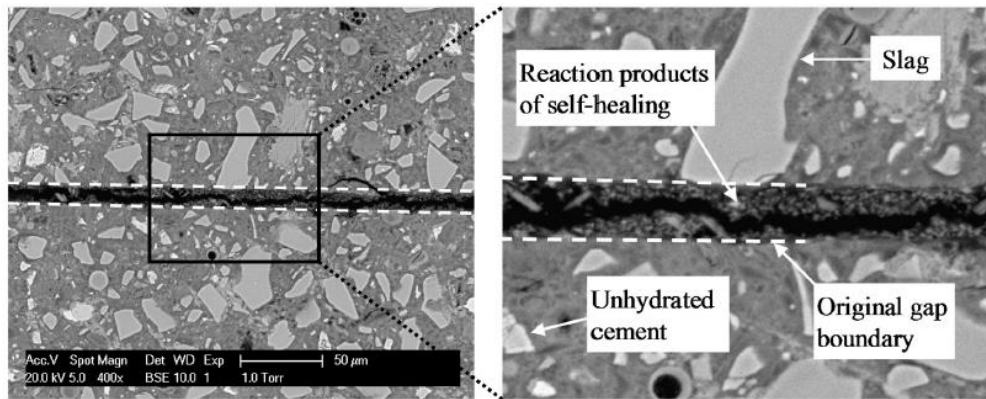


Fig. 2-19 – Morphology of products formed in gaps observed perpendicularly to slice surfaces. Healing starts at the age of 28 days of the specimens and healing time is 220 hours (Huang, et al., 2014).

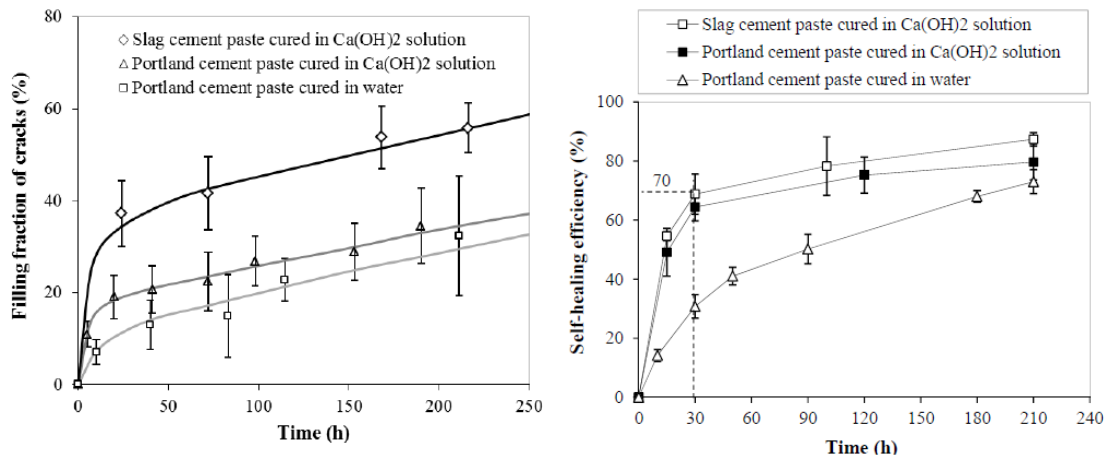


Fig. 2-20 – Comparison between the self-healing behavior of blast furnace slag and ordinary portland cement by measuring filling fraction of cracks (left) or by air permeability (right) (Huang, 2014).

2.3.5.3 Restricting crack width

Other way to improve the self-healing behavior of concrete elements is to restrict crack width, as smaller cracks heal better and in shorter time. There are two main methods to restrict crack width that have been analyzed in order to achieve self-healing: the use of fiber reinforced concrete and the application of compressive strength.

2.3.5.3.1 Fiber-Reinforced Concrete: SHCC+ECC

The use of fiber-reinforced concrete in order to improve autogenous healing is centered in two main types of concrete, which are subtypes of high performance fiber reinforced cementitious composites (HPFRCC): Strain-Hardening Cementitious Composites (SHCC) and Engineered Cementitious Composites (ECC). These materials have high volume of fibers, which permit the

tensional distribution and a ductile behavior, thus presenting multiple cracking with very small cracks ($< 0.05\text{-}0.07\text{ mm}$). Moreover, not only they act as crack restrictions, but they also produce bridging of cracks, which could be precipitation nuclei with different capabilities depending on the fiber composition. Therefore, they were thought as a type of concrete of a high self-healing potential.

The results from Lawler, et al. (2003) show the relation between water flow rate and displacement in fiber-reinforced mortar specimens depending on the type of reinforcement. These results are significant to the healing studies since the measure of water flow for cracked specimens is the methodology of the highest focus in this document. In that research, Lawler, et al. compared the behavior for three types of fiber (long steel, short steel and polyvinyl) combined in different percentages. Their results demonstrate the effect of the fibers type and volume on the flow rate on cracked specimens, since higher volume of fibers and the combination of macro steel fibers and PVA fibers (both added at 0.5% by volume) achieved the lowest water flows (Fig. 2-21).

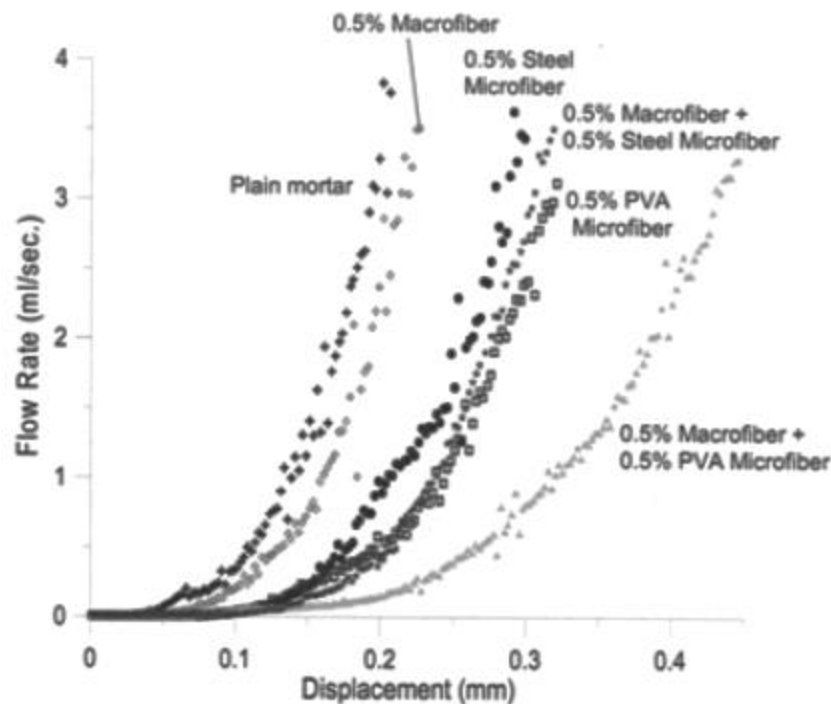


Fig. 2-21 - Direct measurement of permeability for cracked concrete specimens (Lawler, et al., 2003).

In this direction, Desmetre and Charron compared the behavior of normal strength concrete (w/c ratio of 0.6) and fiber-reinforced concrete (with silica fume, w/b = 0.43), showing that autogenous healing overcame the crack propagation effect in fiber-reinforced concrete the, which did not occurred in normal strength concrete (Desmetre, 2011; Desmetre & Charron, 2012). Fig. 2-22 shows the different evolution of permeability-measured healing for the two types of concrete, proving the benefits of FRC in order to achieve better durability on concrete structures due to the thinner and rougher cracks.

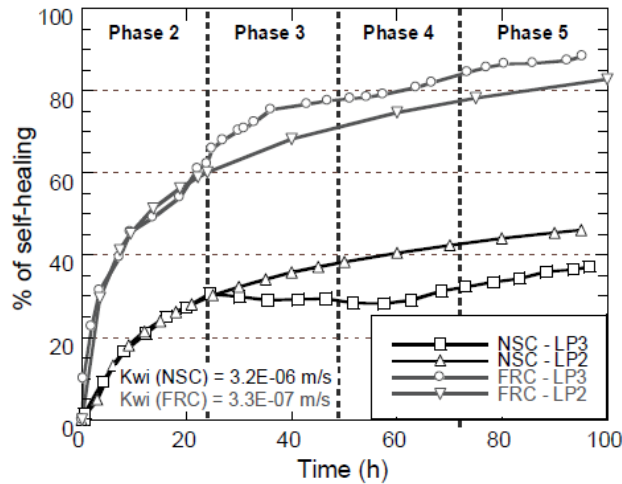


Fig. 2-22 – Evolution of permeability-measured self-healing under constant loading (LP2) and cyclic loading (LP3) for NSC and FRC specimens (Desmettre & Charron, 2012).

In the Japanese group from Tohoku University the focus was made in which type of fiber enhanced more effectively the self-healing phenomena. Homma, et al. (2009) compared polyethylene (PE), steel cord (SC) fibers and a composition of both types. Their results showed a better behavior of polyethylene fibers, as they bridged the cracks more efficiently and crystallization products were attached easily to the fibers. In fact, the mean thickness of the precipitates was higher when using PE fibers, and lowest with SC fibers. The precipitates formed inside the crack were mostly calcium carbonate.

Later, they compared the performance of two types of polyvinyl alcohol (PVA-I and PVA-II), ethylene vinyl alcohol (EVOH), polyacetal (POM) and two polypropylene (PP and C-PP) fibers with similar procedures (Nishiwaki, et al., 2012). When measuring the permeability of pre-cracked specimens, those with PP and EVOH fibers did not present a permeability decrease after healing under water, while the rest of types of fibers (including C-PP) had a significant decrease. However, the only type of fiber that allowed a recovery of permeability coefficient values to that of uncracked specimens, were PVA fibers. By 14 days of healing exposure 0.3 mm cracks were visually closed, except for the PP fibers. However, permeability tests showed that most of the specimens were reacting even at 20-30 days of exposure.

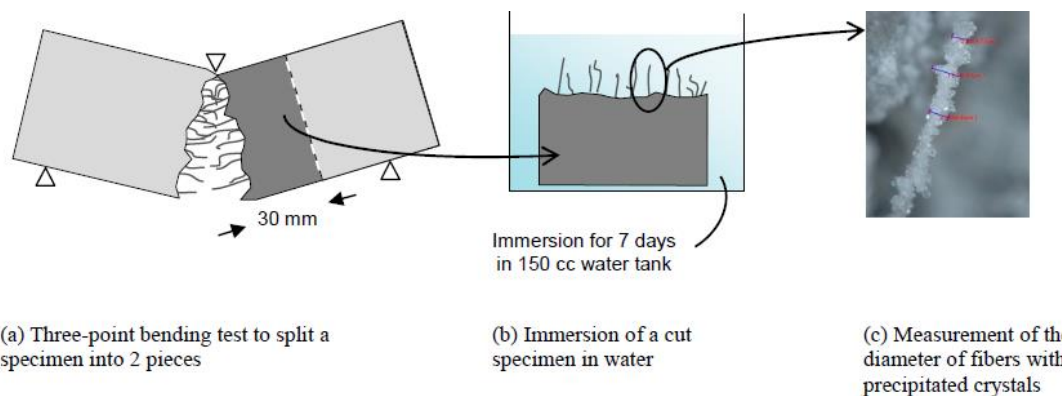


Fig. 2-23 – Methodology followed to measure the thickness of the precipitates (Nishiwaki, et al., 2012).

They also measured the thickness of the crystal precipitates in the different types of fibers, in one concrete surface, in order to measure their potential healing effect, as shown in Fig. 2-23, achieving better results for PVA fibers. This is thought to be caused by their higher polarity strength owing to the OH radical, thus enhancing the precipitation of CaCO_3 (Nishiwaki, et al., 2014). When comparing the recovery ratio of watertightness (lower values mean higher permeability reduction), it can be seen that SC and PE fibers had higher dispersion, EVOH had the worst ratios, while PVA had the best (see Fig. 2-24). They also compared the recovery of energy absorption from first loading and loading after self-healing, which was calculated as the area under the tensile-elongation curve up to a fixed elongation. Their results were similar in the case of PVA fibers, with recoveries around 80-110%, but for the combination of SC+PE the results were quite good (around 80-105%) despite the fact that their cracks were not healed.

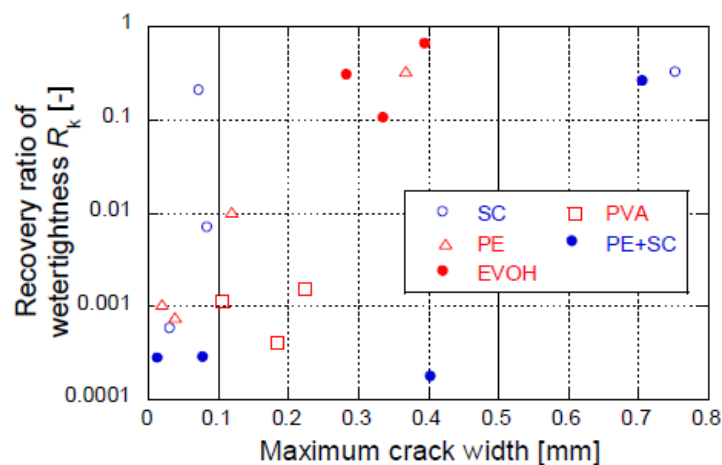


Fig. 2-24 – Relationship between maximum crack width and the recovery ratio (Nishiwaki, et al., 2014).

In a related research, Snoeck & de Belie (2012) analyzed the self-healing properties of cementitious composites reinforced with flax and cottonised flax in order to compare with PVA fibers. According to their results, the self-healing of cracks after exposing specimens to wet/dry cycles, was independent of the fiber type: cracks smaller than 0.03 mm healed completely but cracks around 0.15 mm only partly healed.

The group of V. Li in Michigan studied the enhanced autogenous healing properties for ECC containing Fly Ash and PVA fibers pre-cracked at the age of 6 months, under five different healing exposures (Ying-zi, et al., 2005; Yang, et al., 2011). CR1 and CR2 were two exposures consisting on cycles of water immersion and drying, CR4 was water immersion, and finally CR3 and CR5 were two regimes with different moist conditions. Neither CR3 nor CR5 got significant healing measuring by resonant frequency, confirming the need of direct contact with water. Because of that, only CR4 was compared in terms of recovery of tensile stiffness to the two exposures with cycles (Yang, et al., 2011). Their results show that for small preload tensile strain, the three exposures achieved recoveries higher than 80%, and cycles around 100%, while for moderately damaged specimens the differences between these exposures were not as clear. After

20 days of exposure, the achieved recoveries of resonant frequency were around 87-100% for the exposure CR1 while 77-90% for CR2. Their results showed that self-healing is possible and healed cracks could be of an enough strength (see Fig. 2-25). However when testing to tensile load and comparing the pre-cracking curve with re-loading after healing, their final stiffness were hardly recovered (Yang, et al., 2009). The maximum load was generally recovered but this could be caused by the ECC behavior, with high volumes of fibers.

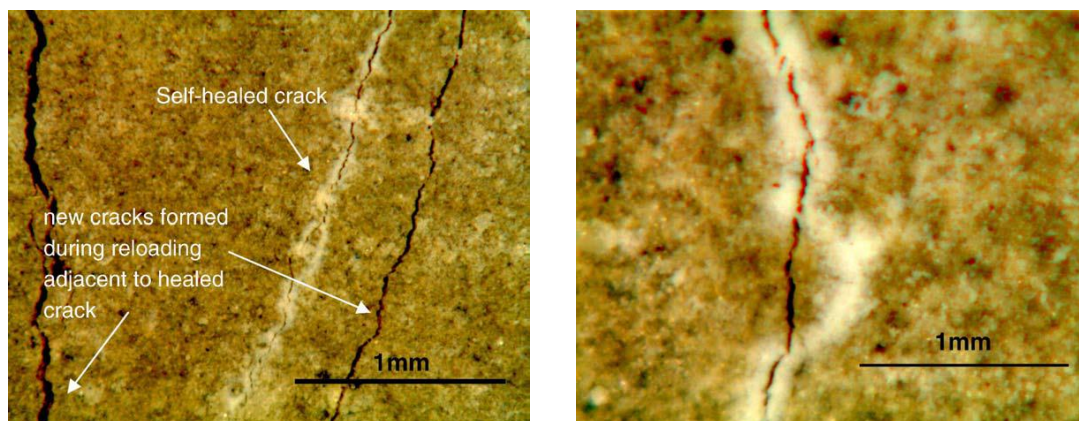


Fig. 2-25 – New crack paths and old healed cracks (with white precipitates) (Yang, et al., 2009).

Later, they also divided the resonant frequency (RF) recovery ratios depending on the crack width of a single crack, before conditioning and after healing with wet-dry cycles. Crack with openings under 0.05 mm heal completely while cracks larger than 0.15 mm showed no recovery regarding to the RF measurements (Yang, et al., 2009).

Later on, Herbert & Li (2013) analyzed if ECC was able to heal under real conditions. In their study, concrete specimens were exposed to environmental conditions in Ann Arbor in Michigan for 12 months, being exposed to a range of temperatures of -11.7 to 32.8°C. They concluded that specimens under a natural exposure could heal; and also that cyclic loading could deteriorate the stiffness recovery, but specimens were still able to heal a certain percentage of the damage.

Qian, et al (2009) analyzed the self-healing behavior of SHCC (similar to the ECC, with fly ash and PVA fibers) incorporating blast furnace slag and limestone powder, in a relatively high water/binder ratio (0.31 to 0.60). Their results show that water curing had always better results than air curing, with recoveries of the deflection capacity about 65-105% in the case of water curing and 40-60% for the latter. The smaller crack widths and low water/binder ratio enhanced the self-healing reactions. In their study, cracks up to 30 μm width were completely healed, but cracks with relatively large width (around 60 μm) showed only partial healing, as shown in Fig. 2-26. This suggests that small crack widths are preferable, since less healing products are needed to fill the crack and it is easier for the products to grow and bridge the crack.

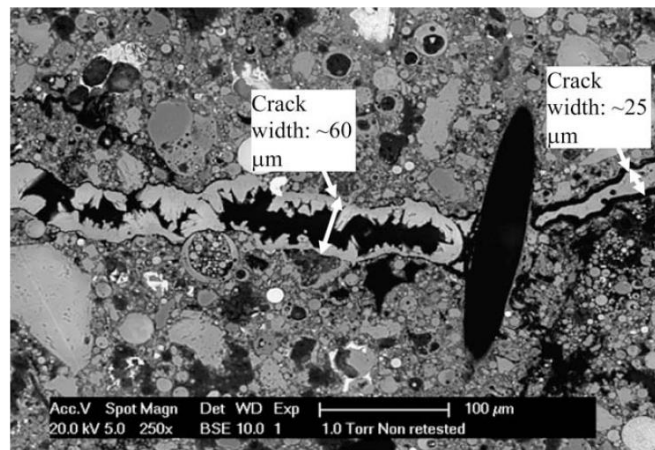


Fig. 2-26 – Partial crack healing after water curing (Qian, et al., 2009).

Recently, in the same direction, Ma, et al. (2014) analyzed the autogenous healing of medium-early-strength ECC for different pre-damage levels and different exposures. According to their results, faster self-healing occurred in the healing condition of water/air cycle but the higher stiffness recovery was achieved combining cycles with different moist contents. Also increasing the pre-loading damage worsened the healing results. The self-healing product were a mixed system consisting of C-S-H and CaCO_3 with predominance of calcite.

Kim, et al. (2014) compared the mechanical behavior of HPSFRC mainly with very small cracks (20 μm) with the standard curve (averaged from at least three specimens) for two exposures: in water or air. Their results show that healing in water could increase stiffness and load recovery in comparison to healing in air (Fig. 2-27). Stiffness at reloading were lower than original stiffness, but it was slightly improved for specimens healed 14 days underwater. The maximum load for specimens healed in water was even higher than for the standard curve. Smaller cracks (< 50 μm) healed completely while medium cracks (around 0.2 mm) remained opened after 28 days of water immersion.

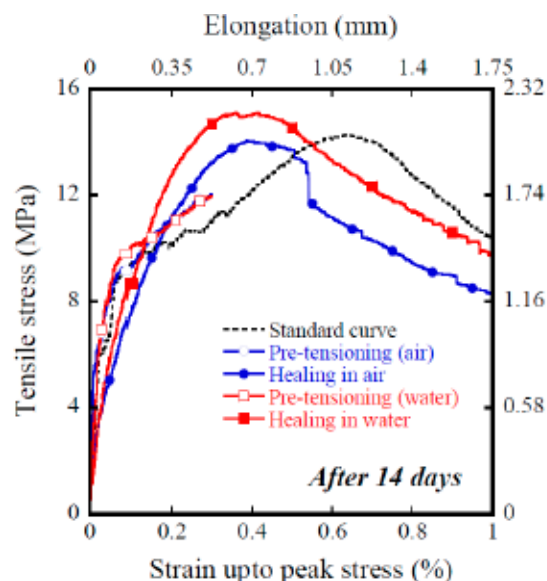


Fig. 2-27 - Tensile stress–strain curve of HPFRCCs after 14 days of healing (Kim, et al., 2014).

2.3.5.3.2 Application of compressive strength

Ter Heide (2005) studied early age cracks and the effect of applying a compressive strength while healing, as it could bring the two crack faces closer. Three-point bending test was used for pre-cracking the specimens to crack widths of 50 μm (before unloading), and also to analyze the strength regain after healing. The main healing parameter studied was the compressive stress applied during healing, by means of a special device designed for this purpose. Her results show that the application of a compressive strength during the healing time improved autogenous healing (Fig. 2-28).

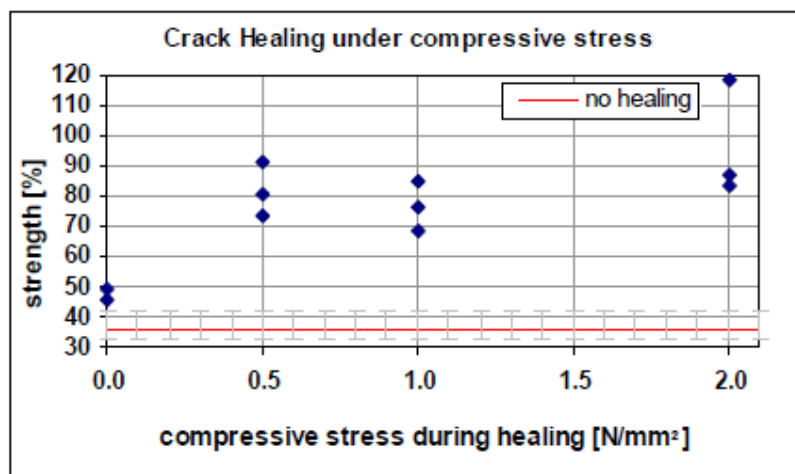


Fig. 2-28 - Influence of compressive strength on healing (ter Heide, 2005).

Parant, et al. (2007) measured a quasi-total recovery of initial stiffness under service load and in the presence of chloride water. The specimens they studied were multiscale fiber-reinforced cement composites (MSFRCC) and were exposed to wet/dry of a chloride solution cycles for 210 days, combining a creep set up with a corrosion inducing storage. They created micro-cracks to the specimens by bending stress and applied fatigue cycles to degrade the bond fiber-matrix. They stored their specimens in four types of environment: highly exposed to corrosion, exposed to flexural creep stress, a combination of both damages and reference exposure, at laboratory conditions. All groups had higher maximum load than reference specimens did and, in the case of the combination of both damages, even the same initial stiffness was reached. The gain of flexural strength is explained here by the positive effect of some fatigue cycles at moderate rate of loading. Micro-cracks were partially or even completely closed.

Also Desmettre (2011) measured the self-healing behavior after 6 days of constant loading, time in which, self-healing had reduced water penetration by 50% and 70% in the NSC and FRC specimens, respectively. She also quantified the stress enhancement needed to reach the initial permeability coefficient for both types of concrete, which was 20-35 MPa for the NSC tie specimens, whereas 40-60 MPa was required for the FRC tie specimens.

Instead of applying compressive strength as an external action, the use of shape memory materials (SMM) has been analyzed to this purpose. Shape memory materials have the property of recovering a shape that was stored in their “memory” under certain conditions. The concept of the use of SMM in order to improve autogenous healing is, to add them in a concept similar to prestressed bars: to apply the activator when a crack appears, thus initiating the shrinkage of the SMM which compresses the specimen.

Jefferson, et al. (2010) used shrinkable polymer tendons, pre-oriented in cementitious beams to this purpose. The tendons were activated thermally thus putting the specimens into a state of axial compression (Fig. 2-29); they proved their capability for closing macro-cracks and enhancing autogenous healing. The effective applied compressive stress was between 1.5 and 2 MPa. They also compared the curing effect and obtained that the combined effect of heating and increasing curing from four days to eight improves the strength of the mortar by approximately 25%.

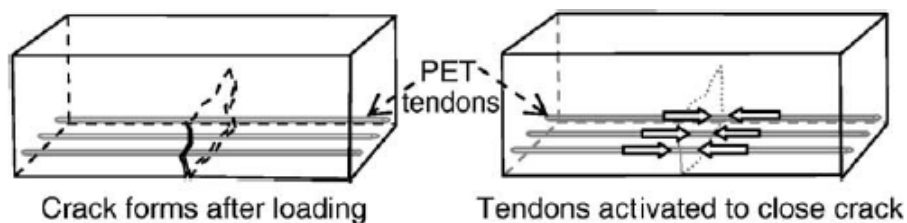


Fig. 2-29 – Concept of shape memory tendons (Jefferson, et al., 2010).

2.3.6 Summary of autogenous healing

Some ideas that have been seen through this section about autogenous healing are:

- It is mostly due to carbonation, though continuing hydration can also affect it.
- High dependence on: age of pre-cracking, crack width and exposure.
- Low dependence on: water/cement ratio and cement content (for traditional dosages of concrete), type of aggregates and type of filler.
- It heal cracks up to 0.05 or up to 0.3 mm depending on the studies. Smaller cracks seem to heal more completely than wide cracks for a specified time but there is a threshold, a critical damage that has to be reached.
- Younger concretes in general heal better than older elements due to the lower degree of hydration.
- The presence of water is essential for all mentioned mechanisms not being enough a high relative humidity (as 95%) for autogenous healing. Dry concrete does not heal. The time in water after damage; the longer the storage time, the more effective the healing.
- Water immersion or wet/dry cycles are the best exposures.
- Most part of the reaction takes place in the first two weeks of exposure.

As it has been explained, different mixture compositions could enhance autogenous healing properties. Despite the lack of consensus for most methods, it can be said that:

- a. Increasing cement content will not necessarily lead to an increase of autogenous healing, but high performance concretes in general are thought to have better healing response.
- b. Different traditional mineral products can affect in different ways. In general, and always comparing with OPC:
 - i. Blast Furnace Slag has lower autogenous healing effect for some authors, and higher for others when the content is around 30-50% by the weight of cement.
 - ii. Fly Ash, some authors say they can improve the autogenous healing effect in contents about 15-25% by cement weight, while others needed 30-40%.
 - iii. Silica fume and limestone powder, have been registered as potential enhancers as well.
- c. Restricting crack width is the most effective way to enhance autogenous healing.

This variability and difficulty to guarantee the autogenous healing effect inspired the design of new engineered healing methods.

2.4 Autonomous healing

2.4.1 Types and classification

Due to the lack of feasibility for autogenous healing, several methods for achieving an engineered self-healing have been designed, which are generally named as “autonomous healing” methods. In general, they are composed of a healing agent that reacts with a catalyst, which can be part of the concrete matrix or an additional product. The way of introducing the healing agent and the catalyst also determines different methodologies. The known options up to the date are displayed in Fig. 2-30.

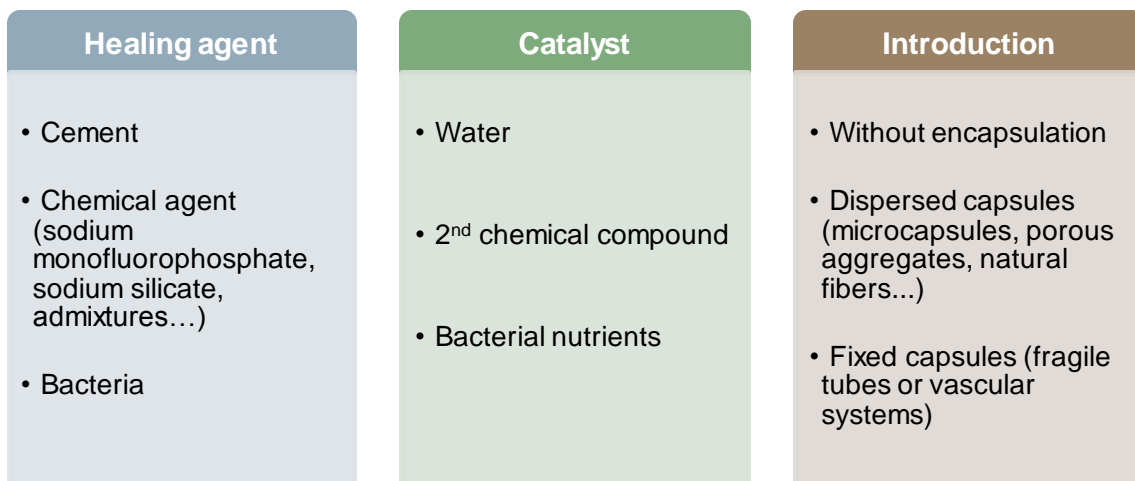


Fig. 2-30 – Types of the three compounds: healing agent, catalyst and introduction method.

Whatever the autonomous healing method, in general four features are needed: 1) detection of the damage, 2) reaction of the agent with the catalyst, 3) transport of the reaction products, and 4) filling of the damage. That is, the healing method must detect the crack when it appears and activate the healing mechanisms, transporting the filling materials to the damaged area.

The healing agent can be introduced as an additional product to the mix process without an encapsulation or protection or can remain inside a capsule until the healing activates it. The main disadvantage of not encapsulating a product is possibility of the consumption of healing potential during mixing or hydration, which will not be available in hypothetical future healing processes. The types of encapsulation can be gathered in two groups: disperse capsules (mostly microcapsules) and located capsules (mostly glass tubes). The first group is thought to be added to the concrete matrix and is a good method for unpredictable or dispersed cracking; while the second needs to be placed in a specific location in a similar way to reinforcement bars, thus being optimal for predictable cracks. These methods need a physical breakage or an increase of the porosity to be activated.

This section has been organized depending on the healing agent and the introduction method inside concrete matrix.

2.4.2 Cement as healing agent

2.4.2.1 Concepts

Cement as healing agent is the continuing hydration effect, having water as the catalyst, which has been explained in Section 2.3. The amount of unhydrated cement stored in order to react at the moment of cracking is an important parameter in order to improve the recovery of properties.

2.4.2.2 Without encapsulation (autogenous healing)

The addition of cement without encapsulation is the ordinary autogenous healing by continuing hydration.

2.4.2.3 Encapsulation of the catalyst (water)

To the knowledge of the author, there are no studies based on the encapsulation of cement. The encapsulation of the catalyst (water) has been of a wide interest, though. Water is fundamental for the hydration of cement. It reacts and goes out of cement matrix because of the physicochemical processes that take place. Two main types of encapsulation of water have been investigated: superabsorbent polymers and natural fibers.

2.4.2.3.1 Superabsorbent polymers

Superabsorbent polymers (SAP) are polymers, generally made of polyacrylic acid cross-linked, also known as hydrogels or water crystals. SAP are hydrophilic, thus they have a high affinity

with water. They have the capability of absorbing huge volumes of water and aqueous solutions, but this capability decreases dramatically when water presents dissolved ions. With pure water, SAP could absorb 100 grams by each gram of SAP, meaning an increase of volume of 100 times the initial volume. In contrast, this absorption could decrease up to 20 grams for impure water. SAP (Imperial College London, 2012).

SAP are used as shrinkage compensators in concrete. When introduced in the concrete matrix they absorb water during the mixing process and releasing it slowly afterwards, while the concrete is drying. This process applied to the design of self-healing concrete is (see also Fig. 2-31):

- i. SAPs are introduced during mixing of concrete
- ii. Concrete suffers a crack in a random location
- iii. SAPs enter in contact with humidity and environmental water, and are filled with it
- iv. SAPs expand and fill pores and parts of the crack, blocking the entrance of contaminants
- v. The slow leaching of water enhances the autogenous healing by continuing hydration or carbonation

The influence of SAPs on the strength of concrete is of a major concern, as they could decrease it just by their addition or because of the frequent additional water that is needed in order to maintain the workability.

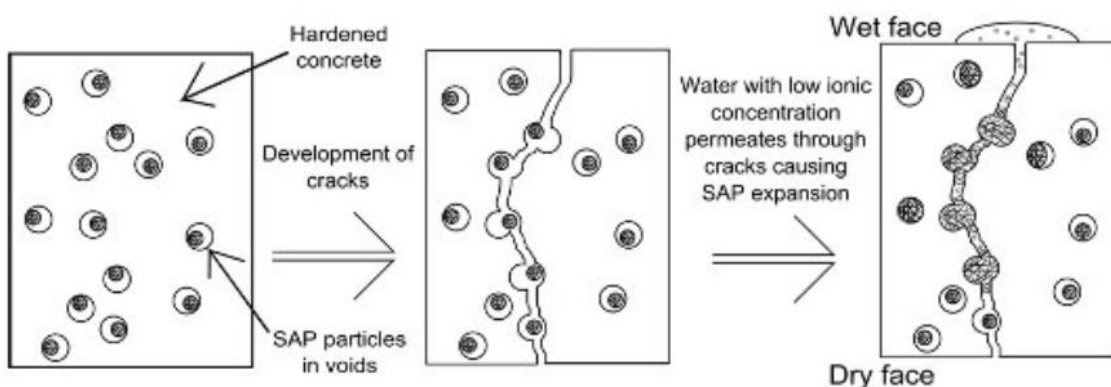


Fig. 2-31 – Mechanism of superabsorbent polymers (Imperial College London, 2012).

Kim & Schlangen (2011) studied this effect in PVA fiber-reinforced mortars with different contents of SAPs. They pre-cracked the specimens at the age of 7 and 28 days and compared the load recovery after 28 days of healing in four exposures: air, water immersion and two types of wet/dry cycles. Their results showed that only water immersion (W) and one of the types of cycles (C) achieved strength improvements after the self-healing process (Fig. 2-32). Reference specimens, without SAPs, (G1) achieved recoveries underwater but negative recoveries under wet/dry exposure, while SAPs specimens (G2 and G3 with increasing contents) achieved notable results in the wet/dry exposure. This indicates the water-pocket effect and the need of direct contact with water when using SAPs.

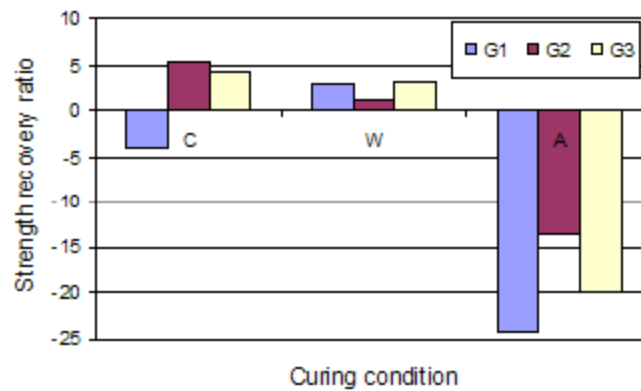


Fig. 2-32 – Development of strength recovery ratio with curing condition with pre-cracking time of 7 days: C cured at cycles, W water immersion, A air conditions (Kim & Schlagen, 2011).

Recent studies (Snoeck, et al., 2013; 2014) compared the self-healing efficiency of adding SAPs to a PVA fiber-reinforced mortar with fly ash. They studied small cracks, around 50 μm with wet/dry cycles (w/d) and exposures with different rates of relative humidity (90% and 60%). Their results show that specimens with SAPs achieved higher recoveries for mechanical properties, being around 80-90% while reference specimens only achieved recoveries around 40-50% (Fig. 2-33). Reference specimens achieved the lower recoveries for flexural strength, while specimens 1B with the higher content of SAPs got the best recovery rates. The healing products were mainly calcium carbonate but also hydration by-products.

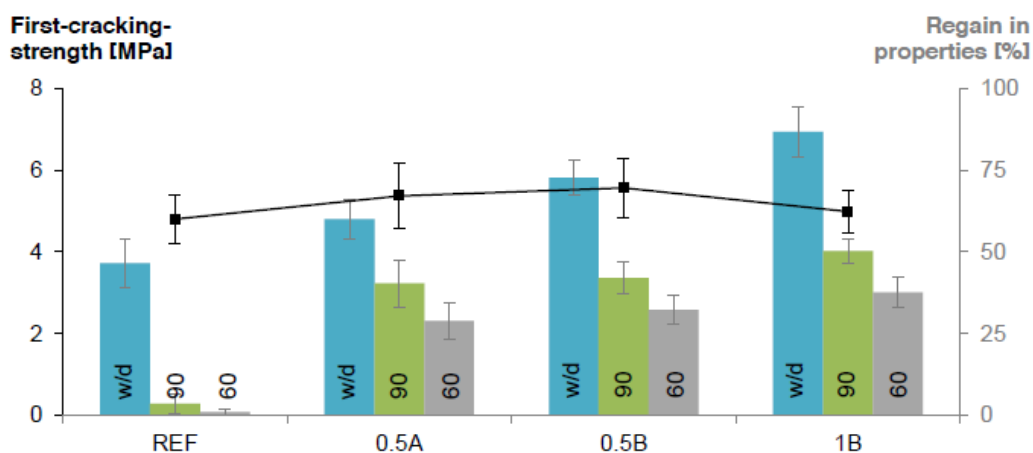


Fig. 2-33 - First crack strength (black lines with square symbols) and recovery of properties (bars) for different exposures: wet/dry (w/d), >90% of relative humidity (90) and 60% of RH (60) (Snoeck, et al., 2013).

2.4.2.3.2 Natural fibers

In a similar strategy, the use of porous natural fibers (coconut and sisal) as water reservoirs have been studied by Toledo Filho, et al. (2005). Specimens were pre-cracked by free and restrained shrinkage and were stored 40 days under water immersion at 22°C afterwards. Specimens with sisal fibers achieved complete healing of cracks under 0.3 mm while coconut fibers only achieved a reduction from 0.2 mm to 0.05 mm width, but the process is quicker in the specimens with coconut fibers, as it can be seen in Fig. 2-34.

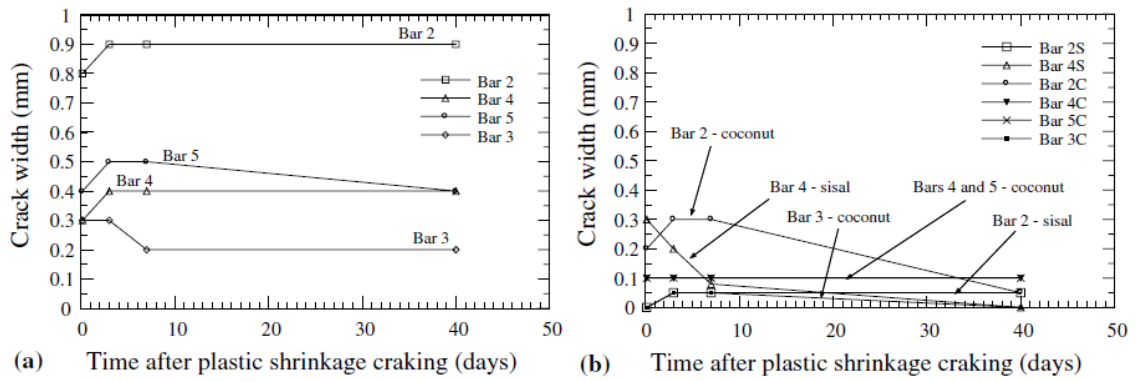


Fig. 2-34 – Evolution of crack width for specimens without natural fibers (left) and with sisal and coconut fibers (right) (Toledo Filho, et al., 2005).

2.4.2.3.3 Other methods for water encapsulation

Qian, et al. (2010) compared that behaviors with mixtures incorporating nanoclay, which was introduced as an additional water supplier, and comparing the exposures of water immersion, air conditions, carbon dioxide cured and wet/dry cycles. They studied the percentage of final cracks that occurred at new locations, instead of re-opening old cracks that should be healed. Their results for mixtures with nanoclay show that the only exposure that had no healing at all was curing at air conditions, demonstrating the need of the water for healing. According to their results, the older the pre-cracking time the higher healing of cracks was produced. It is worth noticing that the addition of nanoclay as internal water supply had no discernible effect to achieve healing effects for air-cured specimens.

2.4.3 Chemical powder or solution as healing agent

2.4.3.1 Concepts

The healing agent can be a different product from any of the matrix compounds. In this group, several types of healing agent can be found, such as mineral powder with chemical actives or different types of adhesives, but they should have a good compatibility with ordinary concrete matrix compounds. Those agents can be added with or without encapsulation to protect them until the moment they are required to act.

2.4.3.2 Without encapsulation (self-healing admixtures)

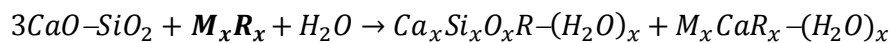
In the group of chemical products able to produce self-healing without encapsulation, there are two types of concrete admixtures: crystalline admixtures and expansive admixtures. The disadvantages of these products is the possibility of consumption of the healing capability before a crack occurrence, as they are not encapsulated. They are thought to store a certain capability in order to heal older age cracks, but their performance is still being studied.

2.4.3.2.1 Crystalline Admixtures

Crystalline admixtures (CA) are a special type of permeability reducer admixtures (PRAs) as reported by the ACI Committee 212 (2010). In contrast to water-repellent or hydrophobic products, these materials are hydrophilic, and this makes them react easily with water. According to that report, when this reaction takes place, it forms water insoluble pore/crack blocking precipitates that increase the density of Calcium Silicate Hydrate (C-S-H) and the resistance to water penetration. The matrix component that would react is the tricalcium silicate (C_3S) and water presence would also be needed. On the contrary, other studies indicate that CA react with portlandite instead of tricalcium silicate (Sisomphon, et al., 2012).

In general, these products are formed by active chemicals contained in cement and sand, which form modified C-S-H, depending on the crystalline promoter, and a precipitate formed from calcium and water molecules. Crystalline deposits become part of the matrix, unlike hydrophobic materials, thus being able to resist pressures as high as 14 bars.

The general reaction described in the ACI report is:



(tricalcium silicate + **crystalline promoter** + water \rightarrow modified calcium silicate hydrate + pore-blocking precipitate)

When comparing the other types of PRAs with CA to improve permeability (see Fig. 2-35), CA showed to be more effective than colloidal silica and pore-blocking admixtures (ACI Committee 212, 2010). Their possibilities as durability enhancers were also demonstrated by (Yodmalai, 2011), but their effect as self-healing agents need further development.

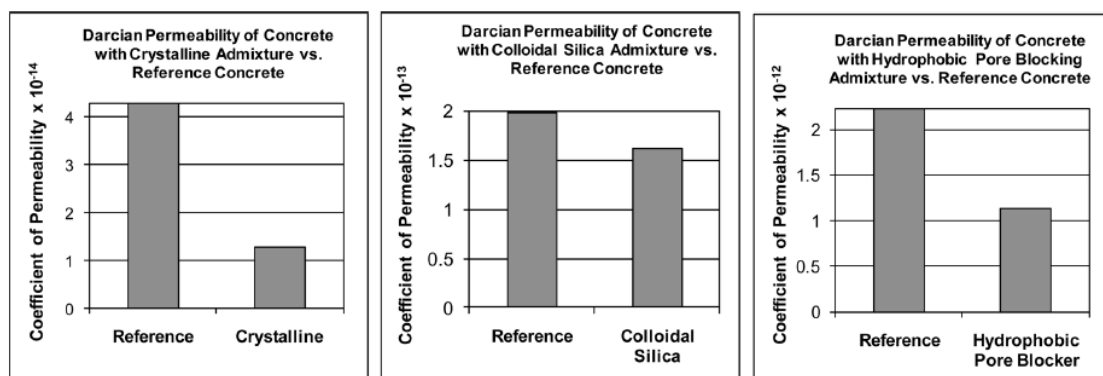


Fig. 2-35 - Comparison of the effectiveness reducing permeability between different PRAs (ACI Committee 212, 2010).

The studies from Jaroenratanapirom & Sahamitmongkol (2011) compared the visual closure for different additions and admixtures, including crystalline admixtures. CA showed their best results for visual closure of cracks for small and early age cracks (< 0.1 mm and 3 days) but they were ineffective for larger cracks (around 0.3 mm) in comparison to OPC mortars.

Similar results were achieved by Sisomphon, et al. (2012), who obtained the as limits of the self-healing capability of crystalline admixture for cracks widths of 150 microns (for 30 days of water immersion), as it can be seen in Fig. 2-36.

Later on, the effect of adding CA in a dosage of 1% by the weight of cement on the strength recovery of ultra-high performance concrete was studied by Ferrara, et al. (2014). They stored the pre-cracked specimens in wet/dry cycles simulating real Italian climate during 4 weeks. The initial pre-cracks were 130 and 270 μm . Reference specimens were healed up to 70% while concrete with CA achieved recoveries around 80% of crack width, thus the addition of CA improved a 14% the self-healing properties of concrete.

This work studies the behavior of crystalline admixtures without encapsulation for the self-healing of concrete specimens.

2.4.3.2.2 Expansive Admixtures

This type of admixtures are used as shrinkage compensators and they are usually designed as EA or as CSA as they are usually composed of calcium sulfoaluminates. They contain calcium hydroxide $\text{Ca}(\text{OH})_2$ and anhydrite CaSO_4 , thus the by-products of the healing reaction are highly compatible with the concrete matrix. However, this process could take place at long term, producing additional stress that could damage concrete because of the secondary formation of ettringite.

In the visual closure studies by Jaroenratanapirom & Sahamitmongkol (2011), they included expansive admixtures. EA showed good behavior for early age and larger cracks (0.1-0.3 mm), but they did not stand out in other situations.

Sisomphon, et al. (2011; 2012) compared the visual closing of mortar specimens incorporating two CSA expansive admixtures, a CA admixture and a combination of an expansive admixture and a crystalline admixture. They pre-cracked the specimens at the age of 28 days and the chosen healing exposure was water immersion. The methodologies used to quantify self-healing were crack closing and decrease of the permeability of cracked specimens. Their results showed that the combination of both agents (10% of CSA and 1.5% of CA by the weight of cement) was the optimal mixture for achieving better healing results (Fig. 2-36). They also obtained that for specimens without admixtures only cracks up to 0.1 mm are able to heal within 28 days of water immersion. On the contrary, specimens with these admixtures could heal cracks up to 0.4 mm within 28 days.

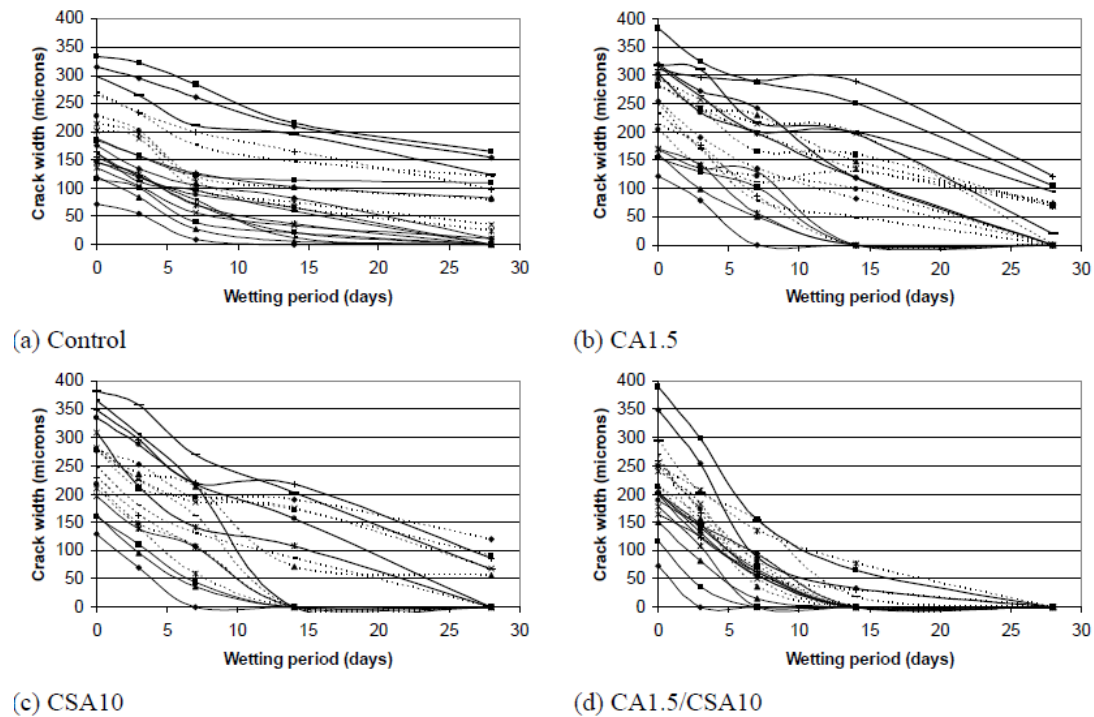


Fig. 2-36 – Crack width reduction for each mix group (Sisomphon & Copuroglu, 2011).

Later on, Sisomphon, et al. (2013) compared the recovery of flexural stiffness and flexural strength for those mixtures in four healing conditions: water immersion in tap water, water immersion in tap water with replacements every 12 hours, wet/dry cycles combining water immersion and drying, 12 hours each cycle and indoor air. The pre-cracking age was 28 days again and the healing time 28 days, as well. Their results showed that specimens under wet/dry cycles achieved the highest recoveries of flexural stiffness and flexural strength, with similar results for reference concrete and those with the admixtures, while specimens at indoor air achieved the lowest. In the case of the recovery of flexural stiffness, results after healing were always lower than virgin stiffness, while regarding the recovery of strength, groups under wet/dry cycles achieved higher final values. With small differences, the mixture with the combination of both admixtures achieved better results than the rest of mixtures.

Ahn & Kishi, (2010) designed a self-healing agent combining three terms: the expansion term given by expansive admixtures (hauyne, anhydrite and free lime), the swelling term given by geopolymers (silica and alumina) and the precipitated term given by chemical agents (including several carbonates: NaHCO_3 , Na_2CO_3 y Li_2CO_3). They looked for a more effective healing promoter with the use of the three compounds. They pre-cracked their specimens to crack widths between 0.1 and 0.3 mm. They concluded that the addition of expansive admixtures was not enough to seal cracks, and that adding the rest of the compounds stabilized and quickened the healing process. With the optimal combination, concrete heals notably 0.15 mm cracks in 3 days and 0.2 mm cracks in 7 days with a complete healing after healing for 28 days under water immersion. The healing products formed by this agent were mostly fibrous C-A-H phases

(hydrogarnet) and calcite (Fig. 2-37). Fibrous phases were formed by the chemical agents and had a great role for bridging cracks.

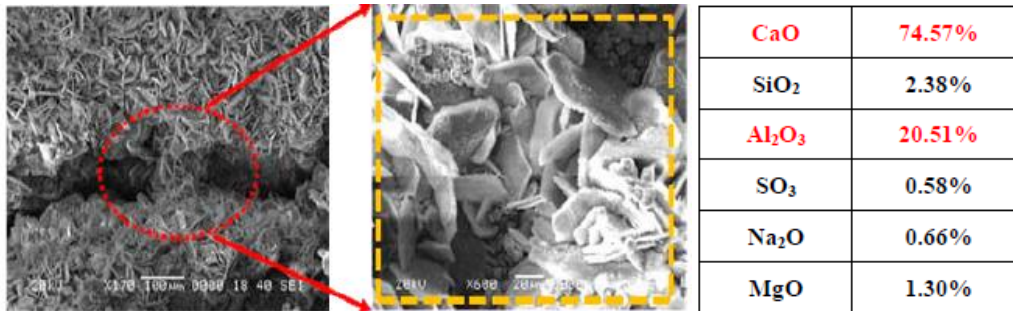


Fig. 2-37 – Self-healing products in a crack, including C-A-H and CaCO₃ (Ahn & Kishi, 2010).

2.4.3.3 Located encapsulation

A different point of view is the introduction of fragile capsules in located positions. These capsules would be activated by cracking in specific locations.

Dry started these designs in the early-mid 90s. She used a design that needed external action, in which methyl methacrylate was used as healing agent, which polymerizes by the action of heat, filling cracks and reducing permeability (Dry, 1994). She also experimented with a passive design that did not require external action. In this case, a three-compound system was used, with methyl methacrylate and one of the initiator in one glass tube and the other initiator inside the contiguous glass tube. When cracks appeared in concrete, glass were broken mechanically, thus releasing the two products, which reacted and filled the cracks. In only one hour, the products set and permit a recovery of strength (Dry & McMillan, 1996). Later, she experimented these systems in true scale models of a bridge deck (Fig. 2-38). The experimental results confirmed the feasibility of this system in order to heal cracks autonomously (Dry, 2000).



Fig. 2-38 – Glass tubes in a bridge deck (Dry, 2000).

Later, this system with glass tubes containing fast air curing superglue of low viscosity has been combined with strain-hardening fiber-reinforced concrete in order to verify its behavior under cyclic loading (Li, et al., 1998). The elastic modulus was found to regain its original value in a repeated loading, supporting this concept for achieving self-healing concrete.

Other authors tried similar designs, embedding ethyl cyanoacrylate in hollow fibers of diameter of 4 mm and 20 cm length (Sun, et al., 2011). They studied cracks of different widths, but only achieved strength recoveries up to 20%.

Tittelboom, et al. (2011) compared the behavior of glass and ceramic tubes with a two-compound system with methyl methacrylate. The pre-cracked up to 0.3 mm mortar cylinders, which contained the tubes inside their matrix, as shown in Fig. 2-39. When the healing agents reacted and filled cracks, the achieved permeability was similar to that of virgin specimens, which is an indicator of the good behavior of this method. Their results show a better behavior for ceramic tubes in comparison to glass tubes.

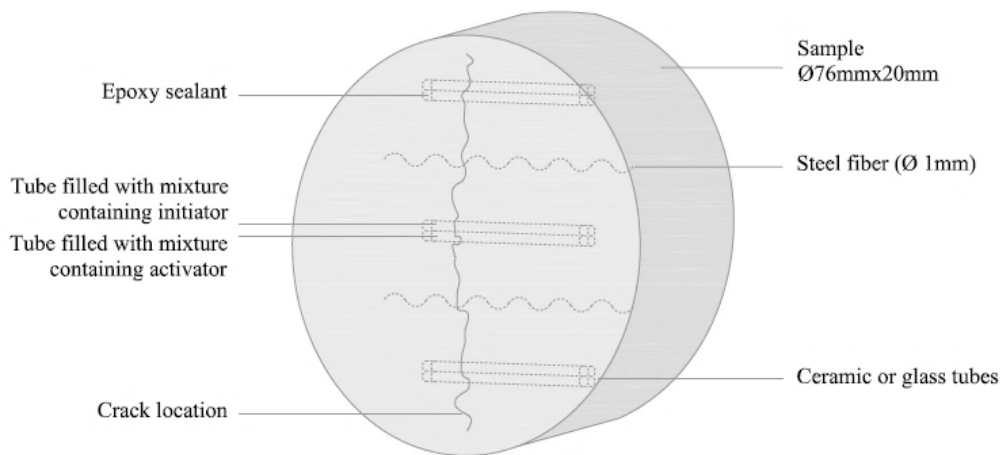


Fig. 2-39 – Mortar cylinders with embedded tubes (van Tittelboom, et al., 2011).

Later they embedded ceramic tubes with a polyurethane pre-polymer and a catalyzer in mortar prisms, which were then embedded in concrete beams. In this way, mortar prisms were a capsule protecting the self-healing encapsulated agent (van Tittelboom, et al., 2012). The load-crack width graphs showed the recovery of mechanical properties that were achieved due to the healing mechanism. Reference specimens did not recover stiffness or load, while self-healed specimens recovered both, with an almost 100% of recovery (see Fig. 2-40).

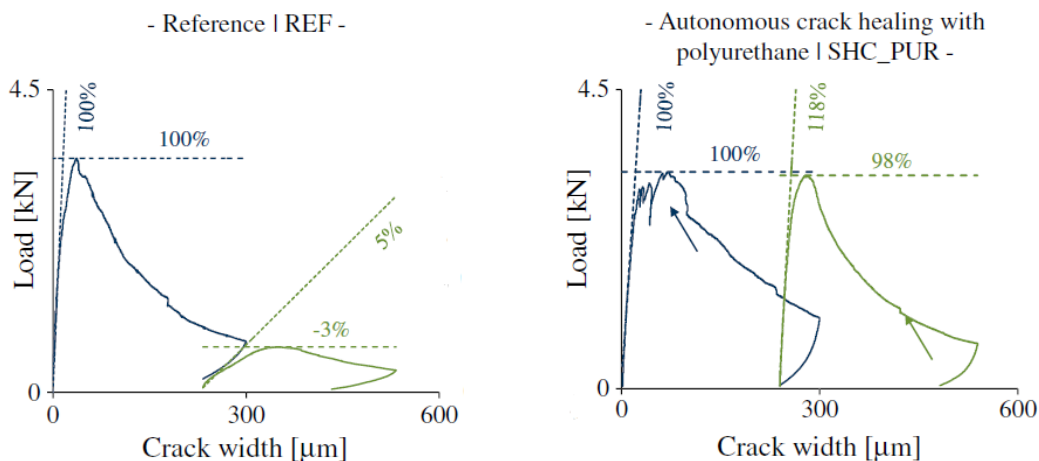


Fig. 2-40 – Load-crack width curves for virgin and healed specimens (van Tittelboom, et al., 2012).

Lastly, Sze Dai, et al. (2011) tested glass tubes with an adhesive in order to design a self-healing beam, a self-healing column and a self-healing slab (Fig. 2-41). They tied the tubes to the reinforcement bars of the structure and achieved recoveries of 84% of flexural strength in the beam, 70% in the column (which was lower due to the different direction of the flow) and 99% of strength recovery for the slab, which was tested to multiple impacts.

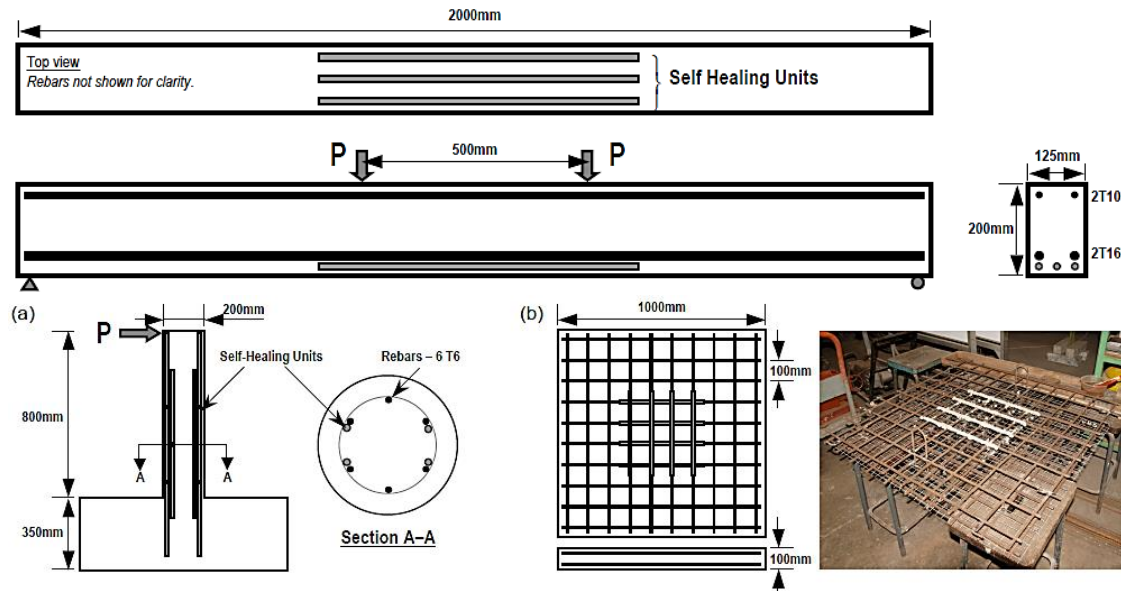


Fig. 2-41 – Self-healing beam, column and slab (Sze Dai, et al., 2011).

2.4.3.4 Dispersed encapsulation

The introduction of dispersed capsules is a better approach to deal with random and disperse cracking than located encapsulation. The three methods for the introduction of dispersed capsules with chemical healing agents are: microcapsules, impregnated natural fibers and impregnated porous aggregates.

2.4.3.4.1 Microcapsules

The method of using microcapsules as carriers of the self-healing agent was developed by White, et al. (2001) in order to design self-healing polymers (Fig. 2-42). This idea is being extrapolated to other types of materials, such as cementitious materials. In this case, the healing agent is stored in microcapsules and the catalyzer can be in the material matrix or in different microcapsules. In this way, when a random crack appears and intersects a microcapsule, it breaks releasing its healing agent (and catalyzer if that is the case) and activating the reaction that would fill the crack by capillary action.

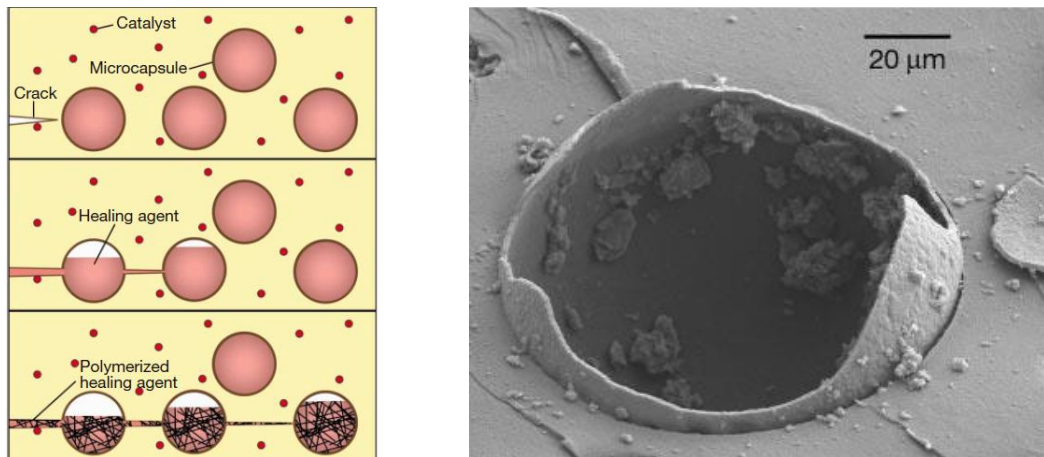


Fig. 2-42 – Process of breakage of a microcapsule (left) and release of healing agent and a broken microcapsule (right) (White, et al., 2001).

Going back to concrete, Yang, et al. (2011) tested mortar with microcapsules (5-40 μm) with oil core and silica gel shell, using methylmethacrylate monomer as healing agent and tri-ethylborane as catalyst. The microcapsules were added in a 1.5% by the weight of cement. The self-healing process was verified by permeability measurements and mechanically using fatigue tests, demonstrating that self-healing mortar (SHM in Fig. 2-43) achieved lower permeability coefficient than control specimens. When comparing the fatigue results, specimens with microcapsules resisted more cycles but at a lower load.

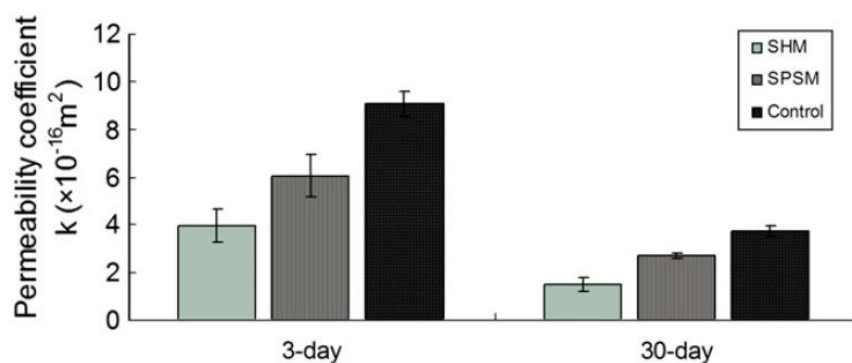


Fig. 2-43 – Permeability coefficients of cement mortar composite at 3-days and 30-day curing ages, after being loaded under 80% of ultimate compressive strength and subsequently set aside for 24 hours (Yang, et al., 2011).

The same year Pelletier, et al. (2011) experimented with polyurethane microcapsules (40-800 μm size) containing a sodium silicate solution. This healing agent would react with calcium hydroxide of concrete matrix forming C-S-H gels that would heal cracks. The final flexural load in the self-healing specimens was 26% of the original value, and only up to 14% in reference specimens.

Dong, et al. (2013) studied custom-designed prismatic fragile polymeric microcapsules with sodium silicate powder. They analyzed the recovery of stiffness and compared specimens cured in air with those cured under water immersion. Their results show that specimens with microcapsules recovered more stiffness, especially for contents of 6.9% of volume of the mixture and sized 3*12*2 mm, reaching a top value of 45% of stiffness recovery.

Zhang, et al. (2013) used urea-formaldehyde resin microcapsules with a dissolved epoxy resin. They achieved higher healing rates when increasing the content of microcapsules for permeability and strength (Fig. 2-44). The healing percentage increased with the size of microcapsules, as well.

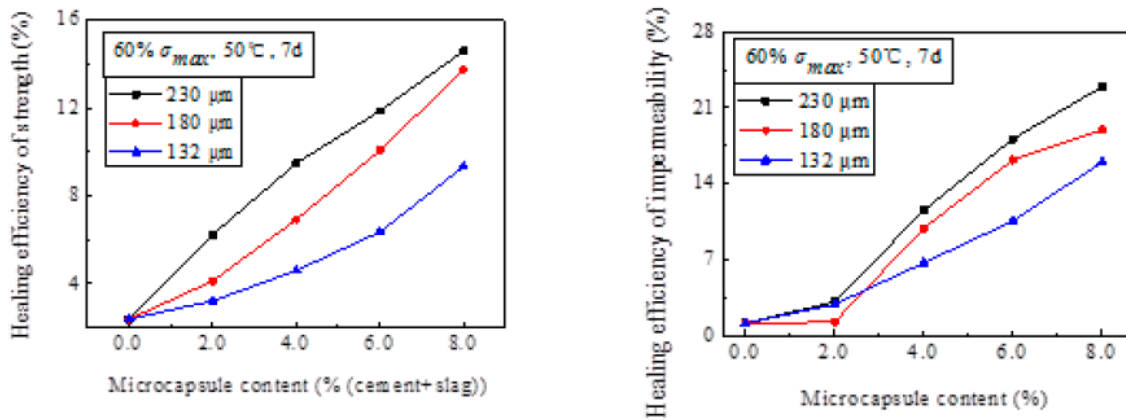


Fig. 2-44 – Strength recovery (left) and permeability healing (right) for different microcapsule contents and sizes (Zhang, et al., 2013).

2.4.3.4.2 Porous aggregates

In a similar concept to microcapsules, porous lightweight aggregates have been also impregnated with healing agents in order to counteract dispersed and random damage. Sisomphon, et al. (2011) used 2-4 mm sized porous clay aggregates that were impregnated with sodium fluorophosphate as healing agent. The aggregates were covered with a layer of cement paste. This time, the damaging agent was the carbonation front, which increased the porosity of the protecting cement layer allowing the release of the healing agent (see Fig. 2-45). The healing products were similar to apatite and were able to seal small pores, which was measured by the capillary absorption.

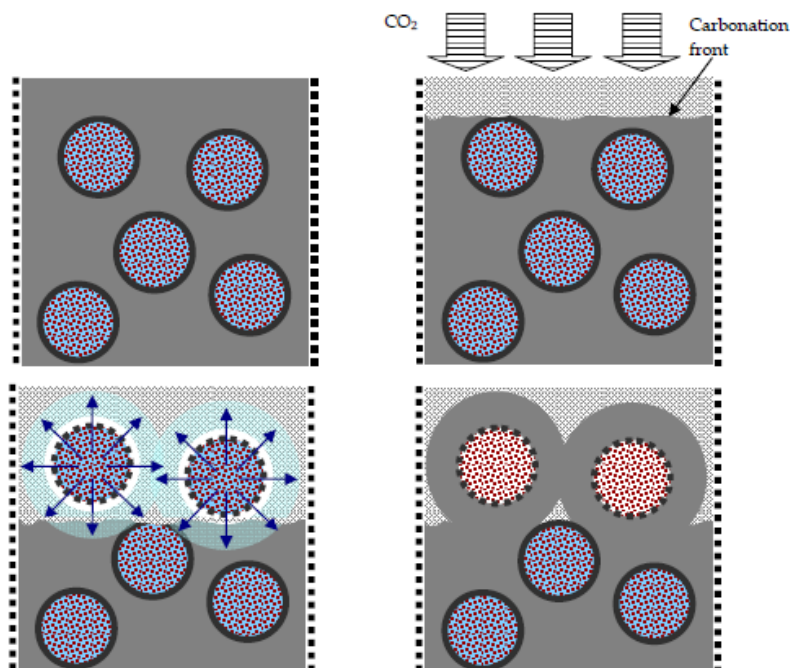


Fig. 2-45 – Self-healing process using impregnated porous aggregates (Sisomphon, et al., 2011).

2.4.3.4.3 *Natural fibers*

Another strategy to achieve dispersed capsules is the use of porous fibers or natural fibers. This was already suggested by Cánovas, et al. (1992) with the use of impregnated sisal fibers in concrete. The healing agents were colophony, tannin or other natural agents, and specimens were stored under water to let the agents act, achieving permeability decreases and durability improvements. Nevertheless, this method needs further development in order to avoid the degradation and treatment of natural fibers and obtaining an effective releasing of the agents.

2.4.4 Bacteria as healing agent

2.4.4.1 Concepts

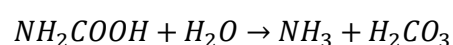
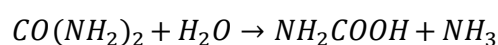
One of the newest healing agents to achieve self-healing concrete is bacteria, in a type of concrete usually named bacterial concrete or bioconcrete. Not every type of bacteria is suitable for this purpose. The main characteristics of these microorganisms should be the endurance to alkaline exposures (*i.e.* concrete) and the capability of precipitating crystals, which is frequently calcium carbonate (Schlegel, 2003). In order to survive to aggressive exposures, it is recommended the use of bacteria that are able to adopt an endospore form, a high-strength survival form intrinsic to some species. Bacteria in endospore form are *dormant* and when the exposure is favorable to their development, that is, contains nutrients and water, bacteria *wake up*. Bacteria are able to live decades, even centuries in the endospore form (Schlangen, et al., 2010). Some of the species that accomplish the requirements are *sporosarcina pasteurii*, *bacillus sphaericus*, *bacillus cohnii* and *bacillus subtilis*.

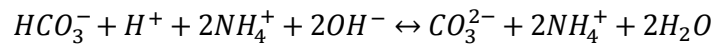
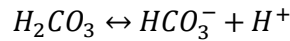
According to Hammes & Verstraete (2002) the process of calcium carbonate precipitation by bacteria depends on four factors: calcium concentration (as a nutrient for bacteria), dissolved inorganic carbon concentration, pH and available precipitation nuclei.

Relating to self-healing, there are two types of reactions that have been investigated to achieve the precipitation of calcium carbonate by the metabolism of this type of bacteria, urea-based and non-urea based. Few studies have been performed regarding the precipitation of silica instead of calcium carbonate (Ghosh, et al., 2009), and they are in an earlier stage of development.

2.4.4.1.1 *Urea-based*

Urea hydrolysis in calcium-rich environments makes bacteria produce calcium carbonate (Siddique & Chahal, 2011). This happens by the urease enzyme production, which catalyzes urea to carbon dioxide (CO₂) and ammonium (NH₄), thus increasing pH and stimulating the carbonate precipitation. The reaction process is the following (van Tittelboom, et al., 2010):



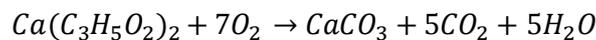


In this process, cellular walls are negatively charged, attracting cations (such as Ca^{+2}), that would react with the carbonate ions (CO_3^{-2}) forming calcium carbonate. These points also act as precipitation nuclei. This urea-based process is a high-efficiency process, as it allows the precipitation of high amounts of $CaCO_3$ in few times (Whiffin, 2004).

The main disadvantage of this method is the decrease of pH (increasing corrosion problems), which is due to the ammonia production (Jonkers, et al., 2010). This is the main reason for the search of different bacterial reactions that precipitate suitable healing products.

2.4.4.1.2 Non-urea-based

Jonkers (2011) used bacteria of different metabolism and calcium lactate as nutrient. In that design, not only bacteria produce calcium carbonate, they also produced carbon dioxide, which would be trapped inside concrete and available to produce even more calcium carbonates, thus being more efficient than the ordinary carbonation reaction of concrete. The reaction that took place in that calcium carbonate precipitation due to bacteria was:



Jonkers also suggested that the higher consumption of oxygen by these bacteria reduces the possible corrosion of reinforcement bars.

The first studies about self-healing bacterial concrete were with bacteria not encapsulated, but later the need of further life and space motivated the research of encapsulation methods.

2.4.4.2 Without encapsulation

Jonkers & Schlangen (2007) published their design for achieving self-healing concrete with *bacillus cohnii* (Fig. 2-46 left), taking advantage of their capability of endospore formation. The bacterial solution was added to concrete in the mixing water. They activated the dormant bacteria curing the specimens with a solution containing the nutrients of the bacteria, which in this case was sodium citrate. Their results showed a 10% decrease of compressive strength of mortar, but bacteria were able to precipitate calcite crystals of 100 μm size (see (Fig. 2-46 right), thus being potential crack sealers (Jonkers & Schlangen, 2008). Later they improved the design, incorporating the nutrients in the mixing water and concluded that bacteria could live only around 4 months due to the continuing decrease of porosity of concrete matrix (produced by continuing hydration), thus limiting the space for bacteria to live (Jonkers, et al., 2010; 2011).

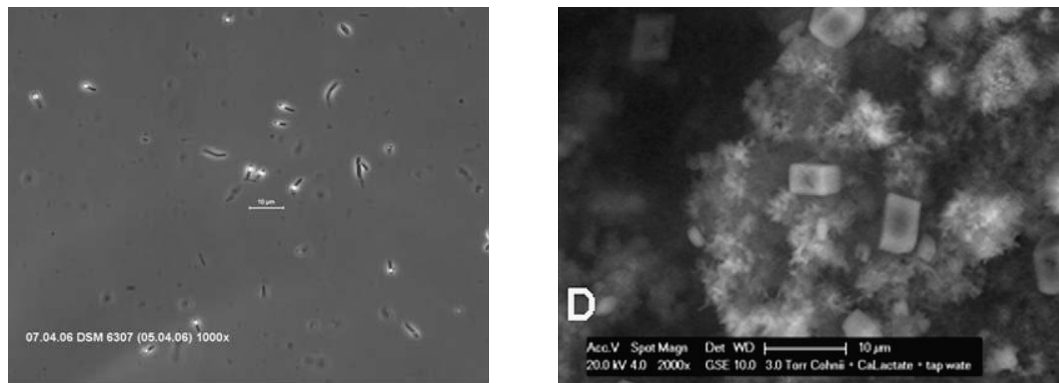


Fig. 2-46 – Endospore formation from *Bacillus cohnii* (left, (Jonkers & Schlangen, 2007)) and final calcite precipitates (Jonkers, et al., 2010).

2.4.4.3 Located encapsulation

In a similar way to the introduction of chemicals inside fragile glass tubes, bacteria can be immobilized and encapsulated in tubes. Wang, et al. (2012) introduced bacteria with the nutrients in sol-gel and in polyurethane (see Fig. 2-47). They compared the results in mortars with the two types of encapsulates with the same specimens but with dead bacteria, in order to isolate the effect due to the microbiological activity. According to their results, bacteria in sol-gel precipitated more calcium carbonate, while specimens with polyurethane tubes achieve the higher strength recoveries (50-80%).



Fig. 2-47 – Glass tubes with bacterial solution are added to mortar disks analogously to steel reinforcement (Wang, et al., 2012).

2.4.4.4 Dispersed encapsulation

In order to encapsulate bacteria in a dispersed method, Jonkers (2011) used lightweight aggregates impregnated with the bacterial solution and nutrients. In this way, bacteria are protected and remain available more years, being hypothesized that more than 50 years, which is a usual value of service life for concrete structures. Jonkers used as reference specimens mortars with bacteria but without nutrients, in order to distinguish the effect due to the metabolism of bacteria. All specimens were pre-cracked at the age of 56 days and cured in water for 24 hours. Self-healing was increased as it can be seen in the crystal formations of Fig. 2-48. After 6 months, bacteria were still alive.



Fig. 2-48 – Control and Bacterial specimens before and after healing (Jonkers, 2011).

Wiktor & Jonkers (2011) quantified the healing effects in prismatic mortar specimens with reinforcement. They generated crack widths between 0.05 and 1 mm that were cured under water immersion in order to activate the healing processes. In this case, they used a bacteria similar to *bacillus alkalinitrilicus*. Their results showed that for 20 days of healing there was not any difference between control and bacterial specimens, but at 40, 70 and 100 days of exposure bacterial concrete had better healing performance.

Wang, et al. (2012) immobilized *bacillus sphaericus* bacteria, urea and yeast in diatomitic earth. This bacterial earth was added to mortar specimens, in different dosages (Fig. 2-49). The method proved to be useful in order to protect bacteria, producing less aggressive pH surroundings for the microorganisms. They achieved complete healing of cracks between 0.15 and 0.17, but with different effectiveness depending on the bacterial concentration and the healing exposure. They achieved higher reductions of the capillary water uptake in bacterial specimens, being reduced 50-70% from the reference specimens. The healing products were calcium carbonate with urea and calcium nitrate crystals.

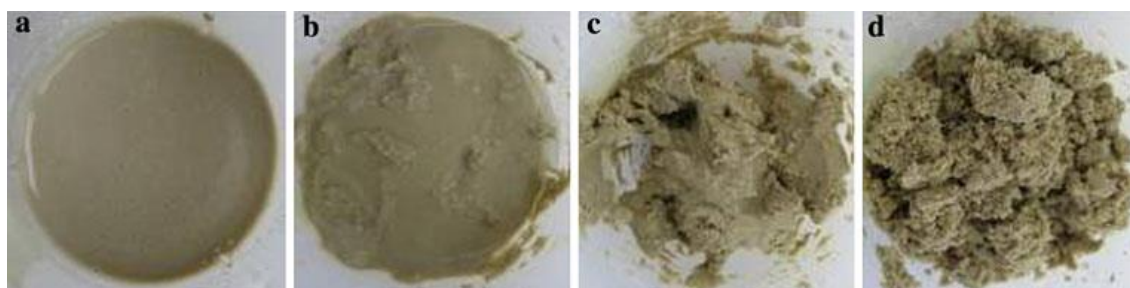


Fig. 2-49 – Different dosages of bacteria and nutrients in diatomitic earth (to right more proportion of earth) (Wang, et al., 2012).

New lines of research are looking for a bacterial encapsulation but are still in early stages.

2.4.5 Summary of autonomous healing

Some of the conclusions from all the different designs explained in this section for achieving autonomous healing are:

- There is a wide range of tailored designs for autonomous healing in concrete, with different grades of development.
- Crystalline and expansive admixtures are the only commercially available product and have a good compatibility with concrete. Their effectiveness is limited but synergies (such as the combination of both agents) and their behavior under different exposures and mix designs can be studied.
- Adhesives have lower compatibility with concrete, but need shorter times for reacting, mostly around 1 day in order to seal small-range cracks.
- Bacteria are promising healing agents, but more studies should be done regarding to their life expectancy inside concrete and their encapsulation possibilities.
- The different designs usually need an activator or catalyst, which can be introduced inside the composition of concrete or can be provided by the external environment, such as by the entrance of water.
- Encapsulation of water by using SAP or natural fibers can promote further autogenous healing due to their effect as water pockets.
- Encapsulation techniques are important to protect healing agents until the required moment, but many types are still in development. The capsule must resist the casting or pouring of concrete, but has to be activated when it is required, for example by cracking.
- Located encapsulation has higher healing capability because of the larger interior volumes, but requires crack prediction. Dispersed encapsulation answers to dispersed cracks, so it is more effective for random cracking, but the damage has to hit the capsules.

2.5 Discussion

This chapter has presented different methodologies for achieving self-healing concrete from two main points of view: enhancing the natural properties of concrete and using specific new designs. Both ways have been mainly focused on healing service cracks (up to 0.3 mm), and the most effective range is often for cracks in the range of the micrometers. Hence, at this stage of development, self-healing should not be considered as a method to repair critically damaged structures. Instead, self-healing is best used in a preventive manner, to increase the service life (and reduce the maintenance costs) of a structure.

Enhancing the intrinsic autogenous healing of concrete is the most immediate way to achieve self-healing. From the literature, it can be thought that carbonation is the main process that causes

autogenous healing. However, this process can increase the corrosion problems of steel reinforcement due to a decrease of the pH inside concrete matrix and the depassivation of the reinforcement. This makes carbonation undesirable in most concrete elements even if it improves autogenous healing. Because of that, autogenous healing by continuing hydration would be a more beneficial process, though it is not likely to happen in a complete absence of carbonation for ordinary structures.

The composition of concrete seems of a minor effect for this type of healing, but some mix designs containing pozzolanas may have higher autogenous healing due to their delayed reaction. Reducing crack width by the use of fiber-reinforced concrete with high volumes of fibers is a reliable method to achieve tighter cracks, which would improve notably the natural healing processes. This type of concrete also presents higher durability, thus is a potential concrete to synergize with healing in order to improve service life of structures.

The autonomous healing designs to achieve self-healing (such as the use of microcapsules, bacteria or admixtures) can improve or give different healing properties depending on the specific type. The main challenge with this group is to protect healing agents inside concrete and activate them only in the required moment. With this purpose, several encapsulation techniques are still being developed, either for bacteria or for chemical solutions. However, the encapsulation adds the difficulty of resisting the casting process of concrete, which needs to be guaranteed before using them in construction. Located encapsulation can partially avoid that problem, as the tubes or capsules are placed before pouring the concrete, in a similar way to reinforcement. In any way, both types have to resist the concrete impact in the moment of pouring while being activated by cracking (or other type of damages) in the concrete element.

Because of the encapsulation difficulties, different groups have studied the use of admixtures with designed activation (such as crystalline admixtures), superabsorbent polymers and impregnated porous fibers or aggregates. These latter designs present a more mature status concerning their addition into concrete, hence they could penetrate earlier in the construction industry. Table 2-3 shows a summary of the advantages and disadvantages of the methods explained in this chapter.

It is also of a great importance that there is no standard methodology in order to evaluate the self-healing properties of a material, not even for a specific type of material, in this case, mortar and concrete specimens. Three main groups have been described in this chapter: permeability and other durability-related tests, mechanical tests and physical closure of cracks. The differences of methodologies and concrete/mortars composition difficult the comparisons between the reported studies and it is not easy to reach clear conclusions, as the testing methodology may influence them.

Group	Type	Advantages	Disadvantages
Cement healing agent	Autogenous healing	Natural process.	Low capability. Low reliability.
	Encapsulation of water	Good compatibility of healing products. SAP and porous fibers.	Inconclusive capability. Inconclusive reliability.
Chemical healing agents	None encapsulation: Admixtures (CA&CSA)	Easy to add. Good compatibility. Availability of commercial products	Activation. Low knowledge. Inconclusive capability. Inconclusive reliability.
	Disperse microencapsulation	Selection of designed healing agents.	Resistance of microcapsules when casting and pouring. Activation when cracking. Still in development.
	Located capsules	Selection of designed healing agents.	Resistance when pouring and activation when cracking. Viscosity of releasing agents.
Biological healing agents	None encapsulation: bacterial solution	Easy to add. Compatible byproducts.	Low life expectancy of bacteria.
	Disperse microencapsulation	Compatible byproducts. Protection of bacteria.	Resistance of microcapsules when casting and pouring. Activation when cracking. Still in development.
	Located capsules	Compatible byproducts. Protection of bacteria.	Resistance when pouring and activation when cracking. Viscosity of releasing agents.

Table 2-3 – Summary of advantages and disadvantages of each specific design for self-healing concrete.

Chapter 3. Experimental phase

3.1 Specific objectives

The specific objectives of the experimental phase are a natural extension of the studies described in Chapter 2. The specific objectives are:

- To establish an experimental methodology in order to evaluate autogenous healing and self-healing by permeability measurements.
- To compare autogenous healing with autonomous healing in concrete with crystalline admixtures.
- To evaluate the influence of initial damage on self-healing, depending on initial crack width.
- To compare the effect of changing water/cement ratio and cement content, with usual values in traditional types of concrete.
- To discern the effectiveness of both types of healing under six different environmental exposures, which would help to identify the optimal types of structures for these products.

3.2 Program of the campaign

The experimental phase was divided in two campaigns, one of them performed during late 2013 and the second during 2014. Both campaigns followed the same methodology, only with minor changes. In the first campaign, the evolution of crack width was analyzed only in half specimens, as permeability was considered the main objective. In the second campaign, all specimens were analyzed by permeability and crack width. One combination or group was repeated in order to represent a link connection between both campaigns. These campaigns were also used to compare methodologies and other parameters that have been included in different research done by this research group (Roig-Flores, et al., n.d.).

The first campaign was designed to determine the influence of four environmental conditions in the autogenous and autonomous healing processes for small cracks (up to 0.25 mm). The four environmental conditions were set to represent usual conditions depending on the environmental water presence: water immersion at 15°C (WI_15), water contact (WC), humidity chamber (HC), and air exposure (AE). The two first exposures had direct contact with water while the others only with moisture in different percentages.

The second campaign evaluated the influence of the quality of concrete, extended the crack range up to medium cracks (up to 0.40 mm), and added two new exposures: water immersion at 30°C (WI_30) and wet/dry cycles (WD). The exposure of WI_15 was the link group between both campaigns.

The following parameters were fixed parameters in the whole research:

- Type of crystalline admixture and content.
- Pre-cracking age of 2 days and healing time of 42 days.
- The rest of mix design parameters, including aggregates and type of cement.
- Type of water used during all the experimental campaign: tap water.

The following parameters were the variables of interest in this research:

1) First campaign:

- Dosage of Crystalline Admixture: 0% (control concrete specimens, CC) and 4% by the weight of cement (crystalline admixture concrete specimens, CAC).
- Initial crack width: between 0.05 and 0.25 mm.
- Exposures: AE, HC, WI_15 and WC.

2) Second campaign:

- Water/Cement and cement content: 0.45 with 350 kg/m³ of cement and 0.60 with 275 kg/m³ of cement content.

- Dosage of crystalline admixture: 0% for control concrete specimens, CC and 4% by the weight of cement for crystalline admixture concrete specimens, CAC.
- Initial crack width: between 0.05 and 0.40 mm.
- Exposures: WI_15, WI_30 and W/D.

Fig. 3-1 represents altogether the parameters of both campaigns and indicates the number of tested specimens for each combination.

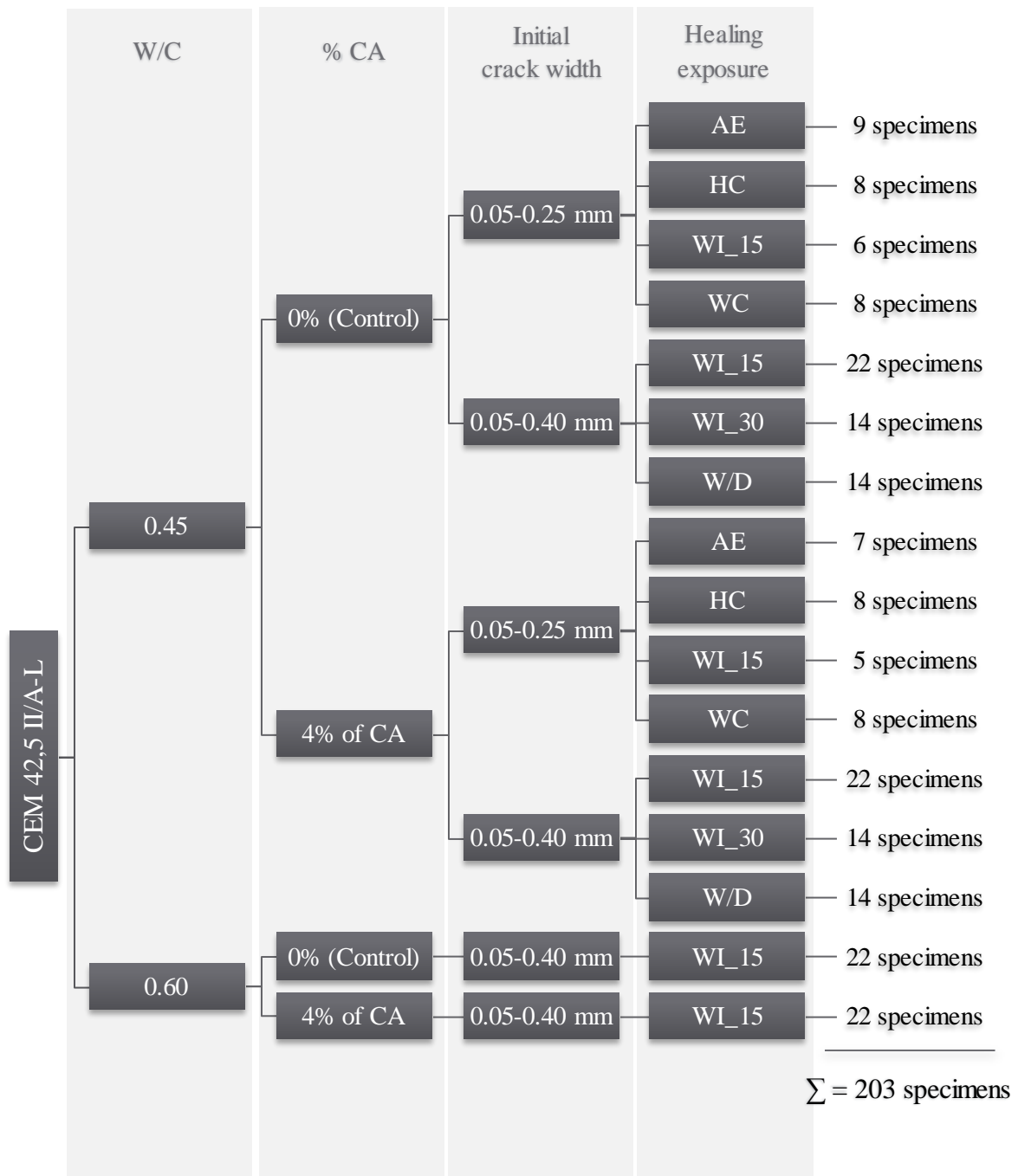


Fig. 3-1 - Experimental program.

3.3 Materials

3.3.1 Cement

The cement used was CEM II/A-L 42.5 R from Elite Cementos S. L. This type of cement has a content of limestone powder of 6-20% and rapid acquisition of strength, since the pre-cracking stage was performed at early age of concrete.

3.3.2 Water

The type of water could affect the healing processes due to its composition. Tap water was used as mixing water in this experimental research due to it is the more likely to be used in the construction stages. The pH of used tap water was measured with pH indicator strips and the results were comprised around seven.

3.3.3 Aggregates and limestone powder

Aggregates' size can affect the results obtained in studies about self-healing properties, as they affect, for example, the transport properties. In this way, when using too large aggregates, the transport of healing agents from the cementitious matrix to the crack might be impossible when maximum size of aggregates is huge.

In this study, it was decided to work with coarse aggregate, in order to have situation closer to real constructions. The coarse aggregates were crushed aggregates of the categories (d_{min}/D_{max}) 7/12 and 4/7. The fine aggregate was natural sand. The different compounds are shown in Fig. 3-2.

In order to adequate the aggregates' size curve to a more continuous it was decided to add limestone powder, due to the lack of fine materials of the laboratory sand. To this purpose, it was decided to add 50 kg/m³ in the casting groups without the mineral admixture, and lower quantities when using them. In any case, the amount of powder fraction is maintained significantly under the limit established by the Spanish Code for concrete EHE (175 kg/m³), even considering the maximum possible amount of lime addition inside cement.



Fig. 3-2 – Main compounds used for casting concrete.

3.3.4 Superplastizer

Superplastizer ViscoCrete-5720 from Sika was added in order to achieve desired workability. In this case, the target was a result in slump test around 14 cm, which is a fluid consistency.

3.3.5 Fibers

It was decided in this study to work with fiber-reinforced concrete. Since the focus of the project was to study the healing effects on pre-cracked specimens, fibers could provide an effective action both in controlling crack width during the pre-cracking process as well as in keeping fixed its value afterwards. The quantity of steel fiber was fixed at 40 kg/m^3 (0.51% by volume) according to the criterion of making the crack opening easily controllable while avoiding excessive branching of cracks. It was decided to work with steel fibers due to their better performance for structural uses and avoiding interaction of precipitation of crystals with high polarity fibers (such as PVA).

Fibers were Dramix® RC 65/35 BN from Bekaert, 35 mm length and 0.55 mm diameter (Fig. 3-3).

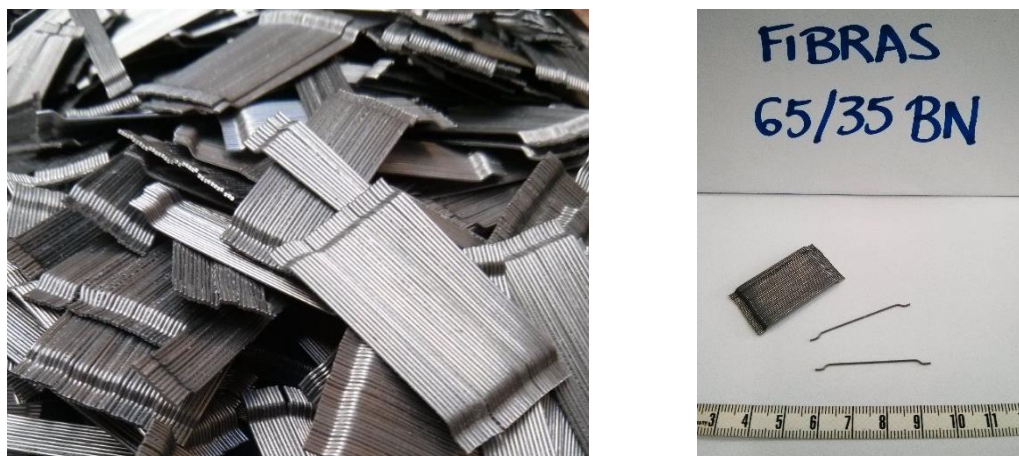


Fig. 3-3 – Steel fibers (Dramix® RC 65/35 BN) used in this research.

3.3.6 Crystalline admixtures

Crystalline admixtures (CA) are a type of permeability reducer admixture for concrete according to the American Concrete Institute, in their Committee 212. A summary of the achieved information about CA was explained in Chapter 2. These products are thought to react when in contact with cement matrix and water, but also it is capable of storing a latent capability. This capability is which allows to activate self-healing mechanisms when a damage occurs in concrete.

Physically is often a green powder, with particle size around 40-150 μm and a density between 1200-1400 kg/m^3 . Its aspect is of a finer cement, as it can be seen in Fig. 3-4. Depending on the type of admixture, it can resist from 40-50 up to 140 water-meter column of pressure. It is usually added in a dosage of 1-2% by the weight of cement and has certain effect as water reducing admixture (between 5-10%). Recommended water/cement ratio is 0.45 or lower. It is able to seal cracks up to 0.40 mm and the by-products of the reaction form integral part of concrete, producing an impermeable concrete. In this way, it protects from corrosion and avoids the entrance of contaminants. It should be remarked that it is not a toxic product, so it can be used for fresh water reservoirs in the same way as cement.



Fig. 3-4 – Aspect of cement and crystalline admixtures used in this research.

3.4 Methodology

3.4.1 Mix design

Two types of concrete were cast, with water/cement ratio of 0.45 and 0.60. A dosage of 4% by the weight of cement of crystalline admixture in powder form was introduced in the CA Concrete whose behavior was compared with control specimens (without crystalline admixture). The four mix designs are shown in Table 3-1.

The group with water/cement ratio of 0.45 are expected to present higher amount of unhydrated cement particles, thus presenting a higher amount of autogenous healing due to continuing hydration.

Material (kg/m ³)	W/C=0.45		W/C=0.60	
	Control	CA Concrete	Control	CA Concrete
Cement II/A-L 42.5 R	350	350	275	275
Water	157.5	157.5	165	165
Gravel (4-12 mm)	950	959	908	915
Natural sand	899	875	987	967
Fibers, Dramix 65/35	40	40	40	40
Limestone powder	50	36	50	39
Crystalline Admixture	-	14	-	11
Average Slump (cm)	13	16	15	14
Average Compressive Strength (MPa)	55	61	38	41

Table 3-1 - Mix design of control and CA concrete for water/cement ratios of 0.40 and 0.60.

The criterion chosen for making concrete mixes with and without crystalline admixture is to maintain constant the sum of limestone powder and crystalline admixture, due to their similar effect on concrete workability since they increase the powder fraction. In fact, they would both act as densifiers of the paste matrix phase. The chosen percentage of crystalline admixture has been 4% by the weight of cement.

Superplasticizer, ViscoCrete 5720, dosage was adjusted in each different group in order to get similar slump (140 mm \pm 20 mm).

In order to calculate the percentages of each aggregate, it has been used the Bolomey method, with parameters $a = 17$ and maximum size 12 for both designs. This is the reason for having slightly different values for each group. For all cases the values of the adjustment are around 3, which are enough good (< 4).

The concrete mixer used for casting concrete was a planetary mixer Betonmass ST 150 CD, with maximum capacity of 150 liters (see Fig. 3-5) and the molds were cylindrical steel standard molds.



Fig. 3-5 – Planetary mixer used for casting concrete (left) and cylindrical molds (right).

After casting the specimens, they were let curing in the mold for 24 hours and after that they were kept in humidity chamber at standard conditions (20°C and 95% of relative humidity) until the time of pre-cracking.

3.4.2 Control tests: slump and compressive strength

For each batch, three $\Phi 150 \times 300$ mm cylindrical specimens were cast according to UNE-EN 12390-2 to determine the compressive strength at 28 days, as per UNE EN 12390-3. All batches were also characterized by their workability with slump test as per UNE EN 12350-2:2009 (Fig. 3-6). These control tests were performed with the objective of verifying the homogeneity of specimens of different batches but belonging to a same mix group (either control or CA) and in order to compare the results between the two mix groups (control and CA).



Fig. 3-6 - Slump test following UNE EN 12350-2:2009.

After averaging the results of all batches for each group (see Fig. 3-7, Table 3-2 and Table 3-3), it was observed that CA concrete had a significantly better compressive strength, about 15% higher than control concrete in the case of water/cement ratio of 0.45 and 8% higher for the group with water/cement ratio of 0.60.

With reference to the slump test results, differences are slightly lower, since the average results are around 13-16 cm for the four groups, which are within the acceptable tolerance limits of slump tests according to the standards.

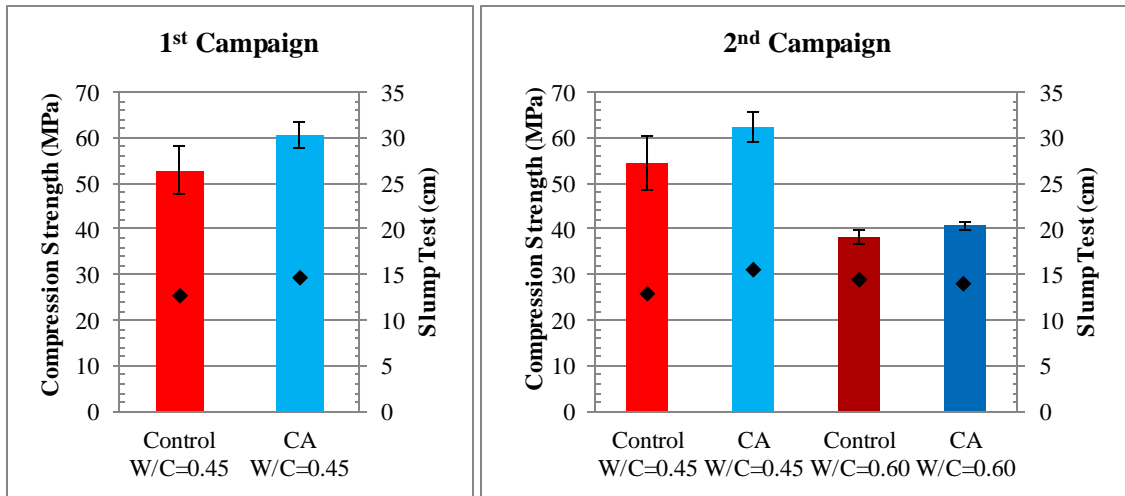


Fig. 3-7 – Average and standard deviation for compressive strength (bars) and slump test (points) for both campaigns.

1 st CAMPAIGN					
W/C	Mix	Slump Test (cm)	Slump Test Deviation (cm)	Average Compression Strength (MPa)	Deviation Compression Strength (MPa)
0.45	Control	12,86	3,13	52,88	5,14
	CA Concrete	14,83	3,66	60,56	2,95

Table 3-2 – Average and standard deviation for compressive strength and slump test for the 1st campaign.

2 nd CAMPAIGN					
W/C	Mix	Slump Test (cm)	Slump Test Deviation (cm)	Average Compression Strength (MPa)	Deviation Compression Strength (MPa)
0.45	Control	13,00	3,61	54,49	5,92
	CA Concrete	15,50	1,73	62,41	3,22
0.60	Control	14,50	0,71	38,33	1,48
	CA Concrete	14,00	2,16	40,73	0,91

Table 3-3 - Average and standard deviation for compressive strength and slump test for the 2nd campaign.

3.4.3 Self-healing methodology

The methodology used in this research has also been used in other works by this group (Roig-Flores, 2013; Roig-Flores, et al., n.d.). It is based on the permeability tests reported in the literature (such as from Edvardsen (1999) or Sisomphon, et al. (2012)) and the standard permeability test for uncracked concrete specimens.

The methodology used in this research to evaluate the effects of self-healing consists of five stages (Fig. 3-8): first, casting of the specimens; second, creation of controlled damage in the specimens; third, measurement of certain properties, such as permeability or crack geometrical parameters; fourth, simulation of the conditions or environmental exposure needed to achieve better healing results and, fifth, evaluation of the recovery of the same property measured in the third stage. More specifically the path that specimens follow in the experimental campaign is displayed in Fig. 3-9.

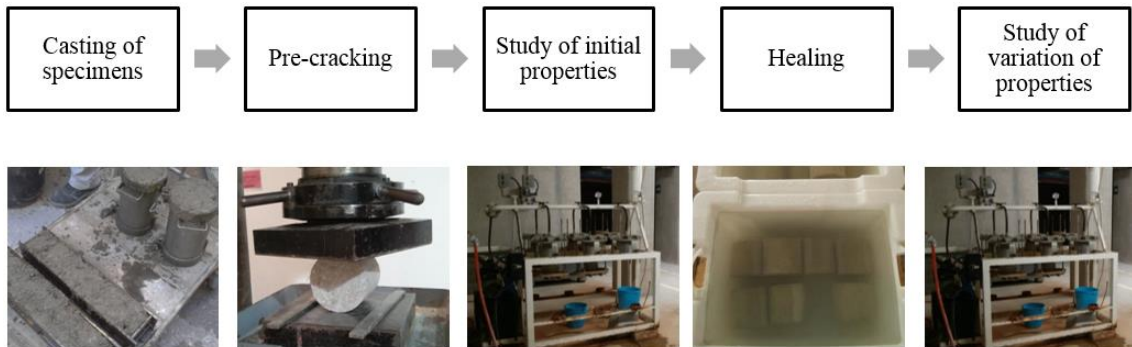


Fig. 3-8 – Methodology procedure.

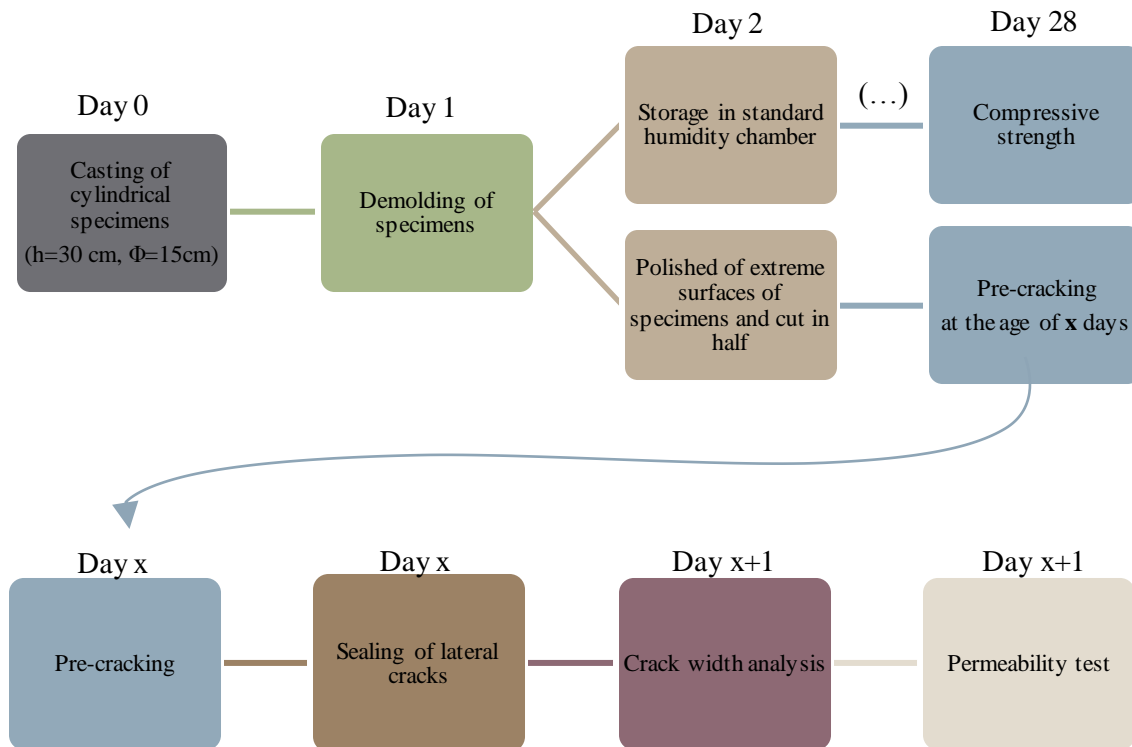


Fig. 3-9 – Scheme of each step of the process.

The size and shape of the concrete specimens was determined by the permeability-based healing test, which conditioned the pre-cracking process together with the available equipment.

3.4.3.1 Creation of a damage: pre-cracking process

Each cylindrical specimen with dimensions of $\Phi 150 \times 300$ mm was cut in half using a circular saw for concrete. In this way, the specimens' size for the permeability test was $\Phi 150 \times 150$ mm. The edge faces of each $\Phi 150 \times 150$ mm cylinder were then polished in order to eliminate mortar layers (in the bottom surface in contact with the molds) and asperities (in the top free surface of the specimen as cast). Fig. 3-10 shows the differences of surface before and after polishing. This process will allow discerning if a crack hits and breaks an aggregate or if it passes through cement paste.



Fig. 3-10 – Irregular surface before polishing with the circular saw (left) and final aspect (right).

The specimens were pre-cracked at the age of 2 days, inducing controlled damage, by means of a splitting test (Fig. 3-11): this was meant as the width of the diameter crack, which was set to reach a target value, controlled by a calibration ruler. The measure of the crack width with the calibration ruler while performing the splitting test has been meant as good enough for the purpose of the campaign. As a matter of fact, though it is an approximate way to measure the crack width, it is also very simple and allows a larger amount of specimens to be cracked in a reasonable time. The calibration ruler has an inherent dispersion due to the human factor but is a good method to obtain crack widths within a range of 0-0.3 mm.



Fig. 3-11 – Pre-cracking process and pre-cracked specimen by splitting test.

Once cracked, lateral cracks are sealed by using an epoxy resin (Sikadur 31-CF and 31-EF). A ring of the crack of one circular surface is sealed as well due to the features of the permeability

test. Fig. 3-12 shows specimens with those areas already sealed. It should be noted that resin does not enter significantly inside the crack, since it is only placed externally.

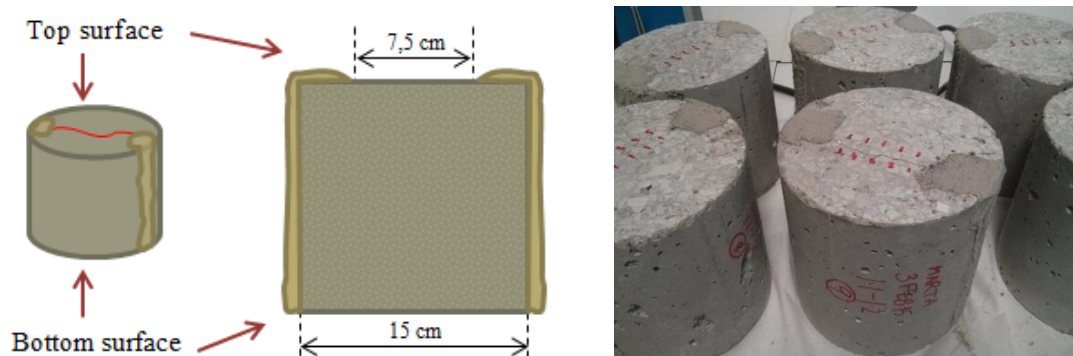


Fig. 3-12 – Sealing of lateral cracks and upper ring with epoxy resin.

3.4.3.2 Evaluation of properties: permeability test

One of the main objectives of crack healing is to improve durability of concrete structures. Visual closing of cracks does not necessarily imply an improvement of durability. Therefore, permeability-based studies of self-healing are of a great importance. There are two main groups of tests for measuring permeability of materials: for high permeability and for almost impermeable elements. Cracked concrete specimens belong to the first category, while virgin and complete healed specimens would belong to the latter. As the main purpose is to verify the process of healing, it was decided to work with a method based on high permeability tests (Darcy's Law). In this way, it will not be possible to discern between different ranges inside impermeable specimens. On the contrary, it would be possible to measure with the same test cracked and healed specimens and identify the healing process.

A method based on the permeability test described in UNE-EN 12390-8 was employed in this study, but measuring the water flow instead of the water depth penetration. To guarantee the impermeability of the specimen lateral surface, the zones of the lateral surface which were in contact with the machine loading platens during the pre-crack splitting tests were sealed with the epoxy resin. A diagram of the test is shown in Fig. 3-13.

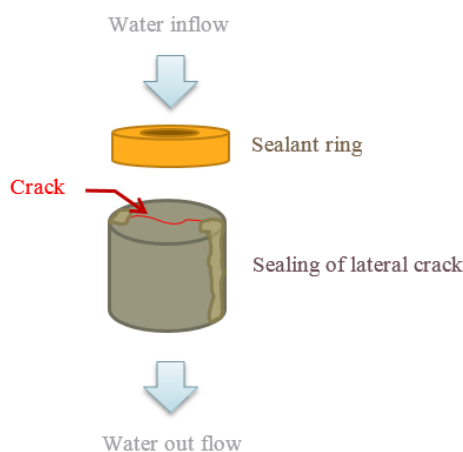


Fig. 3-13 – Diagram of the permeability test for cracked specimens.

Water flow is measured by weighting the amount of water passing through the specimen in the fixed time. The recipient used for collecting water is an ordinary bucket.

The parameters of the test are:

- Head water pressure equal to 2.00 bars. In practice, the initial pressure is set equal to 2.05 bars and as pressure decreases due to water flow, the permeabilimeter turns on again when a pressure of 1.95 bars is reached, recovering the 2.05 bars pressure. Therefore, water pressure is always kept between 1.95 and 2.05 bars.
- The quantity of water passing through the crack was measured during a 5 minutes testing time for small range cracks and 1 minute for medium range cracks due to the capacity limits of the recipients.

Following this method, water passes through the interior of the specimen by the crack and it was experimentally confirmed that, as it was expected, small cracks had smaller water flow while larger cracks presented higher water flows (see Fig. 3-14). In this way, if a crack closes after the healing process, the water flow should have diminished. The permeabilimeter used in the test and the different parts it consists of it are shown in Fig. 3-15.



Fig. 3-14 – Inferior part of an specimen during the permeability test showing water flow for a small crack (left) and a large crack (right).

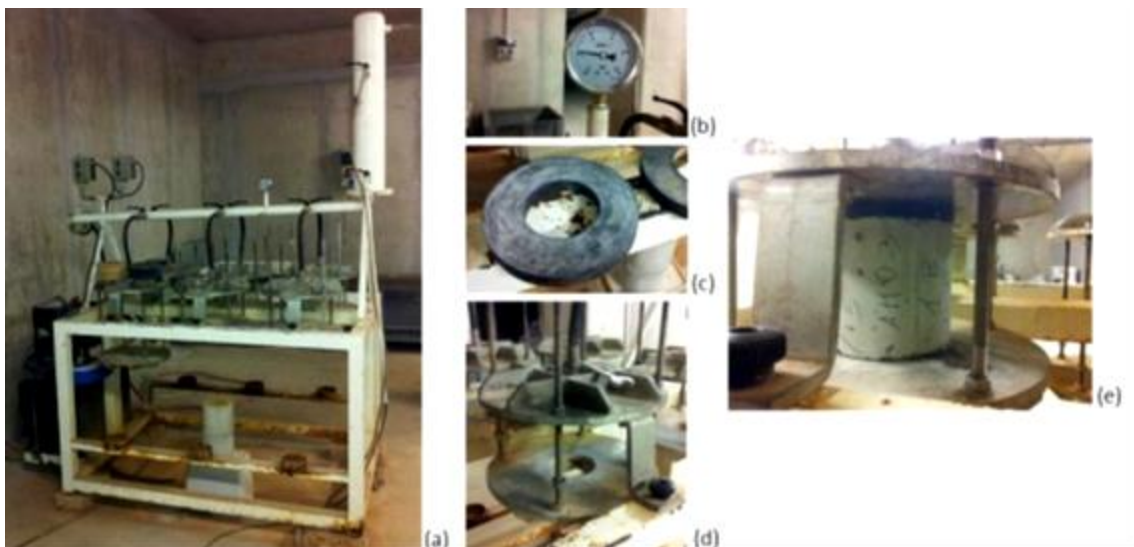


Fig. 3-15 - Permeabilimeter (a) and its parts: manometer (b), sealing ring (c), auxiliary structure (d), prepared specimen (e).

3.4.3.3 Evaluation of properties: study of crack geometrical parameters

In addition to permeability tests, crack width was also measured to support the measurements. An optical microscope and a crack width ruler were used to this purpose (see Fig. 3-16) The photography software Adobe Photoshop CS6 was the tool chosen to measure the parameter. The pictures were taken before and after the healing exposure in order to evaluate autogenous and self-healing. Before taking pictures, all the specimens were cleaned with compressed air.



Fig. 3-16 – Optical microscope connected (left) and crack width ruler (right).

The measurement of crack width was also performed with the purpose of seeking a correlation with the water flow measured in the permeability tests. Water permeability is considered the reference value in order to compare the different methods for quantifying self-healing, since the main objective of closing a crack is to avoid the entrance of liquids, contaminants and aggressive agents.

With reference to the measure of the crack width, the average width w_{avg} was calculated averaging fixed width measurements, taken at prescribed positions along the crack, thus decreasing the uncertainty of the measurement itself. Each concrete specimen has got two cracks (top and bottom), denoted according to the orientation of the same specimen in the permeability test, and the water contact exposure. The research group has already studied other combinations measuring a representative geometrical parameter, and the measure of average crack width was one of the most reliable measures while being more time-effective (Roig-Flores, et al., n.d.). because of that this work only shows the results for averaged crack width.

These photographs, taken with the optical microscope, would also make possible a visual comparison of crack evolution and the formation of precipitates.

3.4.3.4 Exposure simulation

To analyze the activation of autogenous healing and crystalline admixtures is of a major importance the environmental exposure. CA are expected to behave with different rates of

effectiveness under different conditions, mainly depending on the available content of environmental water, analogously to what has been reported for autogenous healing.

Six environmental exposures were studied in order to determine the effect of humidity on the self-healing capability of the tested specimens, comparing the reference concrete with the crystalline admixture concrete (Fig. 3-17).

- a. AE (Air Exposure): storage of the specimens in normal laboratory conditions inside a room without exterior influences, $17\pm 1^\circ\text{C}$ and $40\pm 5\%$ of relative humidity.
- b. HC (Humidity chamber): storage of the specimens inside a standard humidity chamber at 20°C and $95\pm 5\%$ relative humidity.
- c. WC (Water contact): a layer of water with a head pressure of 2 cm-water on the top crack, and storage in humidity chamber at 20°C and $95\pm 5\%$ relative humidity. Additional water was supplied when necessary in order to maintain the 2 cm water layer.
- d. WD (Wet/dry cycles): water immersion at $15\text{-}16^\circ\text{C}$ during three days and a half and air exposure during three days and a half, without renewing water.
- e. WI₁₅ (Water immersion): continuous immersion in tap water at laboratory conditions without renewing the water during the healing period (temperature of water, $15\text{-}16^\circ\text{C}$)
- f. WI₃₀ (Water immersion): continuous immersion in tap water at laboratory conditions without renewing the water during the healing period (temperature of water, 30°C)

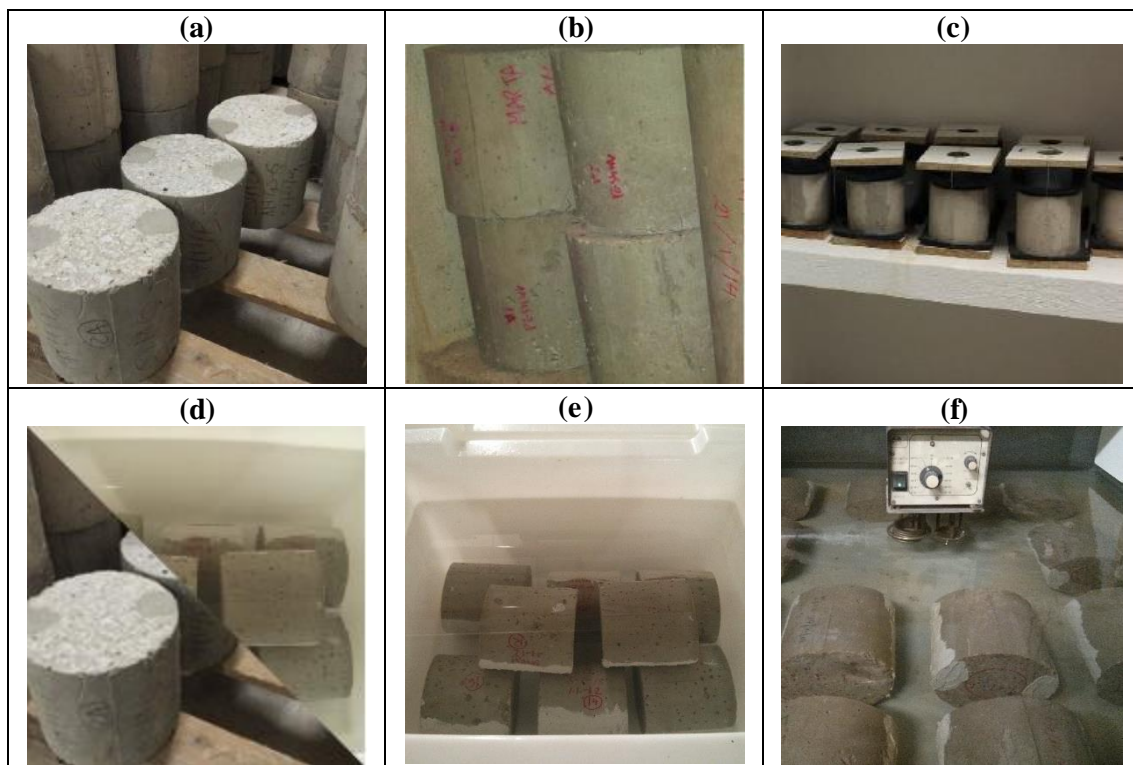


Fig. 3-17 - Six exposures: air exposure (a), humidity chamber (b), water contact (c) wet/dry cycles (d), water immersion at 15°C (e) and water immersion at 30°C (f).

With these six environmental conditions, it is intended to discern if the self-healing will be powerful enough for constructions in several types of environments as above, including those without direct contact with water and those elements in contact with it, either having a small amount of water in contact or totally immersed. Each type of healing exposure has been designed with the objective of simulating real conditions:

- a. AE concrete elements without direct contact with water and average humidity levels
- b. HC simulates concrete elements without direct contact with water but constructed in a high humidity environment
- c. WC simulates situations with a face directly exposed to water with a very low pressure and the other unexposed to it, such as buried walls under the water table
- d. WD simulates structures periodically immersed in water and periodically exposed to a normal humidity environment
- e. WI_15 simulates underwater concrete elements
- f. WI_30 simulates underwater concrete elements in a warm water condition or an accelerated version of WI_15

The specimens immersed in water during the healing period, were divided in two different water recipients, in order to avoid interferences between control concrete and concrete with crystalline admixtures. The immersed specimens were placed on two 3 cm wide wood strips ensuring a separation between specimens of at least 5 cm between the cracked faces and 1 cm between the lateral surfaces, in order to let the water act in the whole specimen.

The setup for the 2 centimeters water contact environment is shown in Fig. 3-18. The equivalent pressure of those 2 cm of water is $1.96 \cdot 10^{-3}$ bars or 0.2 kPa, without pressure in lateral faces of the specimen. In this group, water remains in the upper PVC ring and enters inside the specimen through the crack and does not exit from it because of the lower sheets of insulation material and wood. The parameters that conditioned this design were two: the system should not add an extra day, thus most of adhesive-based products were not suitable; and it should not be permanent, and be easily removable, as parallel studies from the group required to do intermediate permeability tests. After specimens were prepared in the described setup, they were stored inside humidity chamber at 20°C and 95% of relative humidity to minimize water evaporation.

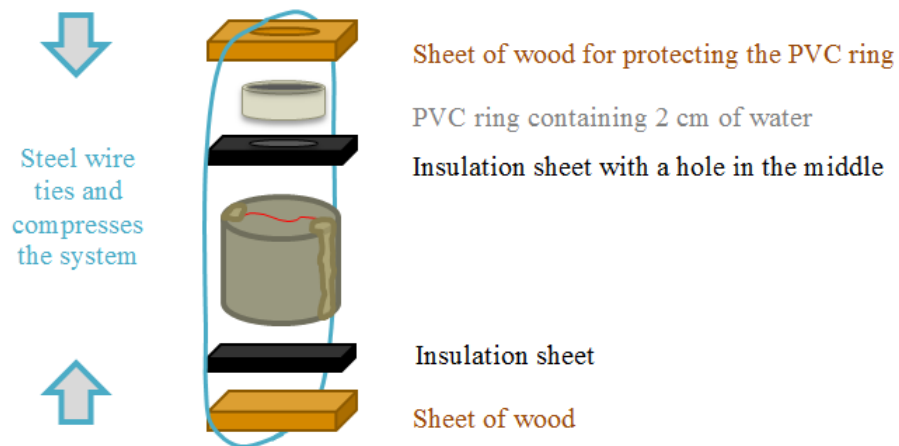


Fig. 3-18 - Setup of the 2 cm water head exposure.

For immersed specimens (either at 15°C or 30°C) and in water contact it was necessary to add extra water each 2/3 days in order to maintain the same water level.

Chapter 4. Results and discussion

4.1 Introduction

This chapter presents the results of the experimental campaigns (Section 4.2) and a discussion on the effect of each objective parameter in the self-healing properties of tested concrete (Section 4.3).

4.2 Presentation of results

4.2.1 Structure of results and parameters

The output results from both campaigns are the initial and final values for water flow and crack width. All of these results can be found in the Appendix, and they are presented as shown in the example of Table 4-1. Empty values represent unmeasured values for those specimens that were only tested to permeability.

1 st CAMPAIGN							
Mixture	W/C	Healing conditions	Specimen	Initial		Final - 42 days	
				Water flow (ml/5min)	Crack width (mm)	Water flow (ml/5min)	Crack width (mm)
Control	0.45	HC	1	302	0,11	293	0,04
			2	2733	0,18	1710	0,15
			3	93	0,16	141	0,11
			4	1645	0,15	1257	0,15
			5	541		96	
			6	243		176	
			7	172		161	
			8	145		173	

Table 4-1 - Permeability and crack width of cracked and healed specimens, 1st campaign, for control specimens with w/c of 0.45 under the humidity chamber exposure.

Self-healing was analyzed from the measures of permeability and crack width before and after the healing process.

As indicated in Chapter 2, the name “healing rate” is commonly used in the literature to indicate a measure of self-healing from the recovery of permeability properties. The term was first coined by Edvardsen (1999), but despite that, there is no commonly-accepted definition for this parameter.

In this research, the Healing Rate was defined as:

$$\text{Healing Rate} = 1 - \frac{\text{Final Flow}}{\text{Initial Flow}} = 1 - \frac{Q_{42}}{Q_0} \leq 0$$

With:

Q_0 the initial water flow

Q_{42} the final water flow for a healing time of 42 days

When the final flow is similar to the initial flow, the Healing Rate would tend to 0; and when the final flow is 0, the Healing Rate would be 1. Negative values of the Healing Rate are considered as 0, meaning that healing has not occurred. The healing produced depending on the initial level of damage can be analyzed by representing the Healing Rates obtained for each specimen versus its initial water flow.

It has been verified that most specimens in exposures in direct contact with water experienced a reduction of water flow.

As for crack width sealing, in the literature it is often estimated by the “self-closing rate” (Jaroenratanapirom & Sahamitmongkol, 2011; van Tittelboom, et al., 2012). In order to maintain

the naming of the self-healing processes in this case it has been named Sealing Rate. Analogously to the Healing Rate, this parameter is defined as:

$$Sealing\ Rate = 1 - \frac{Final\ Crack\ Width}{Initial\ Crack\ Width} = 1 - \frac{\omega_{42}}{\omega_0} \leq 0$$

With:

ω_0 the initial crack width

ω_{42} the final crack width for a healing time of 42 days

The reasoning about the possible results for this parameter is analogous to that for the Healing Rate.

This research considered that the permeability properties were of greater importance regarding the recovery of properties in concrete. Thus, the main parameter in this study was the Healing Rate. This consideration was due to the possibility that a visual closure of cracks, which can occur in the surface, might not have a consequence in effectively blocking of the water flow at the testing pressure. If the crack is visually closed but water can still pass through the specimen, durability is not improved by the closure.

4.2.2 Relation between permeability and crack width measurements

The methodology exposed in Chapter 3 was also used to analyze the relation between average crack width and permeability. From the literature, it is known that the relation follows a cubic expression with only the cubic coefficient (Edvardsen, 1999), but this could be modified by the presence of fibers, as it was reported by Lawler, et al. (2003) (see section 2.3.5.3.1). The dispersion graph Fig. 4-1 displays the values of crack width versus the corresponding values of water flow. It can be seen that the final values experienced notably higher dispersion, which indicates a weaker relation between the final water flow and the final crack width.

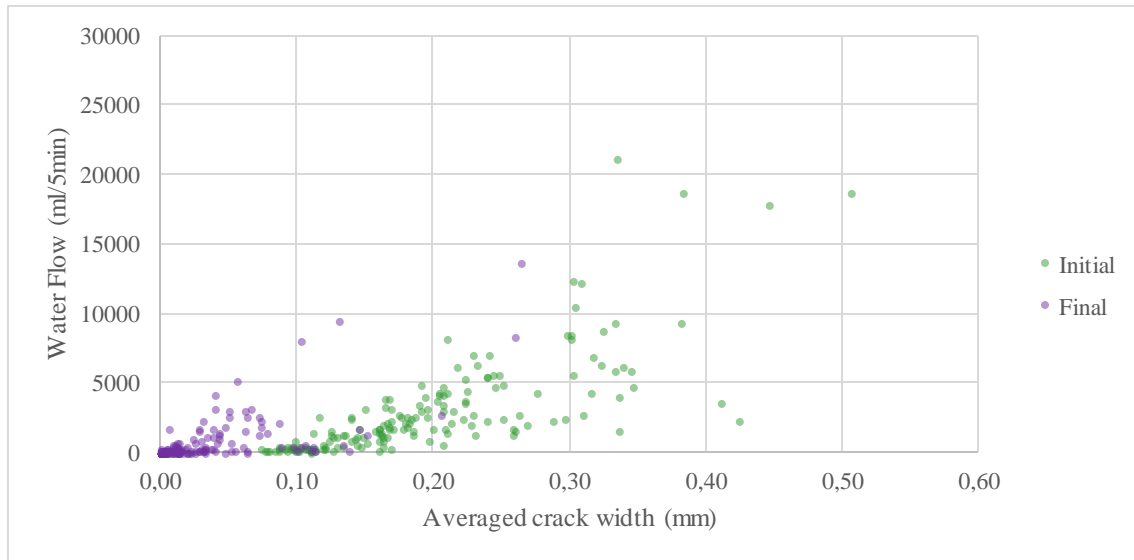


Fig. 4-1 – Average crack width and permeability results.

To better estimate the relation between water flow and crack width, only initial values are considered (169 values). Fig. 4-2 shows the trendlines calculated without robustness and applying two different robustness methods: LAR and Bisquare methods. The applied boundary condition is to adjust to a cubic polynomial curve with only the cubic coefficient.

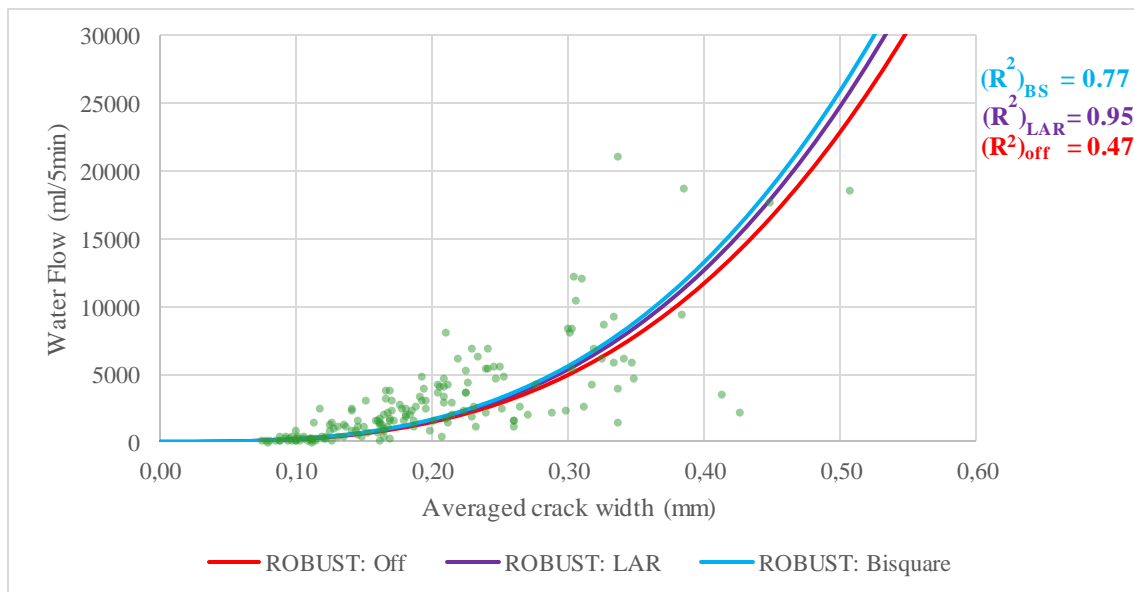


Fig. 4-2 – Initial crack width versus initial water flow with trendline with different adjustments.

These trendlines were used to estimate several theoretical values of initial water flow for each value of initial crack width, as displayed in Table 4-2. Bolded numbers indicate the limit values that will be used to analyze the following results. Thus, an initial damage of crack width 0.25 mm will be equivalent to a result in the permeability test of [2864-3245] ml/5min, while an initial damage of crack width 0.40 mm will be equivalent to a result in the permeability test of [11731-13293] ml/5min. These values will be used as the limits for the graphs in the discussion.

Crack width	Theoretical Water Flow		
	ROBUST: Off	ROBUST: LAR	ROBUST: Bisquare
x (mm)	y ₁ (ml/5min)	y ₂ (ml/5min)	y ₃ (ml/5min)
0	0	0	0
0,05	23	25	26
0,1	183	199	208
0,15	619	670	701
0,2	1466	1588	1662
0,25	2864	3102	3245
0,3	4949	5360	5608
0,35	7859	8511	8905
0,4	11731	12704	13293
0,45	16703	18088	18927
0,5	22913	24813	25963
0,55	30497	33025	34556
0,6	39593	42876	44863

Table 4-2 - Theoretical water flow for different crack widths depending on the type of adjusted curve.

Edvardsen (1999) proposed a model based on Poiseuille Law, which is expressed in equation (1), for water at 20°C, viscosity $\nu = \eta/\rho = 1.00 \text{ mm}^2/\text{s}$ and a visible crack length of 1 meter; where q_0 is the water flow per meter length of crack, I is the hydraulic gradient in meters of water head per meter, w_{avg} is the mean value of crack width and k_t is a correcting parameter for temperature.

$$q_0 \left(\frac{\text{liters}}{\text{m}} \right) = 740 * I * w_{avg}^3 * k_t \quad (1)$$

This expression can be adjusted to the parameters of the present research by changing units and the length of the crack (considered as 75 mm), resulting in the expression (2).

$$Q \text{ (liters)} = 740 * \frac{20}{0.15} * w_{avg}^3 * 1 * 0.075 \quad (2)$$

The theoretical predictions given by equation (2) fit the obtained results of water flow and average crack width in this research reasonably well, particularly for smaller cracks, as displayed in Fig. 4-3. The lower values obtained in this research might be due to the presence of fibers, which could block water flow inside the crack, as it was demonstrated by Lawler, et al. (2003), see Fig. 2-21 in Chapter 2.

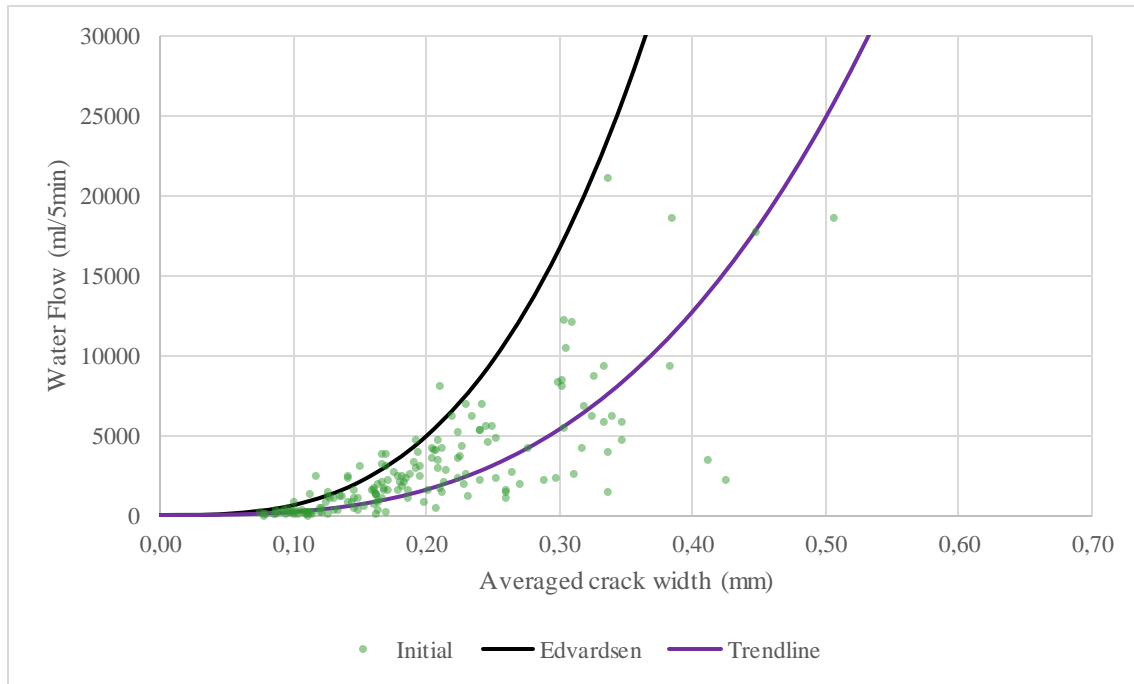


Fig. 4-3 - Comparison between experimental and theoretical water flow and crack width results

The dispersion obtained in the results of this research could be caused by healing in different points of the interior of the crack since crystallization could start easily in the zones with lower crack width. Fig. 4-4 represents a simplification of some of the possible interior morphologies of a crack in a concrete specimen, and the points that might be more suitable in order to start the precipitation of crack healing products. If the morphology of the crack is a concave volume, the interior of the crack may be healing while the visible crack would stay immutable, which could distort the results.

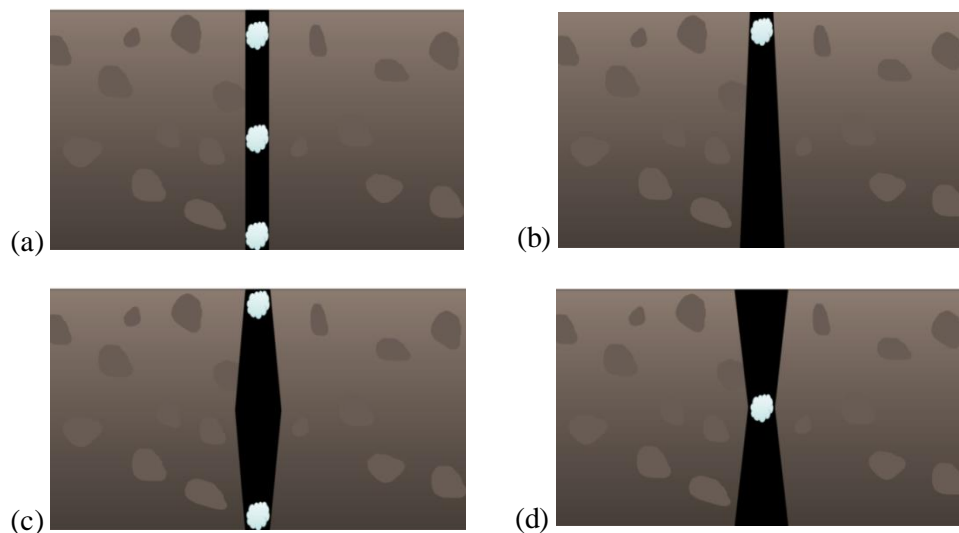


Fig. 4-4 - Simplification of different possibilities for crack geometry in depth: uniform crack, pyramidal frustum, convex and concave forms and their most feasible points for precipitates.

4.2.3 Repeatability of results

This research uses the results from two campaigns. Before comparing their values, the repeatability must be studied by analyzing the results of the groups with coincident parameters. In this case, it was compared using the values of specimens healed under water immersion for initial water flows smaller than 1000 ml/5min, as it is the bracket with the higher density of points, for both control specimens and specimens with crystalline admixtures.

Fig. 4-5 shows these values for the 1st campaign (S1) and for the 2nd (S2). In this graph, it can be seen that CA specimens clearly present the same response for both series. Control specimens show higher dispersion but, since control groups always showed higher dispersion than CA specimens in this research, it was assumed that both campaigns are directly comparable. As consequence, results will be used indistinctly from both campaigns in the discussion in 4.3.

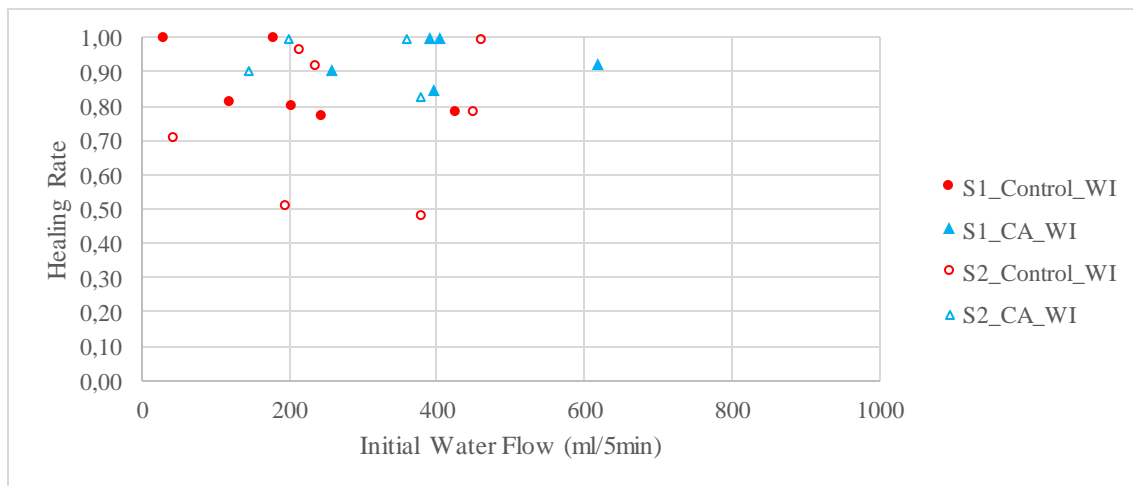


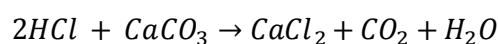
Fig. 4-5 – Comparison between 1st campaign (S1) and 2nd campaign (S2).

4.3 Discussion

This section analyzes the obtained results and the effect of each parameter on the self-healing properties of concrete.

4.3.1 Qualitative evaluation of crack sealing

A qualitative evaluation of the composition of crystals leaching out of the crack was performed both for control specimens and for specimens with crystalline admixtures. The purpose of this evaluation was to discern if the main composition of those products were calcium carbonates (CaCO_3) or a different type of products. To this purpose, chlorhydric acid (HCl) was used since it reacts with carbonates. The reaction between HCl and CaCO_3 is:



This reaction produces clear effervescences due to the release of carbon dioxide.

Fig. 4-6 shows the uptake of crystals samples and the materials used for the test.

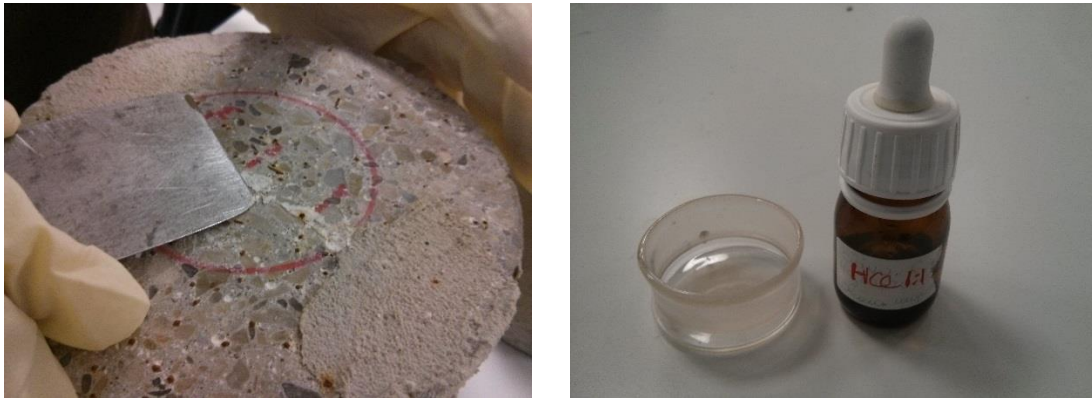


Fig. 4-6 – Sample taking of crystals leaching out of the crack and diluted chlorhydric acid.

The reaction that took place indicated that the products were mostly carbonates, even though the specific type of carbonates could not be discerned by this test. In Fig. 4-7, the aspects of the crystals before and after being in contact with chlorhydric acid is shown.



Fig. 4-7 – Reaction produced between crystals and diluted chlorhydric acid.

In addition, the formation of precipitates inside the crack under different conditions was studied by visual observation of the cracks. As first and immediate aspect of the crack sealing was the appearance of whitish formations in control and CA specimens when immersed in water. As a matter of fact, for specimens conditioned in the “water contact” environment, those white precipitates were only formed on the face in direct contact with water. Consequently, the transportation of water through the crack with a water layer of two centimetres was not enough for ensuring healing of both faces. Despite the smaller reaction of the bottom crack, specimens stored in the WC exposure achieved fairly high Healing Rates, which can be due to the blocking or healing of only one face.

The white precipitates were located all along the surface of the specimens in contact with water, not only inside the crack, but also in some pores. The precipitates were slightly yellowish in some cases, which could have been caused by the oxidation of steel fibres. Fig. 4-8 compares the sealing

of a crack in a specimen in direct contact with water with the sealing of a crack in a specimen under moist conditions (*i.e.*, without direct contact with water).

Another aspect that can be studied through the analysis of the crack pattern is determining whether the healing occurred only when the crack was in the cement paste, or if it also occurred when the crack broke through an aggregate (or in the paste-aggregate interface). This was analysed in the specimens with sealed or almost sealed cracks. It was concluded that most formations were originated in the cement paste, which is logical, because crystalline admixture is dispersed in concrete matrix among with the cement particles, but the healing process was also powerful enough to transport the healing products inside small cracked aggregates, which is an indicator of the effectiveness of the self-healing agent. Fig. 4-9 shows the appearance of sealed cracks in different locations for CAC specimens in the water immersion exposure.

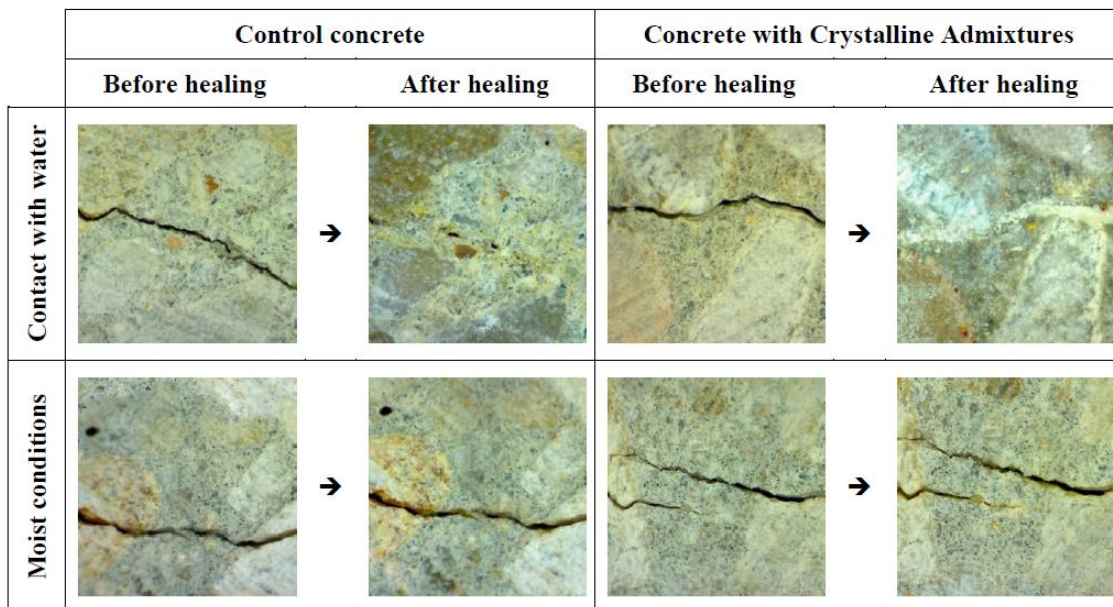


Fig. 4-8 – Comparison between crack aspect at 0 days and after 42 days of healing, for control and CA specimens exposed to environments with and without direct contact with water.

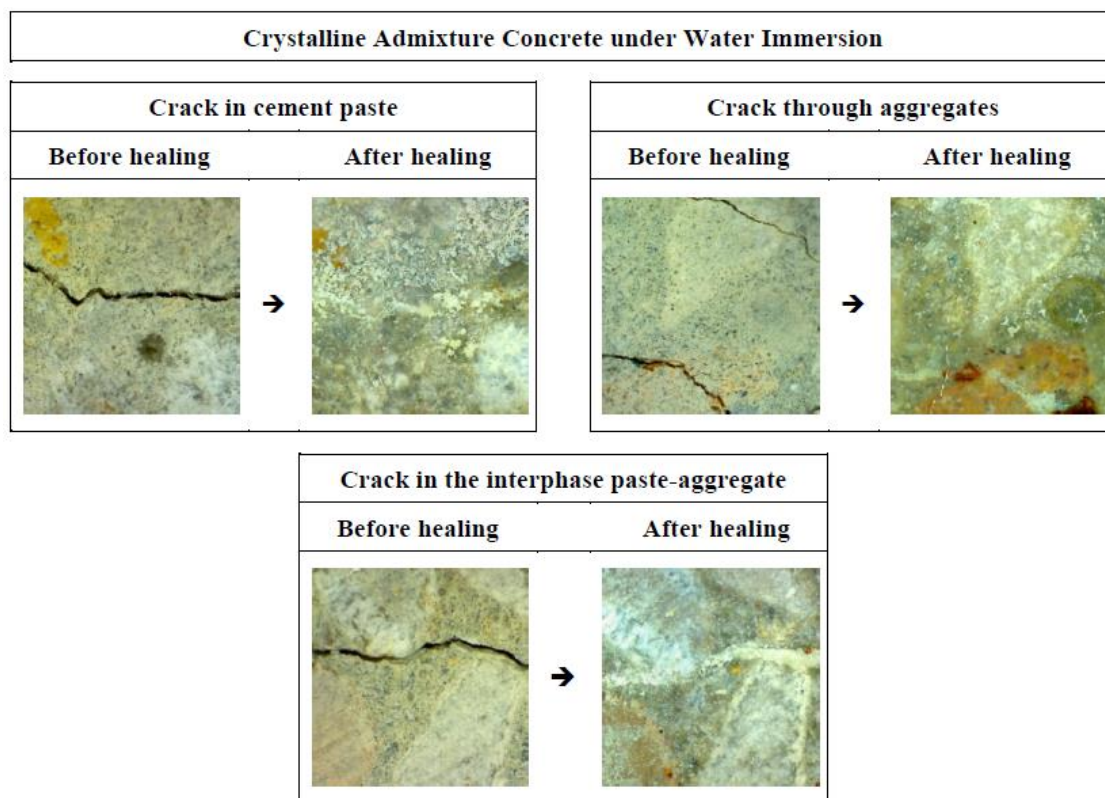


Fig. 4-9 – Comparison between crack aspect at 0 days and after 42 days of healing for CAC specimens exposed to water immersion (WI) for cracks located in: cement paste, aggregates and in the interphase paste-aggregate.

4.3.2 Effect of initial damage on self-healing

As it has been explained in the state of the art, the more damaged a specimen is, the smaller healing properties it will present. However, there was no agreement between the limit values of initial damage in order to achieve complete healing. In this research, cracks up to 0.40 mm have been analyzed (around 13000 ml/5min).

The first analysis on the effect of the initial damage was performed using specimens stored under water immersion at 15°C, for both mix designs, as they are the groups with the higher amount of specimens and it is the most studied exposure in the literature.

Fig. 4-10 shows the obtained values of Healing Rates for permeability tests for these groups. As it was expected, in general, specimens critically damaged achieve lower Healing Rates than those with smaller damages. There is an exception for very small cracks, where there is a high dispersion of results, presenting lower Healing Rates results.

For specimens under water immersion, Healing Rates can be notable even for specimens with large damages. Specimens with initial water flow higher than 4000-5000 ml/5min are unlikely to heal completely. That water flow represents an initial crack opening around 0.30 mm.

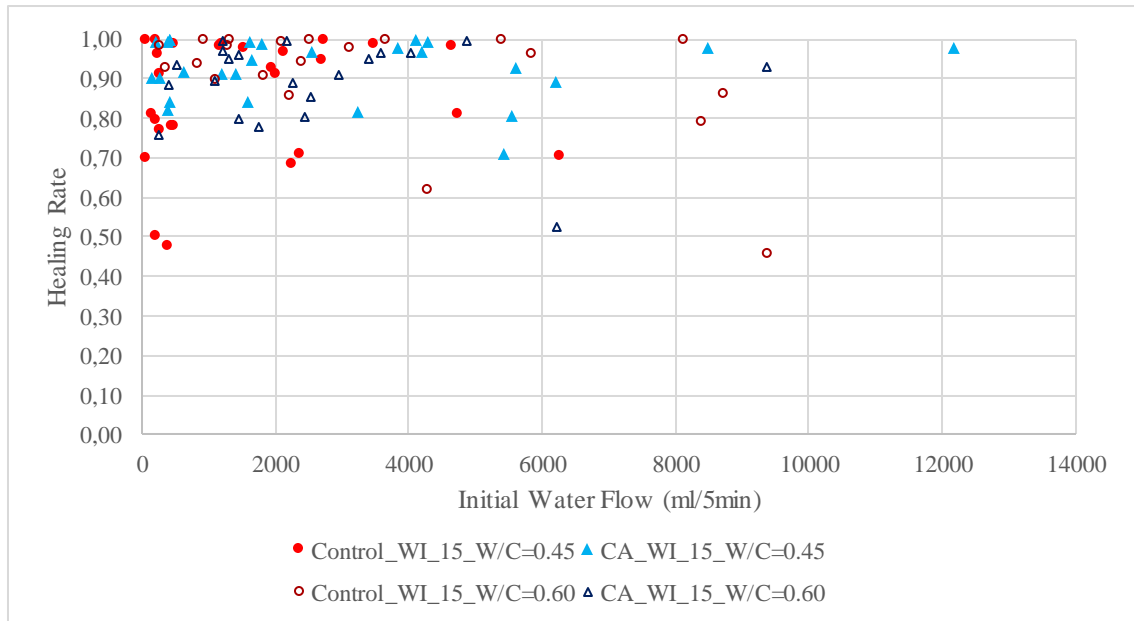


Fig. 4-10 – Healing Rate by permeability of specimens stored under water immersion at 15°C.

More specifically, Fig. 4-11 shows the Healing Rates results for initial water flows under 3000 ml/5min (which is approximately a crack opening of 0.25 mm). This graph clearly shows the high dispersion for low initial water flows, up to 500 ml/5min, which represents a crack width around 0.1-0.15 mm. A more stable response has been achieved after that threshold, in which, as it was expected, the results decrease slowly when increasing the damage.

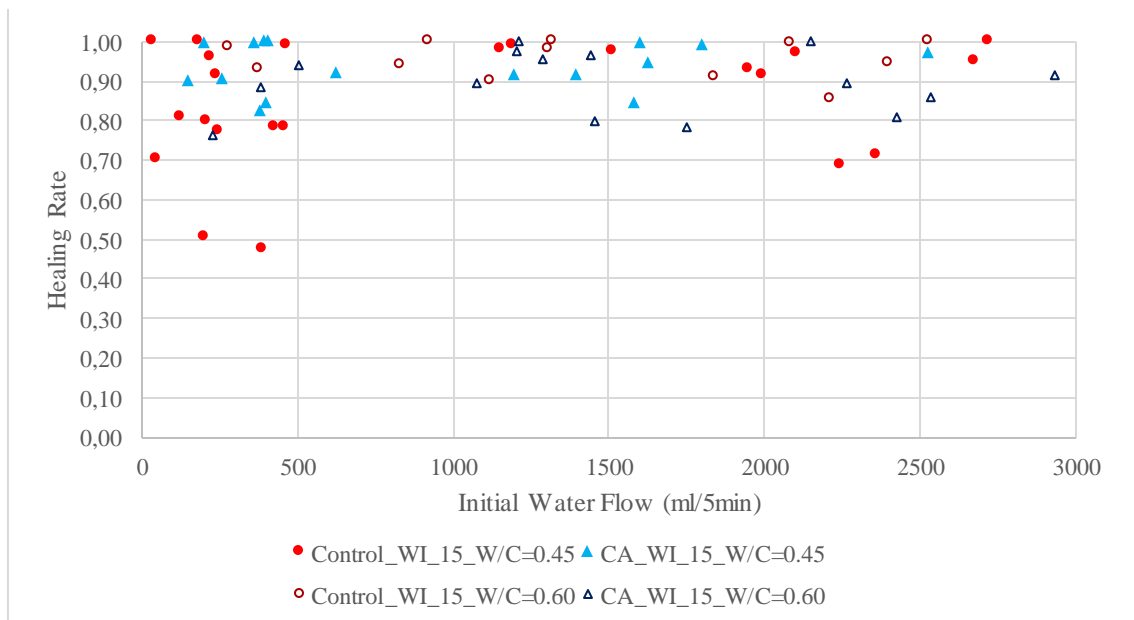


Fig. 4-11 - Healing Rate of specimens stored under water immersion at 15°C and crack width under 0.25 mm.

The Sealing Rates are shown in Fig. 4-12. They are notably higher than Healing Rates, but they follow the same general trends, e.g., specimens with cracks larger than 0.25-0.30 mm were unlikely to heal completely after 42 days of exposure under water immersion at 15°C. Sealing rates also present a high dispersion for very small crack widths.

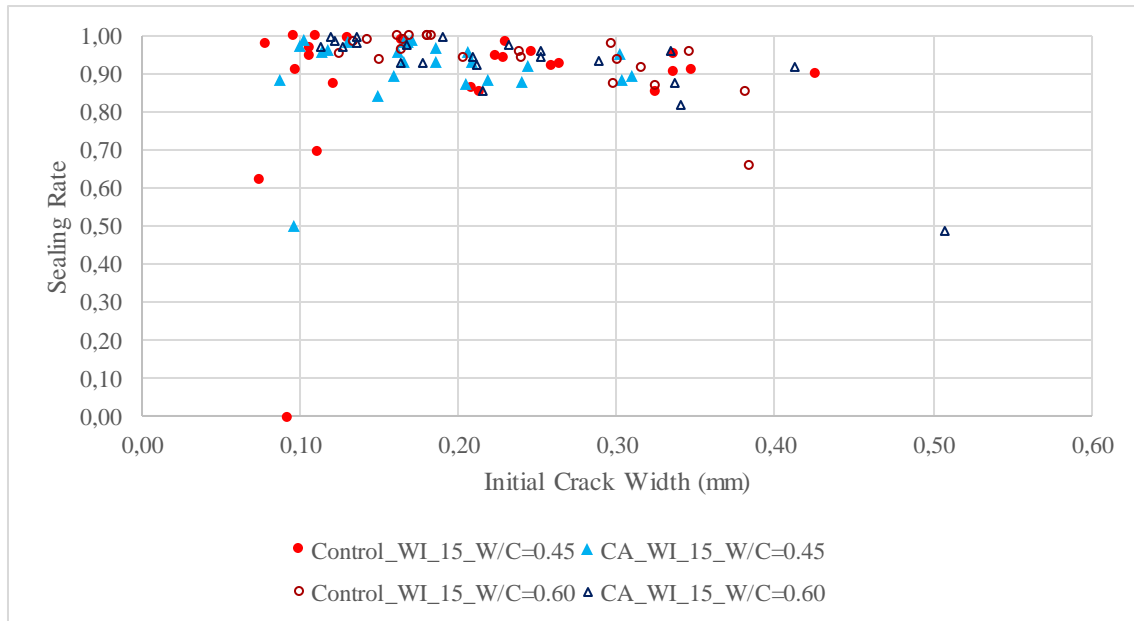


Fig. 4-12 - Sealing Rate by crack closing of specimens stored under water immersion at 15°C.

The high dispersion obtained for smaller initial damages in both parameters could be caused by the precision limits of the method or by the existence of a damage threshold for recovering properties, as it has been indicated in some studies from the literature. This aspect should be further investigated in order to verify the origin of this phenomenon.

Considering Healing Rate higher than 0.90 as a “good” self-healing, it can be said that for both, autogenous and crystalline-based specimens, 0.3 mm cracks are the limit for achieving a good healing when exposed to water immersion during 42 days. This conclusion seem consistent for both CA and CAC specimens.

4.3.3 Effect of water/cement ratio and cement content

One of the objectives of this research was to evaluate the effect of water/cement ratio and cement content for both autogenous healing and crystalline-based self-healing. Fig. 4-13 and Fig. 4-14 show the Healing Rate and Sealing Rate results for the four groups, where it can be seen that there are not notable differences between specimens with w/c ratio of 0.45 and 0.60.

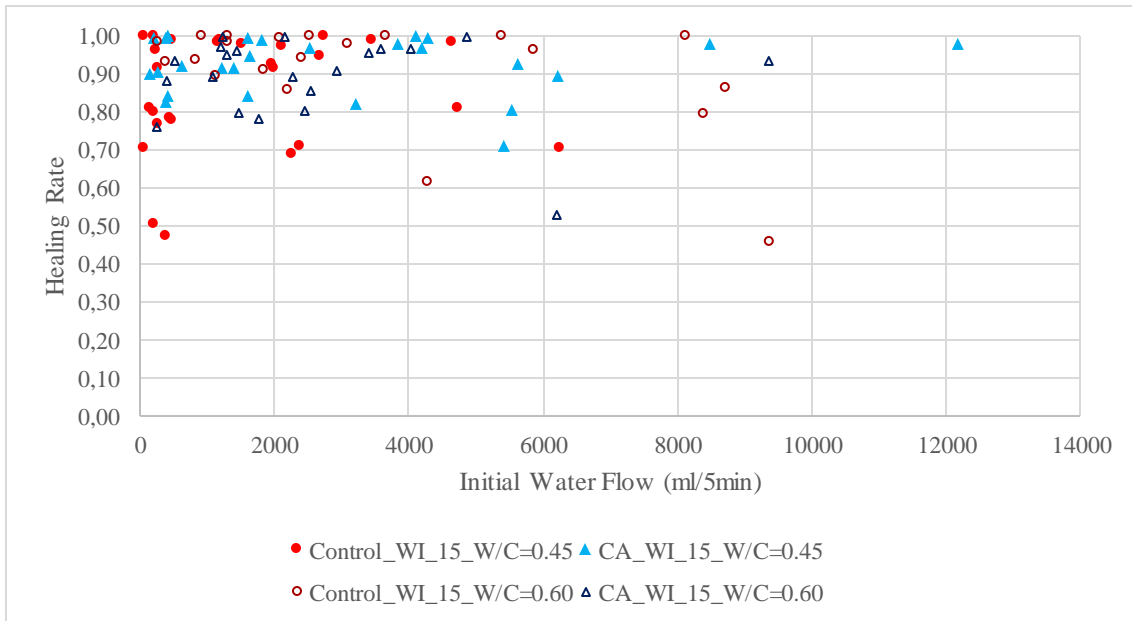


Fig. 4-13 - Healing Rate by permeability of specimens stored WI_15 with w/c of 0.45 and 0.60.

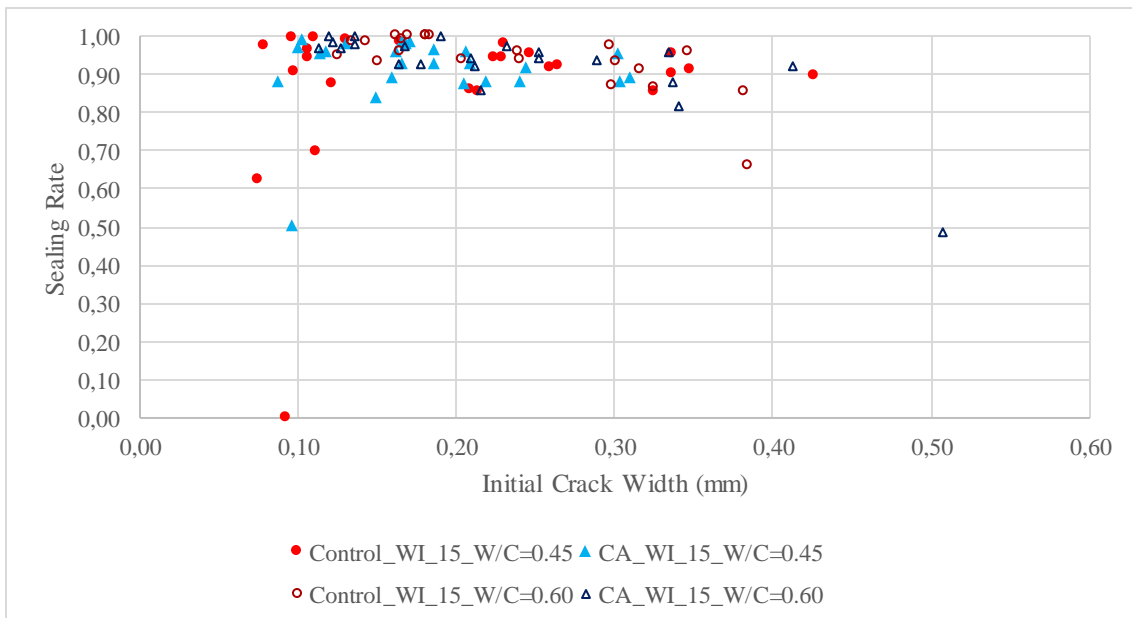


Fig. 4-14 - Sealing Rate by crack closure of specimens stored WI_15 with w/c of 0.45 and 0.60.

More specifically, dividing graphs in one for control specimens and the second for CAC specimens (Fig. 4-15 and Fig. 4-16 respectively) it can be seen that differences for autogenous healing are not notable, but the group with w/c ratio of 0.60 showed slightly better behavior. On the contrary, the trend was the opposite for CAC specimens, with w/c = 0.45 specimens seemingly behaving better, according to the permeability tests. Nevertheless, it should be noted that differences from the different mixtures are not of a huge effect.

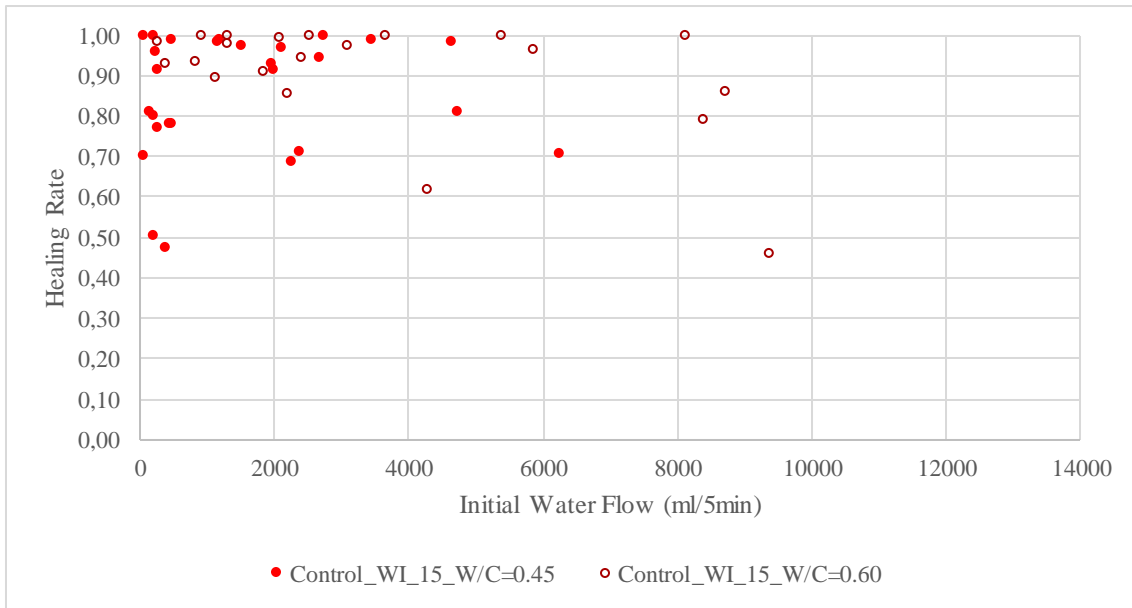


Fig. 4-15 - Healing Rate by permeability of control specimens stored WI₁₅ with w/c of 0.45 and 0.60.

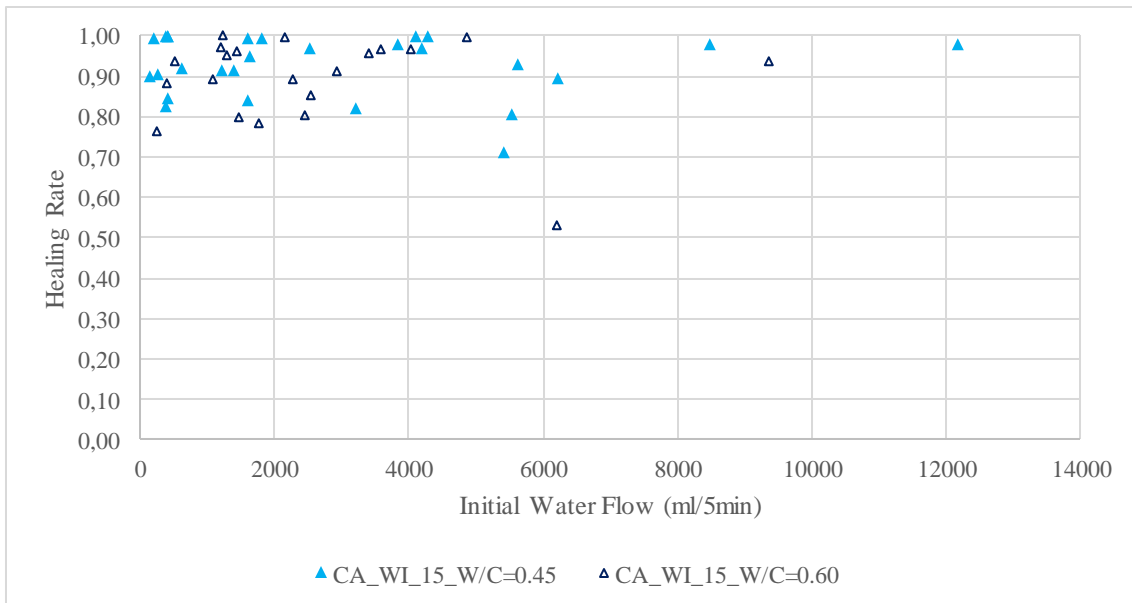


Fig. 4-16 - Healing Rate by permeability of CA specimens stored WI₁₅ with w/c of 0.45 and 0.60.

4.3.4 Effect of crystalline admixtures

Regarding the effect of crystalline admixtures, it can be seen from results that for specimens with W/C ratio of 0.45 and stored under water immersion at 15°C, there was an enhancement of the healing properties. This enhancement was mostly caused by improving the minimum Healing Rate (Fig. 4-17). The maximum value of Healing Rate was not increased by the addition of CA, as there are also control specimens with Healing Rates of almost 1.00. In this way, the effect of the crystalline admixtures on self-healing seemed to be an increase in the stability of the phenomenon.

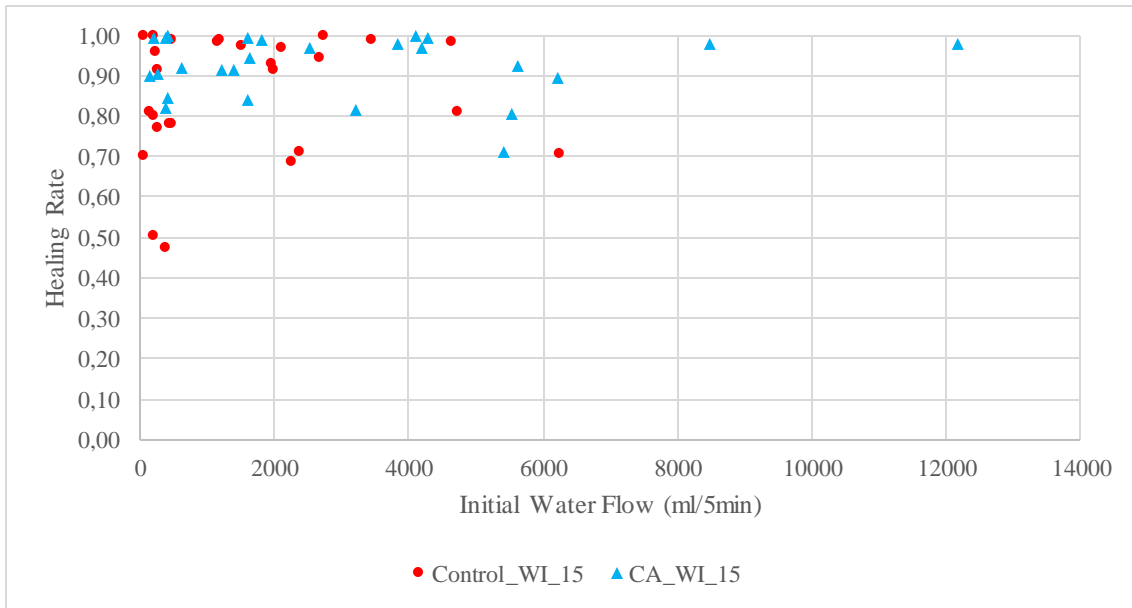


Fig. 4-17 - Healing Rate by permeability of specimens stored under WI at 15°C with w/c of 0.45.

Increasing the temperature of water to 30°C quickened the reaction (see Fig. 4-18), and the results show that in this case all CAC specimens achieved Healing Rates above 0.95. Control specimens also achieved better overall results, but a bit of dispersion still remains.

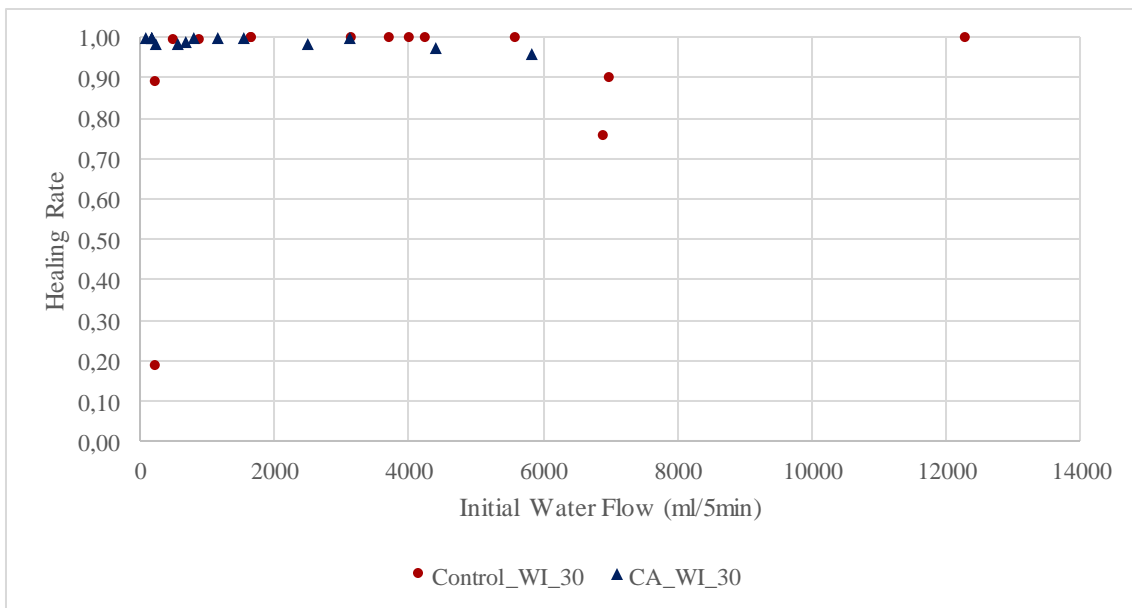


Fig. 4-18 - Healing Rate by permeability of specimens stored under WI at 30°C with w/c of 0.45.

Fig. 4-19 shows the results for w/c ratio of 0.60. In this case, it seems that the addition of CA did not improve self-healing; on the contrary, the autonomous healing induced by the crystalline admixture seemed to be worse than the autogenous healing of control specimens. That contrasts with the slight positive effect on the behavior for w/c ratios of 0.45.

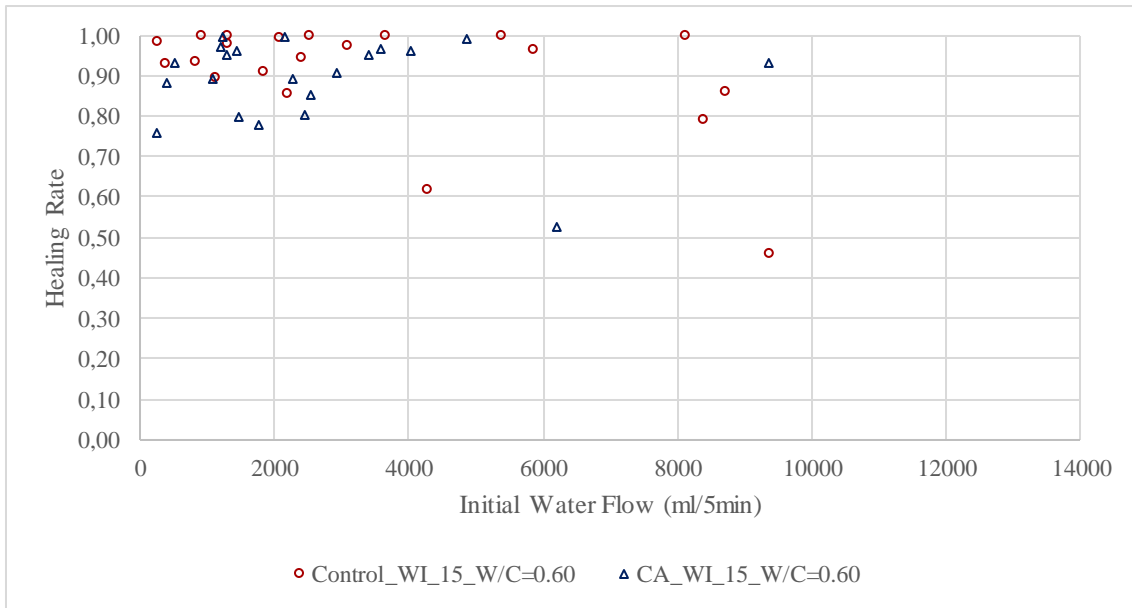


Fig. 4-19 - Healing Rate by permeability of specimens stored under WI at 15°C with w/c of 0.60.

4.3.5 Effect of healing exposure

The healing properties of specimens with w/c ratio of 0.45 have been analyzed under six different exposures, but only in the small range cracks (up to 0.25 mm). The healing results, by means of permeability tests, are shown in Fig. 4-20. It was registered that a few specimens that were stored in low humidity exposures had negative Healing Rates (represented as 0). This can be caused by the lack of moisture to counteract the shrinkage of specimens, thus increasing the crack opening.

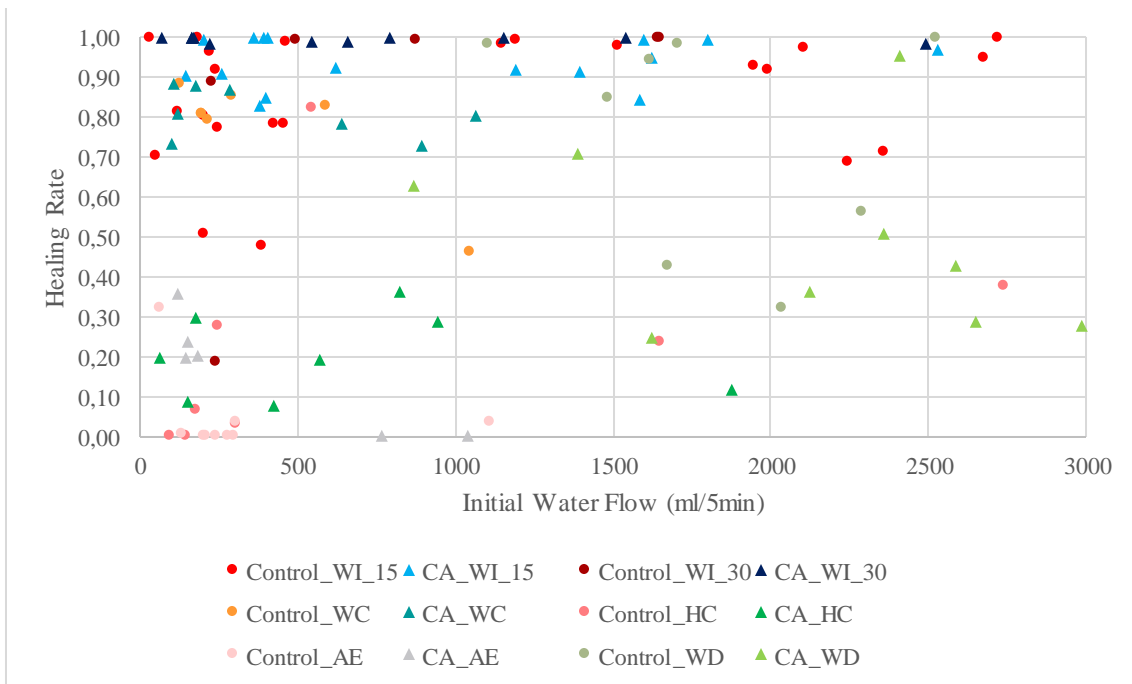


Fig. 4-20 - Healing Rate by permeability of specimens with w/c of 0.45 with small cracks.

Fig. 4-21 and Fig. 4-22 show the effect of the healing exposure for control and CAC specimens respectively. It is worth noticing that only two specimens from the CA group obtained negative

healing rates, and both for the low humidity exposure (AE). Negative healing rates were more frequent in control specimens, taking place for AE and for the Humidity Chamber exposure as well. This could be caused by a possible shrinkage compensation due to the presence of CA. For both cases, higher healing rates were achieved when specimens were stored under water immersion. Wet/dry cycles and water contact of 2 cm of water layer showed similar behaviors for control specimens. In contrast, for CAC specimens, the WC exposure achieved better results and less dispersion than W/D conditions. In general, it is clear that CAC specimens got less dispersion for all exposures, which indicates a more reliable and predictable behavior of concrete with this admixture.

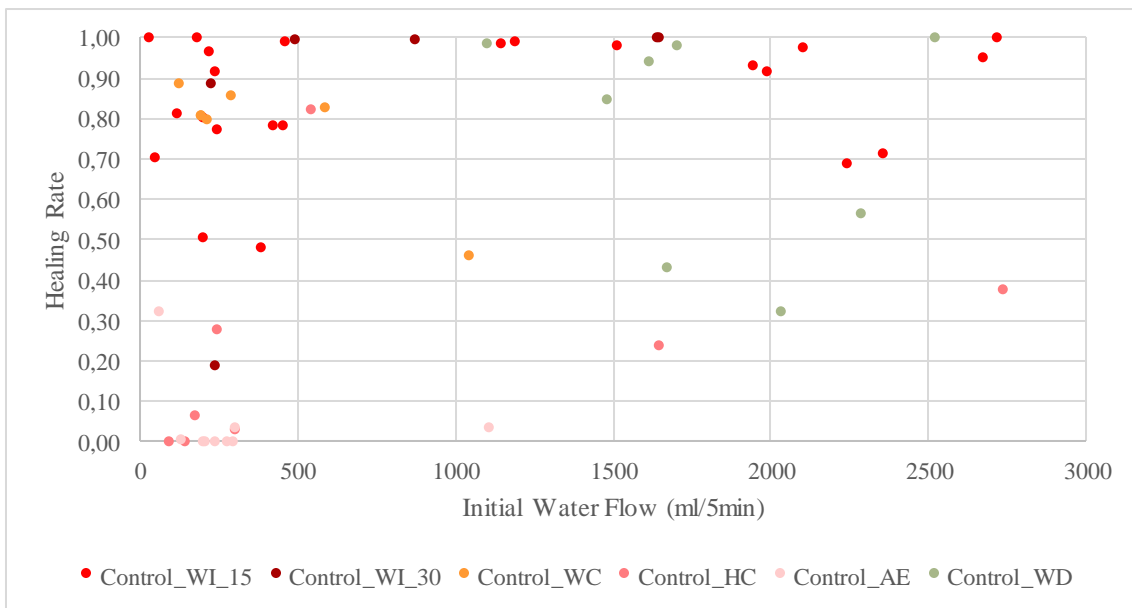


Fig. 4-21 - Healing Rate by permeability of control specimens with w/c of 0.45 with small cracks.

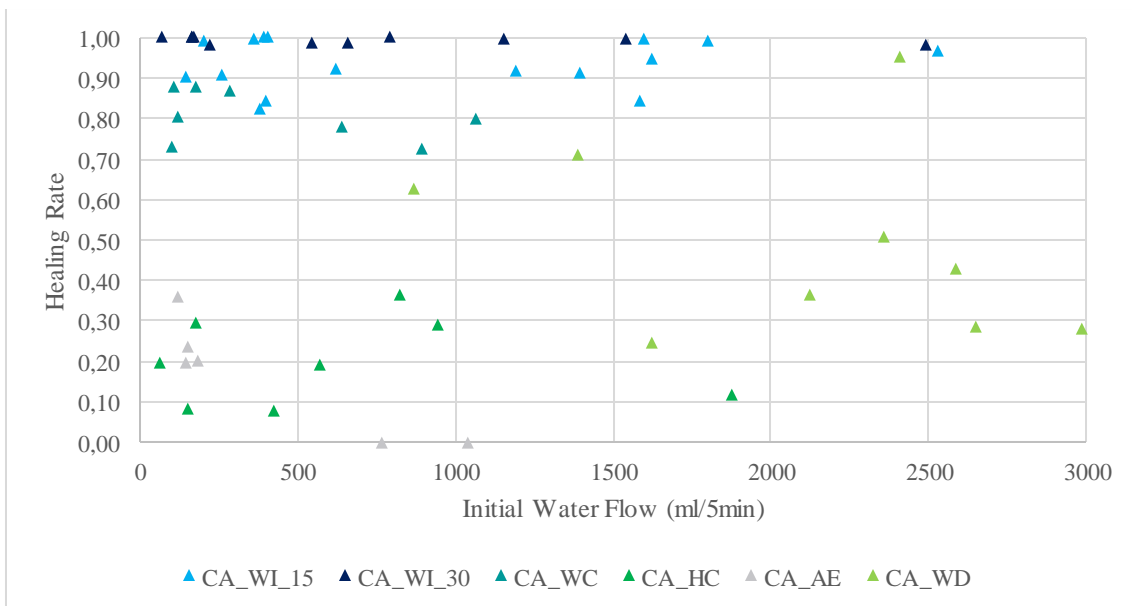


Fig. 4-22 - Healing Rate by permeability of CA specimens with w/c of 0.45 with small cracks.

The results for larger cracks are very similar (see Fig. 4-23), with specimens in direct contact with water obtaining higher Healing Rates than those in different moist conditions. Wet/dry cycles obtained Healing Rates below 0.50 for CA specimens and around 0.50 for control group. That means that for structures under cycling regimes (with periods under water immersion and drying periods) healing phenomena is not effective for achieving a proper response. This contrasts with some of the results described in the state of the art, where specimens under the exposure of wet/dry cycles registered as more efficient than water immersion.

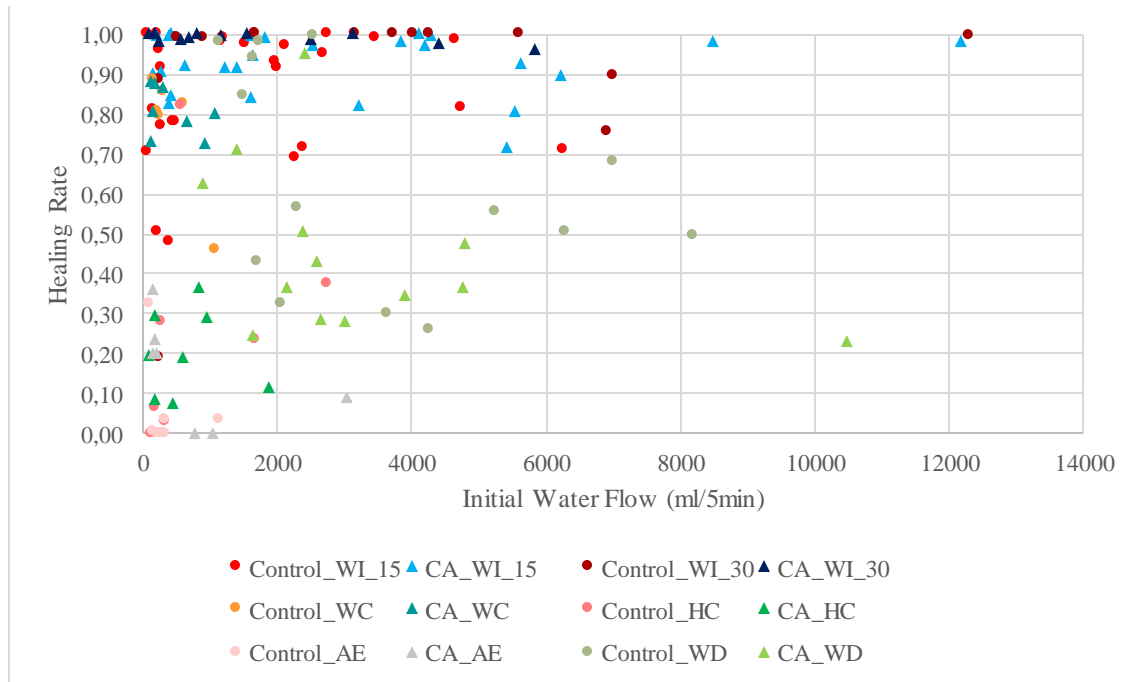


Fig. 4-23 - Healing Rate by permeability of specimens with w/c of 0.45.

Sealing Rates maintained the same trend but in general with higher values (Fig. 4-24). This means that an evaluation of visual closure can overestimate the healing capability in comparison to the recovery of durability properties. Because of that, an evaluation of self-healing only by visual observation could lead to misconceptions of the real recovery of properties. Using the Sealing Rate it was also concluded that WI at 15 and 30°C were the exposures with the best results, and that self-healing was directly correlated with the amount of water available for the reaction. The biggest differences were achieved for specimens in the exposures of WC and WD cycles.

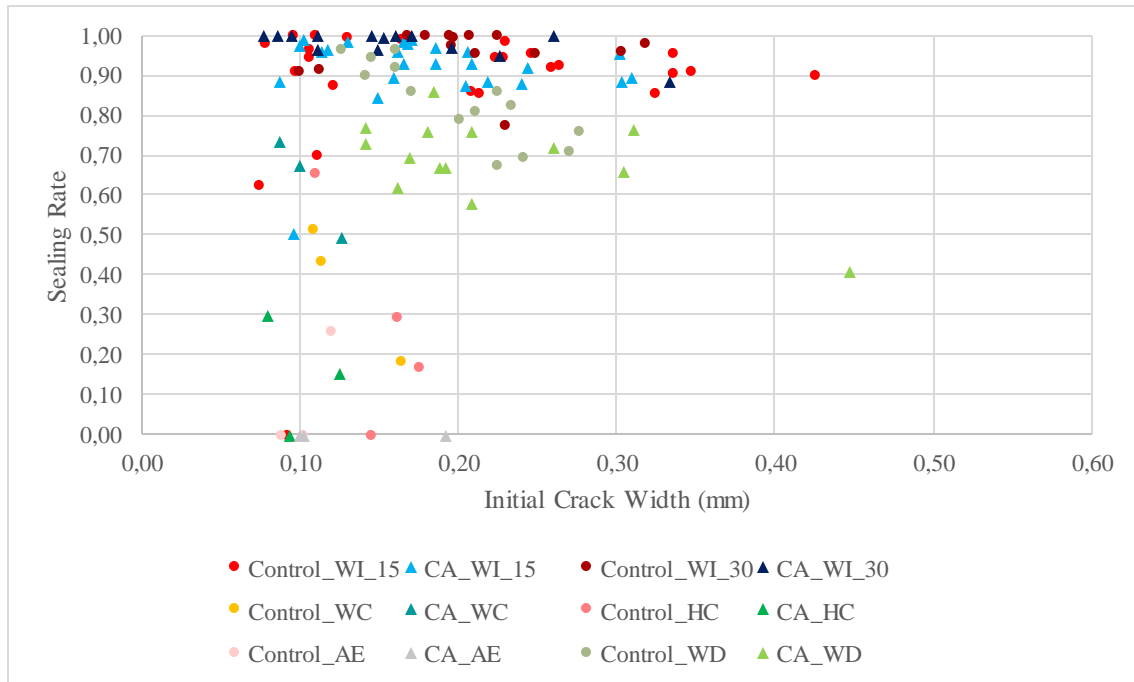


Fig. 4-24 - Sealing Rate by permeability of specimens with w/c of 0.45.

Fig. 4-25 and Fig. 4-26 show the effect of the healing exposure for control and CA specimens respectively for larger cracks. Specimens with initial water flows under 6000 ml/5min were able to heal almost completely under water immersion for both autogenous and CA-based healing. Control specimens showed high dispersion while CAC specimens were gathered in clear groups depending on the exposure. CAC specimens under the AE and W/D exposure had higher dispersion than the rest of exposures for that mixture. For CA groups, increasing the water content clearly increased the healing rates.

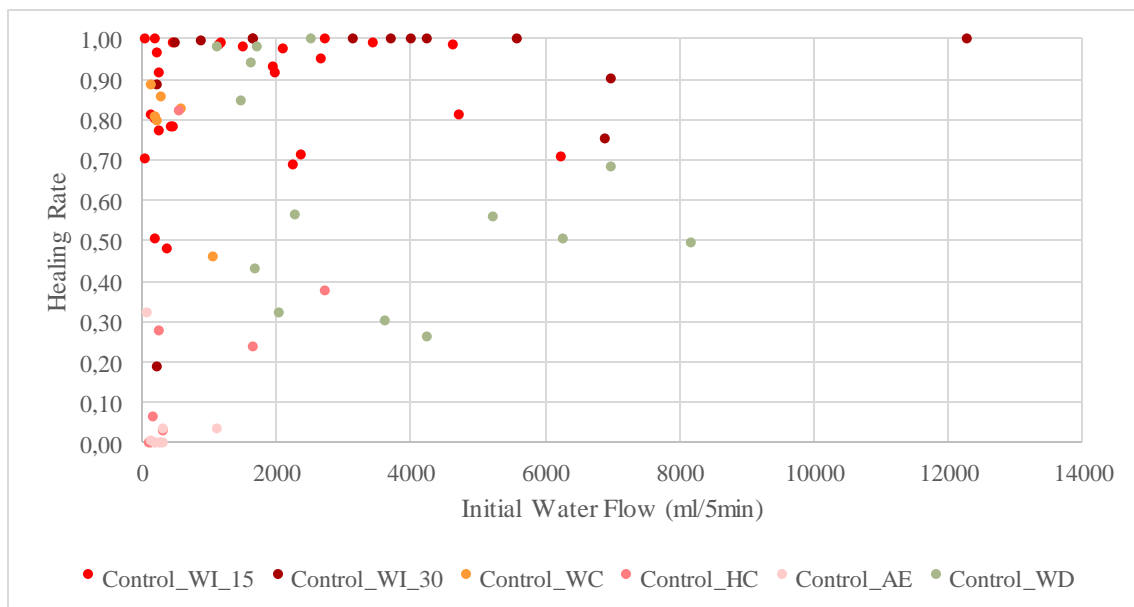


Fig. 4-25 - Healing Rate by permeability of control specimens with w/c of 0.45.

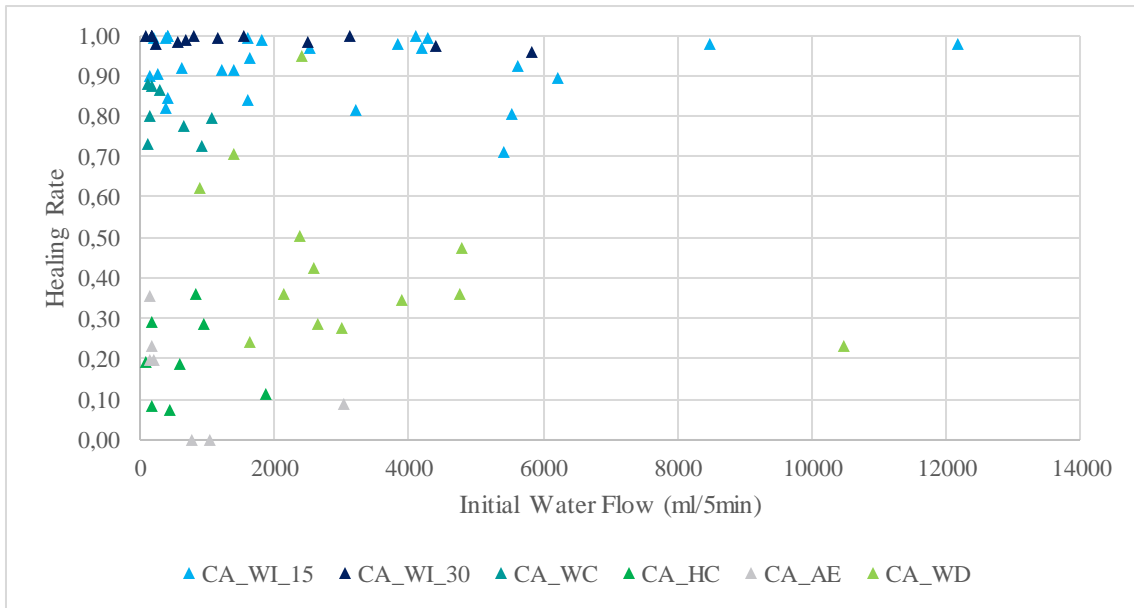


Fig. 4-26 - Healing Rate by permeability of CA specimens with w/c of 0.45.

Fig. 4-27 and Fig. 4-28 analyze separately those specimens in exposures with direct contact with water (WI_15, WI_30, WC and W/D) and pre-cracked to low levels of damage (up to 0.25 mm). For control specimens (Fig. 4-27) there was a high dispersion zone for cracks smaller than 0.10 mm, and several specimens achieved almost complete healing (healing rates around 1.0). For CAC specimens (Fig. 4-28) results were disperse only in the case of W/D exposure. In this case, most of the specimens achieved Healing Rates higher than 0.80.

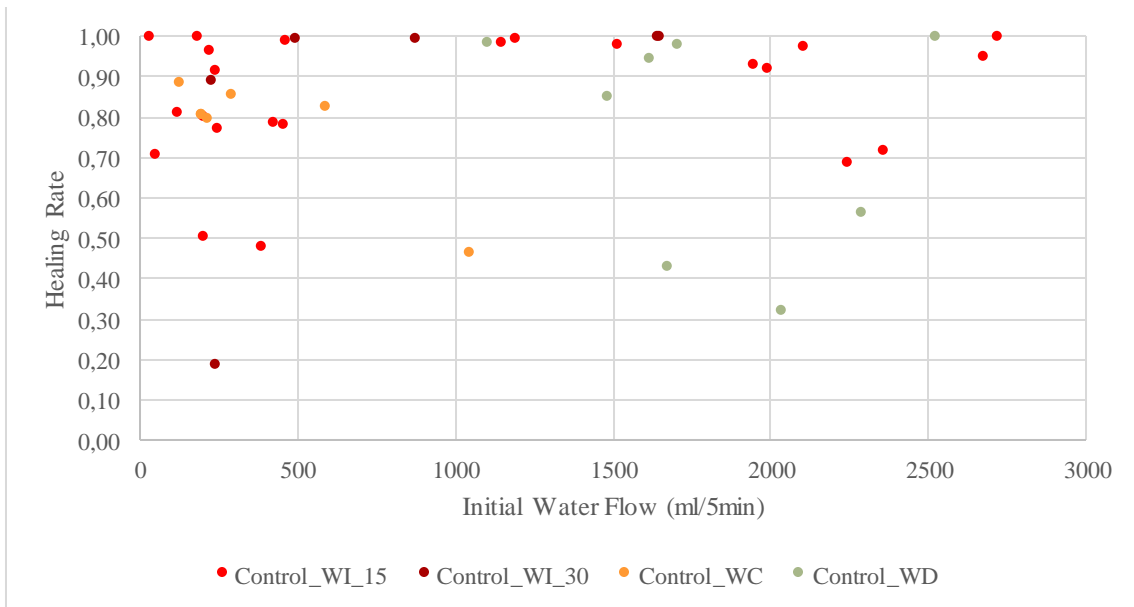


Fig. 4-27 - Healing Rate by permeability of control specimens in exposures in direct contact with water, with w/c of 0.45 and small cracks.

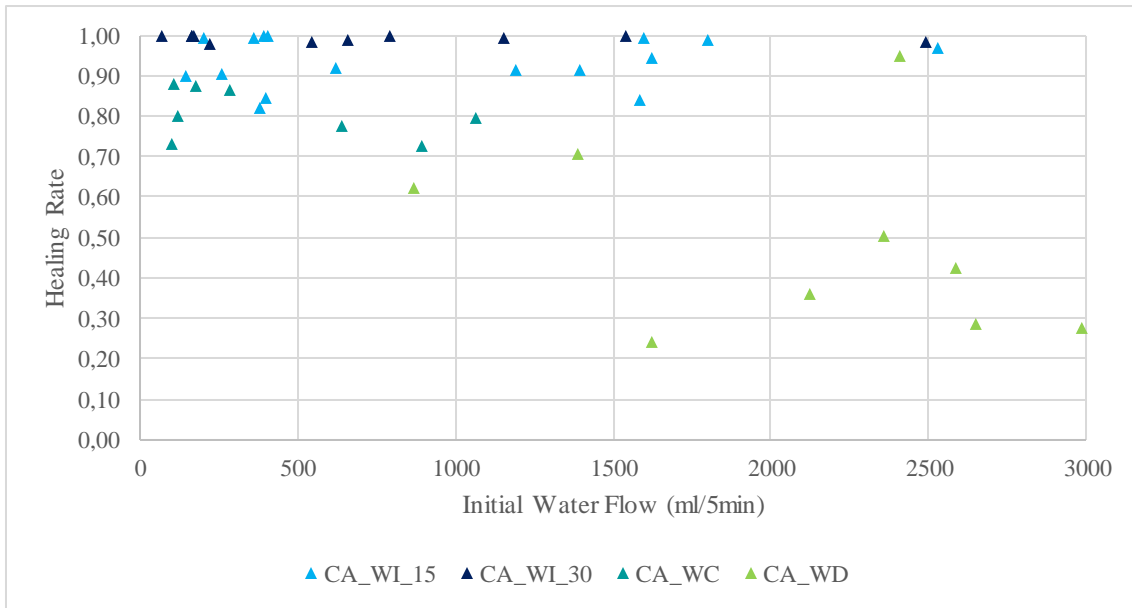


Fig. 4-28 - Healing Rate by permeability of CA specimens in exposures in direct contact with water, with w/c of 0.45 and small cracks.

Fig. 4-29 analyzes the response of specimens in exposures without direct contact with water (HC and AE) and pre-cracked to low levels of damage (up to 0.25 mm). This graph demonstrates the absence of autogenous and CA healing in those exposures, which means that the phenomenons were not reliably for these cases, nor even for high humidity environments (HC).

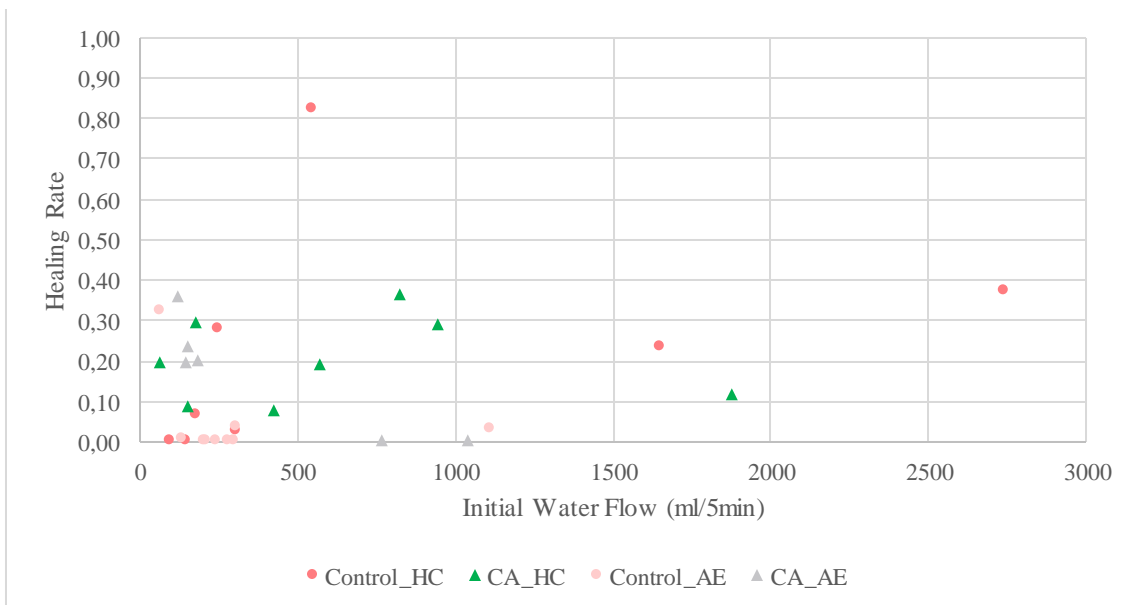


Fig. 4-29 - Healing Rate by permeability of control and CA specimens in exposures without direct contact with water, with w/c of 0.45 and small cracks.

4.3.6 Comparison between parameters

Throughout this section, sealing rates were usually shown to be higher than healing rates. This difference is of great importance in order to define a methodology of analysis for self-healing.

The values for both parameters can be contrasted for the different groups, showing that control specimens were more likely to present higher sealing rates that do not correspond with higher healing rates. This can be seen in Fig. 4-30, which displays values for specimens under water immersion at 15°C.

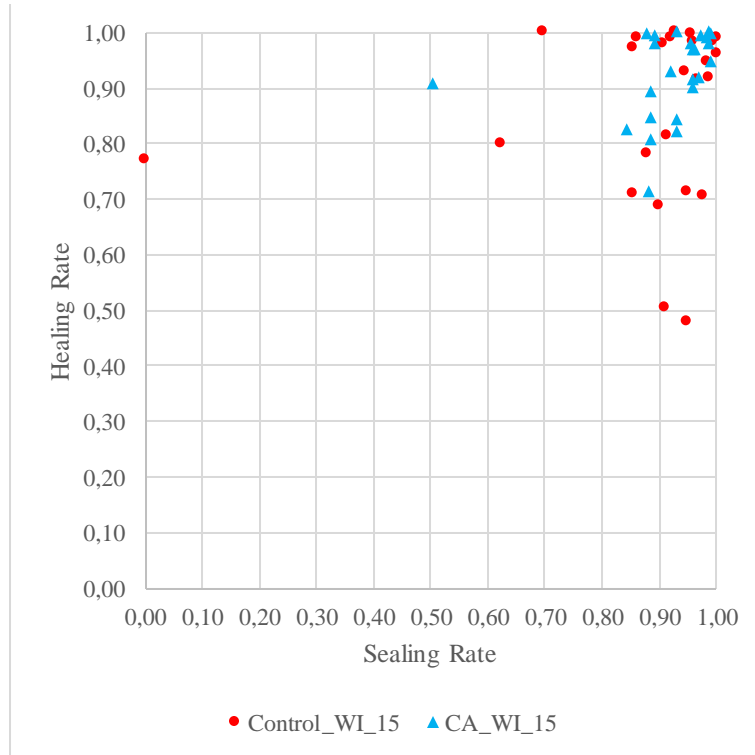


Fig. 4-30 – Healing Rate vs Sealing Rate for specimens with w/c ratio of 0.45 and exposed to water immersion at 15°C.

Comparing the values obtained for the two mix compositions (Fig. 4-31), it can be seen that there were no notable differences. That means that w/c ratio did not change the predominance of the healing or sealing behavior.

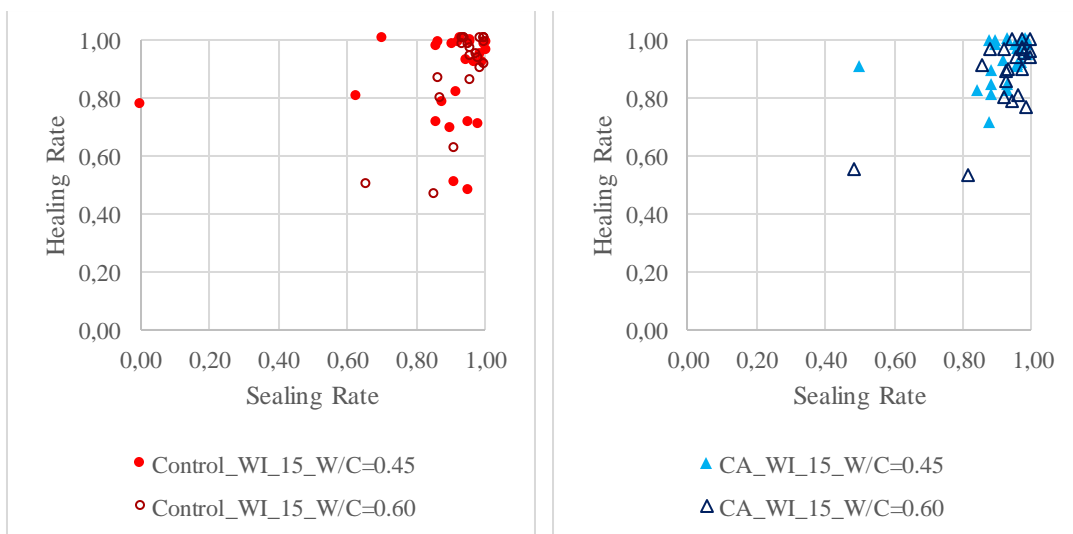


Fig. 4-31 - Healing Rate vs Sealing Rate for control (left) and CA (right) specimens with w/c ratio of 0.45 and 0.60, exposed to water immersion at 15°C.

However, when comparing the results for water immersed specimens with those exposed to wet/dry cycles (Fig. 4-32) it can be seen that the latter exposure achieved much higher Sealing Rates than Healing Rates. This behavior is clear for both groups, CA and control, meaning that the visual sealing of the crack is less related to the permeability healing for specimens under these exposures than for those specimens exposed to water immersion.

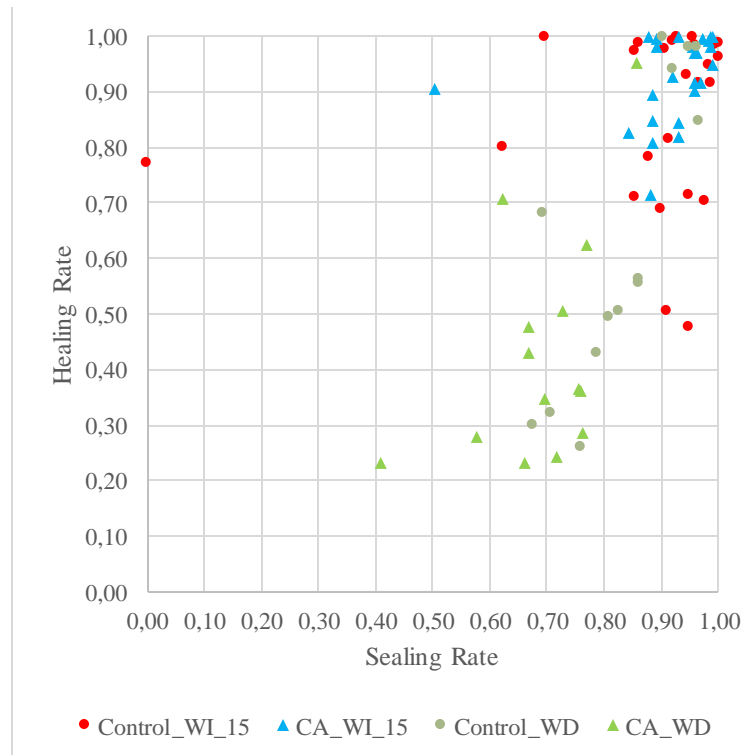


Fig. 4-32 - Healing Rate vs Sealing Rate for control and CA specimens with w/c ratio of 0.45 exposed to water immersion at 15°C and exposed to WD cycles.

It should be noted that specimens under water immersion achieved higher healing and Sealing Rates, while specimens under wet/dry cycles achieved notably worse results. The lower relation between both parameters for the WD exposure could be interpreted as an incomplete healing process in comparison to the WI exposure. As it was seen in Fig. 4-18 the results for water immersion at 30°C were even higher than for those at 15°C, which indicates a possible further development in time of healing phenomena.

The differences between both parameters is of major importance as many studies reported in the state of the art only compared the visual closure of cracks. The study of permeability properties offers more information of the durability properties of concrete structures presenting cracks and their possible healing.

4.3.7 Comparison with other studies

With reference to the Healing Rates for crystalline admixture specimens, similar values have been registered by other authors for permeability properties (Sisomphon, et al., 2012), mechanical

parameters or (Ferrara, et al., 2014; Sisomphon, et al., 2013) closure of crack width (Jaroenratanapirom & Sahamitmongkol, 2011; Sisomphon, et al., 2012) for specimens under water immersion exposure, with values of effectiveness usually around 90% of recovery, or even higher.

The enhancement of effectiveness by crystalline admixtures specimens under water immersion, compared with results of control specimens has been also confirmed by other studies (Ferrara, et al., 2014). These studies CA increased the healing capability about 7-10% with respect to control concrete, which similar to the results obtained in this work. The higher results of specimens from both groups (control and CA) under water immersion WI compared to indoor or air exposure AE specimens obtained in this work are similar to those obtained while studying the recovery of mechanical properties in other studies (Sisomphon, et al., 2013).

Regarding autogenous healing, some studies reported better results for different wet/dry cycles (Ying-zi, et al., 2005; Yang, et al., 2011; Ma, et al., 2014) while others achieved better behavior for water immersed specimens (ter Heide, 2005; Granger, et al., 2005; Qian, et al., 2009). The results from this research coincide with the latter, and concludes that the more water is available, the more healing would be produced.

Chapter 5. Conclusions and Future lines

5.1 Conclusions

This work has presented a state of the art and the results of a study on the self-healing of fibre-reinforced concrete specimens. This analysis has focused on the permeability of the cracked specimens. The objectives were to quantify the self-healing effectiveness of crystalline admixtures as self-healing agents, and to compare the results of concrete specimens with and without the admixture under different environmental exposures and the effect of changing water/cement ratio. The following conclusions can be drawn from this work:

1. The state of the art has remarked the need of tailored designs to achieve reliable self-healing. Differences between several designs for achieving self-healing concrete have been exposed, showing a high variability in the results due to the lack of standardization and the wide array of types of analysis criteria.
2. A methodology to measure self-healing by means of the permeability of cracked specimens has been developed. The methodology is based on the use of a standard permeabilimeter for traditional concrete uncracked specimens. The method is adequate regardless of the chosen healing agent, and can be used in order to compare different methods for achieving self-healing concrete.

3. The Healing Rate, which is calculated from the results of the modified permeability test, is a reliable indicator of the recovery of durability properties. The crack width, evaluated through image analysis techniques, has a clear relation with the water flow results for values measured before healing.
4. Healing Rate using crack width achieved results similar to water flow Healing Rate but often slightly higher, which can be due to a physical closing of crack that has not influence on the actual permeability.
5. Two types of self-healing have been confirmed: autogenous healing of control concrete and autonomous healing caused by crystalline admixtures reactions. Concrete with crystalline admixtures showed a more stable behaviour in healing tests, with data featuring lower dispersion.
6. The groups that achieved the highest Healing Rates were concrete specimens with crystalline admixtures and stored in the water immersion exposure at 15 and 30°C, with values around 95% even for the larger initial crack widths (0.3 mm).
7. The presence of water was essential for the self-healing reactions for both control concrete and crystalline admixture concrete. Specimens in this kind of exposure achieved Healing Rates above 80-90%, respectively for water contact and water immersion, while the specimens exposed only to moisture obtained lower Healing Rates, under 30%. These results indicate that natural humidity was not enough for complete self-healing, even when using crystalline admixtures.
8. The presence of two centimeters water layer on top of the specimen was enough to make the Healing Rate to increase up to 80%.
9. The exposure of cycling water immersion and dry exposures shows higher dispersion and worse values than the water contact exposure.

5.2 Future lines

This work opens new questions and possible future lines of research, such as:

- Analyzing the effectiveness of self-healing in concrete under marine water immersion.
- Analyzing self-healing in high-performance concrete.
- Studying the effective protection for reinforcement given by the autogenous and crystalline-based healings.
- Analyzing the influence on mechanical properties of healing phenomenon.
- Characterizing healing products and their properties.
- Looking for synergies of CA with other admixtures or mineral additions in order to increase their capability.
- In-depth analyzing of crack morphologies and the healing process inside concrete specimens.

References

ACI Committee 212, 2010. Report on chemical admixtures for concrete. *American Concrete Institute (ACI)*, Chapter 15(Report ACI 212-3R-10), pp. 46-50.

AENOR, 2001. Ensayos de hormigón endurecido. Parte 2: Fabricación y curado de probetas para ensayos de resistencia. *UNE-EN 12390-2:2001*.

AENOR, 2001. Ensayos de hormigón endurecido. Parte 8: Profundidad de penetración de agua bajo presión. *UNE-EN 12390-8:2001*.

AENOR, 2003. Ensayos de hormigón endurecido. Parte 3: Determinación de la resistencia a compresión de probetas. *UNE-EN 12390-3:2003*.

AENOR, 2009. Ensayos de hormigón fresco. Parte 2: Ensayo de asentamiento. *UNE-EN 12350-2:2009*.

Ahn, T.-H. & Kishi, T., 2010. Crack Self-healing Behavior of Cementitious Composites Incorporating Various Mineral Admixtures. *Journal of Advanced Concrete Technology*, Junio, Volume 8 (2), pp. 171-186.

Aldea, C.-M., Song, W.-J., Popovics, J. S. & Shah, S. P., 2000. Extent Of Healing Of Cracked Normal Strength Concrete. *Journal of Materials in Civil Engineering*, February, Issue 12, pp. 92-96.

- Cánovas, M. F., Selva, N. H. & Kawiche, G. M., 1992. New economical solutions for improvement of durability of Portland cement mortars reinforced with sisal fibres. *Materials and Structures*, Volume 25, pp. 417-422.
- Desmettre, C., 2011. *Contribution à l'étude de la perméabilité du béton armé sous sollicitations statiques et cycliques*. École Polytechnique de Montréal: s.n.
- Desmettre, C. & Charron, J.-P., 2012. *Water permeability of fiber reinforced concrete subjected to constant and cyclic loading*. UM, Guimarães, Joaquim Barros et al. (Eds).
- Dong, H., Huang, H. & Ye, G., 2013. Inorganic powder encapsulated in brittle polymer particles for self-healing cement-based materials. *International Conference on Self-Healing Materials (ICSHM2013)*.
- Dry, C., 1994. Matrix cracking repair and filling using active and passive modes for smart timed release of chemicals from fibers into cement matrices. *Smart Mater. Struct.*, Volume 3, pp. 118-123.
- Dry, C., 2000. Three designs for the internal release of sealants, adhesives, and waterproofing chemicals into concrete to reduce permeability. *Cement and Concrete Research*, Volume 30, pp. 1969-1977.
- Dry, C. & McMillan, W., 1996. Three-part methylmethacrylate adhesive system as an internal delivery system for smart responsive concrete. *Smart Mater. Struct.*, Volume 5, pp. 297-300.
- Edvardsen, C., 1999. Water Permeability and Autogenous Healing of Cracks in Concrete. *ACI Materials Journal*, Issue 96-M56.
- Edvardsen, C. K., 1996. *Wasserdurchlässigkeit und Selbstheilung von Trennrissen in Beton*. Berlin: Beuth.
- Fagerlund, G. & Hassanzadeh, M., 2010. *Self-healing of cracks in concrete long-term exposed to different types of water: results after 1 year exposure*. s.l.:Report TVBM.
- Fernández Cánovas, M., 1994. *Patología y terapéutica del hormigón armado*. s.l.:ETS de Ingenieros de Caminos, Canales y Puertos de Madrid.
- Ferrara, L., Krelani, V. & Carsana, M., 2014. A “fracture testing” based approach to assess crack healing of concrete with and without crystalline admixtures. *Construction and Building Materials*, Issue 68, p. 535–551.
- Fukuda, D. et al., 2013. Influence of Fracture Width on Sealability in High-Strength and Ultra-Low-Permeability Concrete in Seawater. *Materials 2013*, Issue 6, pp. 2578-2594.
- Gagné, R. & Argouges, M., 2012. A study of the natural self-healing of mortars using air-flow measurements. *Materials and Structures*.

- Ghosh, S., Biswas, M., Chattopadhyay, B. & Mandal, S., 2009. Microbial activity on the microstructure of bacteria modified mortar. *Cement & Concrete Composites*, Volume 31, p. 93–98.
- Granger, S., Loukili, A., Pijaudier-Cabot, G. & Chanvillard, G., 2005. Mechanical characterization of the self-healing effect of cracks in Ultra High Performance Concrete (UHPC). *In Proceedings Third International Conference on Construction Materials, Performance, Innovations and Structural Implications, ConMat*, 5(CANVIAR XARTICLE REVISTA???), pp. 22-24.
- Hammes, F. & Verstraete, W., 2002. Key roles of pH and calcium metabolism in microbial carbonate precipitation. *Re/Views in Environmental Science & Bio/Technology*, Volume 1, pp. 3-7.
- Hearn, N., 1998. Self-sealing, autogenous healing and continued hydration: What is the difference?. *Materials and Structures/Matériaux et Constructions*, October, Volume 31, pp. 563-567.
- Hearn, N. & Morley, C., 1997. Self-sealing property of concrete - Experimental evidence. *Materials and Structures/Matériaux et Constructions*, August-September, Volume 30, pp. 404-411.
- Herbert, E. N. & Li, V. C., 2013. Self-Healing of Microcracks in Engineered Cementitious Composites (ECC) Under a Natural Environment. *Materials*, Issue 6, pp. 2831-2845.
- Homma, D., Mihashi, H. & Nishiwaki, T., 2009. Self-Healing Capability of Fibre Reinforced Cementitious Composites. *Journal of Advanced Concrete Technology*, 7(2), pp. 217-228.
- Huang, H., 2014. *Thermodynamics of Autogenous Self-healing in Cementitious Materials*. Delft: Technische Universiteit Delft.
- Huang, H., Ye, G. & Damidot, D., 2013. Characterization and quantification of self-healing behaviors of microcracks due to further hydration in cement paste. *Cement and Concrete Research*, Issue 52, pp. 71-81.
- Huang, H., Ye, G. & Damidot, D., 2014. Effect of blast furnace slag on self-healing of microcracks in cementitious materials. *Cement and Concrete Research*, Volume 60, p. 68–82.
- Igarashi, S., Kunieda, M. & Nishiwaki, T., 2009. *Technical Committee on Autogenous Healing in Cementitious Materials*. s.l.:Digest. Edition.
- Imperial College London, 2012. *Self-sealing cracks with superabsorbent polymer*. [Online] Available at: <http://www3.imperial.ac.uk/concretedurability/researchprojects/selfsealingconcrete> [Accessed 23 February 2015].

Jacobsen, S., Granl, H. C., Sellevold, E. J. & Bakke, J. A., 1995. High Strength Concrete - Freeze/Thaw Testing and Cracking. *Cement and Concrete Research*, 25(8), pp. 1775-1780.

Jacobsen, S., Marchand, J. & Homain, H., 1995. SEM Observations Of The Microstructure Of Frost Deteriorated And Self-Healed Concretes. *Cement and Concrete Research*, 25(8), pp. 1781-1790.

Jacobsen, S. & Sellevold, E. J., 1996. Self Healing of High Strength Concrete after Deterioration by Freeze/Thaw. *Cement and Concrete Research*, 26(1), pp. 55-62.

Jaroenratanapirom, D. & Sahamitmongkol, R., 2011. Effects of Different Mineral Additives and Cracking Ages on Self-Healing Performance of Mortar. *Annual Concrete Conference 6*.

Jaroenratanapirom, D. & Sahamitmongkol, R., 2011. Self-Crack Closing Ability of Mortar with Different Additives. *Journal of Metals, Materials and Minerals*, 21(1), pp. 9-17.

Jefferson, A. et al., 2010. A new system for crack closure of cementitious materials using shrinkable polymers. *Cement and Concrete Research*, Issue 40, p. 795–801.

Jonkers, H. M., 2011. Bacteria-based Self-healing Concrete. *HERON*, 56(1/2).

Jonkers, H. M. & Schlangen, E., 2007. Crack repair by Concrete-Immobilized Bacteria. *Proceedings of the First International Conference on Self Healing Materials*, 18-20 April.

Jonkers, H. M. & Schlangen, E., 2008. Development of a bacteria-based self healing concrete. *Tailor Made Concrete Structures*, pp. 425-430.

Jonkers, H. M. et al., 2010. Application of bacteria as self-healing agent for the development of sustainable concrete. *Ecological Engineering*, Volume 36, pp. 230-235.

Joos, M., 2001. Leaching of Concrete under thermal influence. *Otto-Graf-Journal*, Volume 12, pp. 51-68.

Kim, D. J., Kang, S. H. & Ahn, T.-H., 2014. Mechanical Characterization of High-Performance Steel-Fiber Reinforced Cement Composites with Self-Healing Effect. *Materials*, Volume 7, pp. 508-526.

Kim, J. S. & Schlangen, E., 2011. Self-Healing in ECC stimulated by SAP under flexural cyclic load. *Proceedings of 3rd International Conference on Self Healing Materials, Bath, UK*, pp. 27-29.

Lawler, J. S., Wilhelm, T., Zampini, D. & Shah, S. P., 2003. Fracture processes of hybrid fiber-reinforced mortar. *Materials and Structures / Matériaux et Constructions*, Volume 36, pp. 197-208.

- Li, V. C., Limb, Y. M. & Chanc, Y.-W., 1998. Feasibility study of a passive smart self-healing cementitious composite. *Composites*, Volume 29B, p. 819–827.
- Li, Z., Zhou, Z., Xu, D. & Yu, J., 2011. Influence of Cement Coarse Particle on the Self-Healing Ability of Concrete Based on Ultrasonic Method. *Advanced Materials Research*, Volume 177, pp. 526-529.
- Lubelli, B., Nijland, T. G. & van Hees, R. P. J., 2011. Self-healing of lime based mortars: microscopy observations on case studies. *HERON*, 56(1/2), pp. 75-92.
- Ma, H., Qian, S. & Zhang, Z., 2014. Effect of self-healing on water permeability and mechanical property of Medium-Early-Strength Engineered Cementitious Composites. *Construction and Building Materials*, Issue 68, pp. 92-101.
- Ministerio de Fomento, 2008. Instrucción de Hormigón Estructural (EHE-08).
- Morandau, A., Thiérya, M. & Dangla, P., 2014. Investigation of the carbonation mechanism of CH and C-S-H in terms of kinetics, microstructure changes and moisture properties. *Cement and Concrete Research*, Volume 56, p. 153–170.
- Na, S.-H., 2013. *Experimental investigation on self-healing performance of cementitious composite incorporating fly ash and ground granulated blast furnace slag*. s.l.:Muroran Institute of Technology, Academic Resources Archive.
- Neville, A. M., 1986. *Properties of Concrete*. First ed. s.l.:Longman.
- Neville, A. M., 2011. *Properties of Concrete*. Fifth ed. s.l.:Pearson.
- Nijland, T. G. et al., 2007. Self healing phenomena in concretes and masonry mortars: a microscopic study. *Proceedings of the First International Conference on Self Healing Materials*, 18-20 April.
- Nishiwaki, T. et al., 2012. Experimental Study on Self-Healing Capability of FRCC Using Different Types of Synthetic Fibers. *Journal of Advanced Concrete Technology*, Volume 10, pp. 195-206.
- Nishiwaki, T. et al., 2014. Self-Healing Capability of Fiber-Reinforced Cementitious Composites for Recovery of Watertightness and Mechanical Properties. *Materials*, Issue 7, pp. 2141-2154.
- Olivier, K., Darquennes, A., Benboudjema, F. & Gagné, R., 2013. Etude de l'auto-cicatrisation des matériaux cimentaires avec additions minérales après fissuration au jeune âge par retrait gene. *31èmes Rencontres de l'AUGC, E.N.S. Cachan,, 29 au 31 mai*.
- Parant, E., Pierre, R. & Le Maou, F., 2007. Durability of a multiscale fibre reinforced cement composite in aggressive environment under service load. *Cement and Concrete Research*, Issue 37, p. 1106–1114.

- Pelletier, M. M., Brown, R., Shukla, A. & Bose, A., 2011. Self-healing concrete with a microencapsulated healing agent. *Cement and Concrete Research*.
- Qian, S. et al., 2009. Self-healing behavior of strain hardening cementitious composites incorporating local waste materials. *Cement & Concrete Composites*, Issue 31, p. 613–621.
- Qian, S., Zhou, J. & Schlangen, E., 2010. Influence of curing condition and precracking time on the self-healing behavior of Engineered Cementitious Composites. *Cement & Concrete Composites*, Issue 32, p. 686–693.
- Reinhardt, H.-W. & Jooss, M., 2003. Permeability and self-healing of cracked concrete as a function of temperature and crack width. *Cement and Concrete Research*, Issue 33, p. 981–985.
- Roig-Flores, M., 2013. *Caracterización del efecto de un aditivo cristalino en la capacidad de autosanación de un hormigón. Aplicación práctica en dos intervenciones en el auditorio de Cartagena (Murcia)*, s.l.: Final Project for Civil Engineering Degree. Universitat Politècnica de València.
- Roig-Flores, M., Moscato, S., Serna, P. & Ferrara, L., n.d.. Self-healing capability of concrete with crystalline admixtures in different environments. "Manuscript submitted for publication".
- Sahmaran, M., Yildirim, G. & Erdem, T. K., 2013. Self-healing capability of cementitious composites incorporating different supplementary cementitious materials. *Cement & Concrete Composites*, Issue 35, p. 89–101.
- Schlangen, E., Jonkers, H., Qian, S. & Garcia, A., 2010. *Recent advances on self healing of concrete*. Jeju, Korea, Proceedings FRAMCOS7.
- Schlangen, E., ter Heide, N. & van Breugel, K., 2006. Crack Healing of early age cracks in concrete. In: M. Konsta-Gdoutos, ed. *Measuring, Monitoring and Modeling Concrete Properties*. s.l.:Springer, p. 273–284.
- Schlegel, H. G., 2003. *General Microbiology*. Séptima ed. s.l.:Cambridge University Press.
- Siddique, R. & Chahal, N. K., 2011. Effect of ureolytic bacteria on concrete properties. *Construction and Building Materials*, Volume 25, p. 3791–3801.
- Sisomphon, K. & Copuroglu, O., 2011. Self healing mortars by using different cementitious materials. *International RILEM Conference on Advances in Construction Materials through Science and Engineering*. Eds. Christopher Leung, and KT WAN. RILEM Publications SARL: Hong Kong, China, 27-29 Junio.
- Sisomphon, K., Copuroglu, O. & Fraaij, A., 2011. Application of encapsulated lightweight aggregate impregnated with sodium monofluorophosphate as a self-healing agent in blast furnace slag mortar. *HERON*, 56(1/2).

- Sisomphon, K., Copuroglu, O. & Koenders, E., 2013. Effect of exposure conditions on self healing behavior of strain hardening cementitious composites incorporating various cementitious materials. *Construction and Building Materials*, Volume 42, p. 217–224.
- Sisomphon, K., Copuroglu, O. & Koenders, E. A. B., 2012. Self-healing of surface cracks in mortars with expansive additive and crystalline additive. *Cement & Concrete Composites*, Issue 34, p. 566–574.
- Snoeck, D. & de Belie, N., 2012. Mechanical and self-healing properties of cementitious composites reinforced with flax and cottonised flax, and compared with polyvinyl alcohol fibres. *Biosystems Engineering*, Volume III, pp. 325-335.
- Snoeck, D., Dubruel, P. & De Belie, N., 2013. Microfibres and hydrogels to promote autogenous healing in cementitious materials.. *4th International conference on Self-Healing Materials (ICSHM 2013)*, pp. 17-20.
- Snoeck, D. et al., 2014. Self-healing cementitious materials by the combination of microfibres and superabsorbent polymers. *Journal of Intelligent Material Systems and Structures*, Volume 25(1), pp. 13-24.
- Sun, L., YU, W.-Y. & Ge, Q., 2011. Experimental research on the self - healing performance of micro – cracks in concrete bridge. *Advanced Materials Research*, Volume 250-253, pp. 28-32.
- Sze Dai, P., Phuoc Thao, T. D. & and Ser Tong, Q., 2011. Self-Healing Concrete Structural Elements. *3rd International Conference on Self-Healing Materials*, 27-29 Junio.
- ter Heide, N., 2005. *Crack healing in hydrating concrete*. Delft: Delft University of Technology, Faculty of Civil Engineering and Geosciences.
- Termkhajornkit, P., Nawa, T., Yamashiro, Y. & Saito, T., 2009. Self-healing ability of fly ash–cement systems. *Cement & Concrete Composites*, Issue 31, p. 195–203.
- Toledo Filho, R. D., Ghavami, K., Sanjuán, M. A. & England, G. L., 2005. Free, restrained and drying shrinkage of cement mortar composites reinforced with vegetable fibres. *Cement & Concrete Composites*, Issue 27, p. 537–546.
- van Breugel, K., 2007. Is there a market for self-healing cement-based materials?. *Proceedings of the First International Conference on Self Healing Materials, Noordwijk aan Zee, The Netherlands*, 18-20 April.
- van Tittelboom, K. et al., 2011. Methyl methacrylate as a healing agent for self-healing cementitious materials. *Smart Mater. Struct.*, Volume 20.

- van Tittelboom, K., de Belie, N., Lehmann, F. & Grosse, C. U., 2012. Acoustic emission analysis for the quantification of autonomous crack healing in concrete. *Construction and Building Materials*, Volume 28, p. 333–341.
- van Tittelboom, K., de Belie, N., Muynck, W. D. & Verstraete, W., 2010. Use of bacteria to repair cracks in concrete. *Cement and Concrete Research*, Issue 40, p. 157–166.
- van Tittelboom, K., Gruyaert, E., Rahier, H. & de Belie, N., 2012. Influence of mix composition on the extent of autogenous crack healing by continued hydration or calcium carbonate formation. *Construction and Building Materials*, Issue 37, p. 349–359.
- van Tittelboom, K., Snoeck, D., Wang, J. & De Belie, N., 2013. Most recent advances in the field of self-healing cementitious materials. *International Conference on Self-Healing Materials ICSHM2013*, pp. 406-413.
- Wang, J., van Tittelboom, K., de Belie, N. & Verstraete, W., 2012. Use of silica gel or polyurethane immobilized bacteria for self-healing concrete. *Construction and Building Materials*, Volume 26, p. 532–540.
- Wang, J. Y., de Belie, N. & Verstraete, W., 2012. Diatomaceous earth as a protective vehicle for bacteria applied for self-healing concrete. *J Ind Microbiol Biotechnol*, Volume 39, p. 567–577.
- Whiffin, V. S., 2004. *Microbial CaCO₃ precipitation for the production of Biocement*. Murdoch University: Doctoral dissertation, Murdoch University.
- White, S. R. et al., 2001. Autonomic healing of polymer composites. *NATURE*, 15 February. Volume 409.
- Wiktor, V. & Jonkers, H. M., 2011. Quantification of crack-healing in novel bacteria-based self-healing concrete. *Cement & Concrete Composites*, Volume 33, p. 763–770.
- Yang, Y., Lepech, M. D., Yang, E.-H. & Li, V. C., 2009. Autogenous healing of engineered cementitious composites under wet–dry cycles. *Cement and Concrete Research*, Volume 39, p. 382–390.
- Yang, Y., Yang, E.-H. & Li, V. C., 2011. Autogenous healing of engineered cementitious composites at early age. *Cement and Concrete Research*, Volume 41, pp. 176-183.
- Yang, Z., Hollar, J., He, X. & Shi, X., 2011. A self-healing cementitious composite using oil core/silica gel shell microcapsules. *Cement & Concrete Composites*, Volume 33, p. 506–512.
- Yildirim, G., Sahmaran, M. & Ahmed, H. U., 2014. Influence of Hydrated Lime Addition on the Self-Healing Capability of High-Volume Fly Ash Incorporated Cementitious Composites. *Journal of Materials in Civil Engineering*.

- Ying-zi, Y., Lepech, M. D. & Li, V. C., 2005. Self-healing of Engineered Cementitious Composites under cycling wetting and drying. *Proceedings International Workshop on Durability of Reinforced Concrete under Combined Mechanical and Climatic Loads (CMCL), Qingdao, China*, pp. 231-242.
- Yodmalai, D., 2011. *Durability Properties of Concrete with Crystalline Admixtures*. s.l.:Master Thesis, Sirindhorn International Institute of Technology, Thammasat University.
- Zhang, M. et al., 2013. Evaluation of a Microcapsule based self-healing system for cementitious materials. *International Conference on Self-Healing Materials (ICSHM2013)*.
- Zhang, Z., Qian, S. & Ma, H., 2014. Investigating mechanical properties and self-healing behavior of micro-cracked ECC with different volume of fly ash. *Construction and Building Materials*, Issue 52, p. 17–23.
- Zhong, W. & Yao, W., 2008. Influence of damage degree on self-healing of concrete. *Construction and Building Materials*, Issue 22, p. 1137–1142.
- Zhou, Z., Li, Z., Xu, D. & Yu, J., 2011. Influence of Slag and Fly Ash on the Self-healing Ability of Concrete. *Advanced Materials Research*, Volume 306-307, pp. 1020-1023.

Appendix

The results from both campaigns are displayed in this Appendix. These tables indicate the type of mixture (control or specimens with crystalline admixtures), the healing conditions (AE, HC, WC, WD, WI_15 or WI_30), the identification number of each specimen and the obtained values of the healing tests: initial and final values for water flow and crack width.

1 st CAMPAIGN							
Mixture	W/C	Healing conditions	Specimen	Initial		Final - 42 days	
				Water flow (ml/5min)	Crack width (mm)	Water flow (ml/5min)	Crack width (mm)
Control	0.45	AE	1	296	0,10	398	0,11
			2	278	0,12	323	0,09
			3	197	0,09	460	0,10
			4	131		130	
			5	239		440	
			6	303		292	
			7	205		491	
			8	62		42	
			9	1103		1066	

Table 0-1 - Permeability and crack width of cracked and healed specimens, 1st campaign, for control specimens with w/c of 0.45 under the air exposure conditions.

1 st CAMPAIGN							
Mixture	W/C	Healing conditions	Specimen	Initial		Final - 42 days	
				Water flow (ml/5min)	Crack width (mm)	Water flow (ml/5min)	Crack width (mm)
Control	0.45	HC	1	302	0,11	293	0,04
			2	2733	0,18	1710	0,15
			3	93	0,16	141	0,11
			4	1645	0,15	1257	0,15
			5	541		96	
			6	243		176	
			7	172		161	
			8	145		173	

Table 0-2 – Permeability and crack width of cracked and healed specimens, 1st campaign, for control specimens with w/c of 0.45 under the humidity chamber exposure.

1 st CAMPAIGN							
Mixture	W/C	Healing conditions	Specimen	Initial		Final - 42 days	
				Water flow (ml/5min)	Crack width (mm)	Water flow (ml/5min)	Crack width (mm)
Control	0.45	WC	1	1043	0,16	562	0,13
			2	211	0,11	43	0,06
			3	191	0,11	37	0,05
			4	588		102	
			5	191		37	
			6	286		42	
			7	125		15	

Table 0-3 - Permeability and crack width of cracked and healed specimens, 1st campaign, for control specimens with w/c of 0.45 under the water contact exposure.

1 st CAMPAIGN							
Mixture	W/C	Healing conditions	Specimen	Initial		Final - 42 days	
				Water flow (ml/5min)	Crack width (mm)	Water flow (ml/5min)	Crack width (mm)
Control	0.45	WI_15	1	29	0,11	0	0,03
			2	201	0,07	40	0,03
			3	243	0,09	55	0,10
			4	118		22	
			5	423		92	
			6	177		0	

Table 0-4 - Permeability and crack width of cracked and healed specimens, 1st campaign, for control specimens with w/c of 0.45 under the water immersion at 15°C exposure.

1 st CAMPAIGN							
Mixture	W/C	Healing conditions	Specimen	Initial		Final - 42 days	
				Water flow (ml/5min)	Crack width (mm)	Water flow (ml/5min)	Crack width (mm)
CA	0.45	AE	1	3021	0,19	2748	0,21
			2	119	0,10	76	0,11
			3	147	0,10	112	0,14
			4	1034		1181	
			5	139		112	
			6	181		145	
			7	764		1182	

Table 0-5 - Permeability and crack width of cracked and healed specimens, 1st campaign, for CA specimens with w/c of 0.45 under the air exposure conditions.

1 st CAMPAIGN							
Mixture	W/C	Healing conditions	Specimen	Initial		Final - 42 days	
				Water flow (ml/5min)	Crack width (mm)	Water flow (ml/5min)	Crack width (mm)
CA	0.45	HC	1	824	0,12	524	0,11
			2	424	0,09	392	0,10
			3	174	0,08	123	0,06
			4	939		669	
			5	151		138	
			6	569		461	
			7	63		50	
			8	1872		1654	

Table 0-6 - Permeability and crack width of cracked and healed specimens, 1st campaign, for CA specimens with w/c of 0.45 under the humidity chamber exposure.

1 st CAMPAIGN							
Mixture	W/C	Healing conditions	Specimen	Initial		Final - 42 days	
				Water flow (ml/5min)	Crack width (mm)	Water flow (ml/5min)	Crack width (mm)
CA	0.45	WC	1	893	0,10	244	0,03
			2	98	0,13	26	0,06
			3	117	0,09	23	0,02
			4	106		13	
			5	282		37	
			6	172		21	
			7	1060		212	
			8	637		140	

Table 0-7 - Permeability and crack width of cracked and healed specimens, 1st campaign, for CA specimens with w/c of 0.45 under the water contact exposure.

1 st CAMPAIGN							
Mixture	W/C	Healing conditions	Specimen	Initial		Final - 42 days	
				Water flow (ml/5min)	Crack width (mm)	Water flow (ml/5min)	Crack width (mm)
CA	0.45	WI_15	1	389	0,13	0	0,00
			2	256	0,10	24	0,05
			3	396	0,09	61	0,01
			4	617		48	
			5	402		0	

Table 0-8 - Permeability and crack width of cracked and healed specimens, 1st campaign, for CA specimens with w/c of 0.45 under water immersion at 15°C exposure.

2 nd CAMPAIGN							
Mixture	W/C	Healing conditions	Specimen	Initial		Final - 42 days	
				Water flow (ml/5min)	Crack width (mm)	Water flow (ml/5min)	Crack width (mm)
Control	0.45	WI_15	1	196	0,10	97	0,01
			2	450	0,12	98	0,01
			3	4725	0,35	880	0,03
			4	2240	0,43	698	0,04
			5	381	0,11	199	0,01
			6	237	0,11	20	0,00
			7	3450	0,21	38	0,03
			8	1945	0,23	138	0,01
			9	4640	0,25	71	0,01
			10	6250	0,32	1818	0,05
			11	44	0,08	13	0,00
			12	2715	0,26	0	0,02
			13	1187	0,26	11	0,02
			14	1510	0,34	33	0,03
			15	1146	0,13	19	0,00
			16	2355	0,22	674	0,01
			17	21155	0,34	52	0,01
			18	2100	0,21	58	0,03
			19	1990	0,16	166	0,00
			20	215	0,11	8	0,00
			21	460	0,10	5	0,00
			22	2670	0,23	137	0,00

Table 0-9 - Permeability and crack width of cracked and healed specimens, 2nd campaign, for control specimens with w/c of 0.45 under water immersion at 15°C exposure.

2 nd CAMPAIGN							
Mixture	W/C	Healing conditions	Specimen	Initial		Final - 42 days	
				Water flow (ml/5min)	Crack width (mm)	Water flow (ml/5min)	Crack width (mm)
Control	0.45	WI_30	1	6975	0,23	709	0,05
			2	3710	0,22	2	0,00
			3	3150	0,20	3	0,00
			4	6900	0,32	1700	0,01
			5	1640	0,17	0	0,00
			6	489	0,21	4	0,00
			7	5580	0,25	3	0,01
			8	12270	0,30	19	0,01
			9	234	0,11	190	0,01
			10	1645	0,18	0	0,00
			11	4230	0,21	0	0,01
			12	872	0,20	6	0,00
			13	222	0,10	25	0,01
			14	4005	0,19	0	0,00

Table 0-10 - Permeability and crack width of cracked and healed specimens, 2nd campaign, for control specimens with w/c of 0.45 under water immersion at 30°C exposure.

2 nd CAMPAIGN							
Mixture	W/C	Healing conditions	Specimen	Initial		Final - 42 days	
				Water flow (ml/5min)	Crack width (mm)	Water flow (ml/5min)	Crack width (mm)
Control	0.45	WD	1	1481	0,13	226	0,00
			2	1100	0,15	20	0,01
			3	1699	0,16	33	0,01
			4	2286	0,17	996	0,02
			5	2518	0,14	7	0,01
			6	2029	0,27	1375	0,08
			7	6980	0,24	2228	0,07
			8	8165	0,21	4119	0,04
			9	6275	0,23	3108	0,04
			10	4255	0,28	3144	0,07
			11	3620	0,22	2531	0,07
			12	1669	0,20	953	0,04
			13	5235	0,22	2320	0,03
			14	1614	0,16	95	0,01

Table 0-11 - Permeability and crack width of cracked and healed specimens, 2nd campaign, for control specimens with w/c of 0.45 under the wet/dry exposure.

2 nd CAMPAIGN							
Mixture	W/C	Healing conditions	Specimen	Initial		Final - 42 days	
				Water flow (ml/5min)	Crack width (mm)	Water flow (ml/5min)	Crack width (mm)
Control	0.60	WI_15	1	8735	0,33	1211	0,04
			2	920	0,14	0	0,00
			3	5860	0,35	214	0,01
			4	2395	0,30	140	0,01
			5	2085	0,18	10	0,00
			6	276	0,17	5	0,00
			7	827	0,16	53	0,01
			8	2210	0,24	322	0,01
			9	8120	0,30	7	0,02
			10	2525	0,18	0	0,00
			11	3655	0,20	3	0,01
			12	9375	0,38	5076	0,06
			13	18695	0,38	9452	0,13
			14	8395	0,30	1743	0,04
			15	498	0,12	32	0,00
			16	1200	0,23	32	0,01
			17	1211	0,14	0	0,00
			18	1073	0,13	113	0,00
			19	2150	0,17	4	0,00
			20	3395	0,19	154	0,00
			21	2425	0,25	473	0,01
			22	1750	0,21	382	0,01

Table 0-12 - Permeability and crack width of cracked and healed specimens, 2nd campaign, for control specimens with w/c of 0.60 under water immersion at 15°C exposure.

2 nd CAMPAIGN							
Mixture	W/C	Healing conditions	Specimen	Initial		Final - 42 days	
				Water flow (ml/5min)	Crack width (mm)	Water flow (ml/5min)	Crack width (mm)
CA	0.45	WI_30	1	790	0,16	0	0,00
			2	2490	0,20	38	0,01
			3	163	0,09	0	0,00
			4	69	0,08	195	0,00
			5	4390	0,23	108	0,01
			6	1540	0,26	2	0,00
			7	168	0,09	0	0,00
			8	1153	0,15	3	0,01
			9	216	0,11	4	0,00
			10	164	0,11	0	0,00
			11	3110	0,17	0	0,00
			12	5825	0,33	239	0,04
			13	543	0,15	8	0,00
			14	656	0,15	7	0,00

Table 0-13 - Permeability and crack width of cracked and healed specimens, 2nd campaign, for CA specimens with w/c of 0.45 under water immersion at 30°C exposure.

2 nd CAMPAIGN							
Mixture	W/C	Healing conditions	Specimen	Initial		Final - 42 days	
				Water flow (ml/5min)	Crack width (mm)	Water flow (ml/5min)	Crack width (mm)
CA	0.45	WD	1	864	0,14	324	0,03
			2	2404	0,18	112	0,03
			3	2355	0,14	1163	0,04
			4	4790	0,19	2512	0,06
			5	10480	0,30	8053	0,10
			6	1619	0,26	1224	0,07
			7	4745	0,21	3016	0,05
			8	2646	0,31	1889	0,07
			9	1384	0,16	404	0,06
			10	2121	0,18	1351	0,04
			11	2583	0,19	1475	0,06
			12	17730	0,45	13606	0,26
			13	2986	0,21	2155	0,09
			14	3880	0,17	2538	0,05

Table 0-14 - Permeability and crack width of cracked and healed specimens, 2nd campaign, for CA specimens with w/c of 0.45 under the wet/dry exposure.

2 nd CAMPAIGN							
Mixture	W/C	Healing conditions	Specimen	Initial		Final - 42 days	
				Water flow (ml/5min)	Crack width (mm)	Water flow (ml/5min)	Crack width (mm)
CA	0.45	WI_15	1	5410	0,24	1552	0,03
			2	3835	0,17	76	0,00
			3	2525	0,12	76	0,00
			4	3210	0,17	579	0,01
			5	197	0,10	1	0,00
			6	359	0,10	1	0,00
			7	5520	0,30	1070	0,03
			8	1620	0,17	85	0,00
			9	1795	0,17	15	0,00
			10	4090	0,21	0	0,01
			11	4185	0,21	126	0,01
			12	12165	0,31	242	0,03
			13	8470	0,30	166	0,01
			14	5600	0,24	402	0,02
			15	1146	0,13	19	0,00
			16	2355	0,22	674	0,01
			17	21155	0,34	52	0,01
			18	2100	0,21	58	0,03
			19	1990	0,16	166	0,00
			20	215	0,11	8	0,00
			21	460	0,10	5	0,00
			22	2670	0,23	137	0,00

Table 0-15 - Permeability and crack width of cracked and healed specimens, 2nd campaign, for CA specimens with w/c of 0.45 under water immersion at 15°C exposure.

2 nd CAMPAIGN							
Mixture	W/C	Healing conditions	Specimen	Initial		Final - 42 days	
				Water flow (ml/5min)	Crack width (mm)	Water flow (ml/5min)	Crack width (mm)
CA	0.60	WI_15	1	4015	0,34	137	0,04
			2	1438	0,11	52	0,00
			3	1452	0,21	292	0,02
			4	4860	0,25	21	0,01
			5	18595	0,51	8326	0,26
			6	6205	0,34	2921	0,06
			7	381	0,16	44	0,01
			8	3560	0,41	120	0,03
			9	223	0,12	53	0,00
			10	2260	0,29	242	0,02
			11	2530	0,18	366	0,01
			12	1285	0,14	61	0,00
			13	9355	0,33	611	0,01
			14	2930	0,21	261	0,03
			15	498	0,12	32	0,00
			16	1200	0,23	32	0,01
			17	1211	0,14	0	0,00
			18	1073	0,13	113	0,00
			19	2150	0,17	4	0,00
			20	3395	0,19	154	0,00
			21	2425	0,25	473	0,01
			22	1750	0,21	382	0,01

Table 0-16 - Permeability and crack width of cracked and healed specimens, 2nd campaign, for CA specimens with w/c of 0.605 under water immersion at 15°C exposure.